

ABSTRACT

Title of Document: ANALYZING THE EFFECTS OF BLAST LOADS ON BRIDGES USING PROBABILITY, STRUCTURAL ANALYSIS, AND PERFORMANCE CRITERIA

Degree Candidate: Erin Elizabeth Mahoney

Degree and Year: Master of Science, 2007

Directed By: Professor Chung C. Fu
Department of Civil and Environmental Engineering

Recent years have seen an upsurge in terrorist activity. Many studies have shown that the United States' transportation infrastructure is vulnerable to attack. This is especially true for bridges. While the probability of an attack's occurrence is very low, the structural response and consequences could be substantial. Bridge owners need a way to assess the vulnerability of their facilities, in order to make well-informed decisions regarding risk management and mitigation. This thesis proposes a method to evaluate the effects of a man-made attack using vehicle-bound conventional explosives on a highway bridge. The body of knowledge in performance-based seismic design is extended to blasts, using performance criteria to characterize structural response. The expected value of three major consequences is estimated: structural damage, casualties, and downtime. Probability distributions are used throughout to account for uncertainty. Three case studies apply the proposed method to different functional bridge types of an existing long-span bridge.

**ANALYZING THE EFFECTS OF BLAST LOADS ON BRIDGES
USING PROBABILITY, STRUCTURAL ANALYSIS, AND
PERFORMANCE CRITERIA**

By

Erin Elizabeth Mahoney

Thesis submitted to the Faculty of the Graduate School of the
University of Maryland, College Park, in partial fulfillment
of the requirements for the degree of

Master of Science

August, 2007

Advisory Committee:

Professor Chung C. Fu, Chair/Advisor

Professor M. Sherif Aggour

Professor Amde M. Amde

© Copyright by
Erin Elizabeth Mahoney
2007

Acknowledgements

I would like to take this opportunity to thank my advisor, Dr. Chung C. Fu, for his knowledge and guidance this past year. I have truly enjoyed my time working for him, and I appreciate his enthusiasm for learning. His research opportunities allowed me to pursue my degree immediately following my undergraduate education, and for that I am very grateful.

I also thank Dr. Aggour and Dr. Amde for being on my thesis committee. Their time is valuable, so I thank them for reading my work and providing their insight and comments.

I would like to thank Dr. Bilal Ayyub for his suggestions and comments regarding my research, the motivation for which began in his class.

Finally, I thank my family, friends, and fellow graduate students. I appreciate their support and encouragement during my pursuit of a Master's degree.

Table of Contents

Acknowledgements.....	ii
Table of Contents.....	iii
List of Tables.....	vi
List of Figures.....	viii
1.0 INTRODUCTION.....	1
1.1 Background.....	1
1.1.1 Risk and Consequence.....	2
1.2 Purpose and Scope.....	3
1.3 Document Organization.....	4
2.0 LITERATURE REVIEW.....	5
2.1 Introduction.....	5
2.2 Transportation Infrastructure Vulnerability Analyses.....	6
2.2.1 Qualitative Risk Analysis Methods.....	6
2.2.2 Quantitative Risk Analysis Methods.....	10
2.3 Characterizing Terrorist Attack Scenarios.....	14
2.4 Blast Resistant Bridge Design.....	15
2.5 Performance-Based Design.....	17
2.5.1 Performance-Based Earthquake Engineering (PBEE).....	18
2.5.2 Recent Developments in PBEE.....	20
2.5.3 Performance-Based Blast Engineering (PBBE).....	23
2.5.4 Performance-Based Approach to Bridges.....	25
2.6 Closing Remarks.....	26
3.0 PROPOSED METHOD.....	28
3.1 Introduction.....	28
3.2 Proposed Method.....	28
4.0 METHOD DEMONSTRATION.....	32
4.1 Define Attack Scenarios.....	32
4.1.1 Introduction.....	32
4.1.2 Attack Location.....	33
4.1.3 Attack Magnitude.....	35
4.2 Create Bridge Model.....	36
4.2.1 Structural Analysis Software.....	36
4.3 Apply Attack Scenarios to Bridge Model.....	37
4.3.1 Blast Loads.....	37
4.3.2 Equivalent Static Loads.....	38
4.4 Analyze Structural Response.....	41
4.4.1 Nonlinear Analysis.....	41
4.4.2 Performance Levels.....	42

4.5 Consequence Assessment	45
4.5.1 Structural Damage	47
4.5.2 Casualties	50
4.5.3 Downtime.....	51
4.5.4 Total Consequence Cost	54
5.0 CASE STUDY 1: PRESTRESSED CONCRETE (PC) BEAM BRIDGE.....	56
5.1 Geometry and Material Properties	56
5.2 Attack Scenarios	57
5.3 Bridge Model	58
5.3.1 Bridge Deck	58
5.3.2 Tendons.....	60
5.3.3 Completed Model.....	61
5.4 Apply Attack Scenarios to PC Beam Bridge Model.....	62
5.5 Analyze Structural Response	64
5.6 Consequence Assessment	67
5.6.1 Structural Damage	67
5.6.2 Casualties	68
5.6.3 Downtime.....	68
5.6.4 Total Consequences for PC Beam Bridge	69
6.0 CASE STUDY 2: STEEL PLATE GIRDER (SG) BRIDGE.....	71
6.1 Geometry and Material Properties	71
6.1.1 Steel Plate Girders and Stringers	72
6.2 Attack Scenarios	72
6.3 Bridge Model	72
6.3.1 Bridge Deck	73
6.3.2 Abutments and Bents	75
6.3.3 Completed Model.....	76
6.4 Apply Attack Scenarios to SG Bridge Model.....	77
6.5 Analyze Structural Response	79
6.6 Consequence Assessment	82
6.6.1 Structural Damage	82
6.6.2 Casualties	83
6.6.3 Downtime.....	83
6.6.4 Total Consequences for Steel Plate Girder Bridge	84
7.0 CASE STUDY 3: DECK CANTILEVER TRUSS (DT) BRIDGE.....	86
7.1 Geometry and Material Properties	86
7.1.1 Truss Members.....	87
7.1.2 Floorbeams and Stringers	88
7.2 Attack Scenarios	89
7.2 Attack Scenarios	90
7.3 Bridge Model	90
7.3.1 Bridge Deck	90
7.3.2 Completed Model.....	92

7.4 Apply Attack Scenarios to DT Bridge Model.....	93
7.5 Analyze Structural Response	95
7.6 Consequence Assessment	97
7.6.1 Structural Damage	98
7.6.2 Casualties	98
7.6.3 Downtime.....	98
7.6.4 Total Consequences for Deck Cantilever Truss Bridge.....	99
8.0 CONCLUSIONS.....	101
8.1 Study Results	101
8.2 Recommended Areas of Future Research.....	102
Appendix.....	104
References.....	126

List of Tables

Table 2-2: Building Performance Levels per FEMA 273 [26].....	19
Table 2-3: Possible Performance Levels for Blast-Type Loadings [27].....	24
Table 4-1: Randomly Generated Attack Locations	34
Table 4-2: Attack Location along Bridge Length for Bridge Types.....	34
Table 4-3: Randomly Generated Blast Magnitudes.....	36
Table 4-4: Replacement Cost by Performance Level	47
Table 4-5: CALTRANS Comparative Bridge Costs [8].....	48
Table 4-6: Replacement Bridge Costs	49
Table 4-7: Bridge Replacement Times	52
Table 5-1: Attack Scenarios for PC Beam Bridge.....	58
Table 5-2: Prestressed Concrete Beam Bridge Deck Elements.....	60
Table 5-3: Attack Scenario 1 (674 lbs TNT) Static Equivalent Load Calculations...	63
Table 5-4: PC Beam Bridge Structural Damage Costs.....	68
Table 5-5: Cost of Casualties for PC Beam Bridge	68
Table 5-6: PC Beam Bridge Downtime	69
Table 5-7: PC Beam Bridge Downtime Costs	69
Table 5-8: PC Beam Bridge Consequence Costs.....	70
Table 6-1: Attack Scenarios for Steel PG Bridge	72
Table 6-2: Continuous Steel Plate Girder Bridge Deck Elements.....	74
Table 6-3: Attack Scenario 1 (674 lbs TNT) Static Equivalent Load Calculations...	78
Table 6-4: SG Bridge Structural Damage Costs	82
Table 6-5: Cost of Casualties for SG Bridge	83
Table 6-6: SG Bridge Downtime	83
Table 6-7: SG Bridge Downtime Costs	84
Table 6-8: SG Bridge Consequence Costs.....	85
Table 7-1: Attack Scenarios for DT Bridge.....	90
Table 7-2: DT Bridge Deck Elements	92
Table 7-3: Attack Scenario 1 (674 lbs TNT) Static Equivalent Load Calculations...	94
Table 7-4: DT Bridge Structural Damage Costs.....	98
Table 7-5: Cost of Casualties for DT Bridge.....	98
Table 7-6: DT Bridge Downtime	99
Table 7-7: DT Bridge Downtime Costs.....	99
Table 7-8: DT Bridge Consequence Costs.....	100
Table 8-1: Structural Damage Summary	101
Table 8-2: Results Summary.....	101
Table 8-3: Expected Value of Costs by Consequence Type.....	102
Table A-1: PC Beam Attack Scenario 1 Static Equivalent Load Calculations.....	104
Table A-2: PC Beam Attack Scenario 2 Static Equivalent Load Calculations.....	105
Table A-3: PC Beam Attack Scenario 3 Static Equivalent Load Calculations.....	106
Table A-4: PC Beam Attack Scenario 4 Static Equivalent Load Calculations.....	107
Table A-5: PC Beam Attack Scenario 5 Static Equivalent Load Calculations.....	108

Table A-6: SG Bridge Attack Scenario 1 Static Equivalent Load Calculations.....	113
Table A-7: SG Bridge Attack Scenario 2 Static Equivalent Load Calculations.....	114
Table A-8: SG Bridge Attack Scenario 3 Static Equivalent Load Calculations.....	115
Table A-9: SG Bridge Attack Scenario 4 Static Equivalent Load Calculations.....	116
Table A-10: SG Bridge Attack Scenario 5 Static Equivalent Load Calculations....	117
Table A-11: DT Bridge Attack Scenario 1 Static Equivalent Load Calculations....	121
Table A-12: DT Bridge Attack Scenario 2 Static Equivalent Load Calculations....	121
Table A-13: DT Bridge Attack Scenario 3 Static Equivalent Load Calculations....	122
Table A-14: DT Bridge Attack Scenario 4 Static Equivalent Load Calculations....	122
Table A-15: DT Bridge Attack Scenario 5 Static Equivalent Load Calculations....	123

List of Figures

Figure 2-1: Components in Risk Assessment for an Individual Facility [2]	7
Figure 2-2: Criticality and Vulnerability Matrix [1].....	9
Figure 2-3: PEER Framework [19].....	21
Figure 3-1: Proposed Method	29
Figure 4-1: Attack Location in Center Lane	33
Figure 4-2: Relative Location of Blast Centroid.....	34
Figure 4-3: Blast Magnitude Probability Distribution	35
Figure 4-4: Blast Pressure vs. Time	37
Figure 4-5: AT-Blast Screenshot	39
Figure 4-6: Explosion Incidence Orientation.....	40
Figure 4-7: Typical Plastic Hinge [17]	42
Figure 4-8: Deformation-Controlled M3 Hinge Data	44
Figure 5-1: Prestressed Concrete Beam Typical Half Section.....	56
Figure 5-2: AASHTO Type III Beam Cross-sections.....	57
Figure 5-3: Prestressed Concrete Beam Bridge Deck Section.....	59
Figure 5-4: Grid of Deck Frame Elements for PC Beam Bridge.....	60
Figure 5-5: Prestressing Tendon Layout.....	61
Figure 5-6: SAP2000 Model of Prestressed Concrete Beam Bridge.....	62
Figure 5-7: Attack Scenario 1 (674 lbs TNT) Static Equivalent Joint Loads.....	64
Figure 5-8: Attack Scenario 1 Response (Step 11).....	65
Figure 5-9: Attack Scenario 2 Response (Step 11).....	65
Figure 5-10: Attack Scenario 3 Response (Step 11).....	66
Figure 5-11: Attack Scenario 4 Response (Step 11).....	66
Figure 5-12: Attack Scenario 5 Response (Step 11).....	67
Figure 6-1: Continuous Steel Plate Girder Bridge Typical Section.....	71
Figure 6-2: Plate Girder Bridge Deck Section.....	73
Figure 6-3: Grid of Deck Frame Elements for PG Bridge.....	75
Figure 6-4: Bent Cap Beam	76
Figure 6-5: SAP2000 Model of Continuous Steel PG Bridge.....	76
Figure 6-6: Attack Scenario 1 (674 lbs TNT) Static Equivalent Joint Loads.....	79
Figure 6-6: Attack Scenario 1 Response (Step 10).....	80
Figure 6-7: Attack Scenario 2 Response (Step 3).....	80
Figure 6-8: Attack Scenario 3 Response (Step 2).....	81
Figure 6-9: Attack Scenario 4 Response (Step 25).....	81
Figure 6-10: Attack Scenario 5 Response (Step 6).....	82
Figure 7-1: Deck Cantilever Truss Configuration.....	86
Figure 7-2: Truss Member Cross Sections.....	87
Figure 7-3: Deck Cantilever Truss Typical Section.....	89
Figure 7-4: Deck Cantilever Truss Bridge Deck Section	91
Figure 7-5: SAP2000 Model of Deck Cantilever Truss Bridge.....	92
Figure 7-6: SAP2000 Model of Deck Cantilever Truss Bridge (Zoomed In)	93

Figure 7-7: Attack Scenario 1 (674 lbs TNT) Static Equivalent Joint Loads	94
Figure 7-8: Attack Scenario 1 Response (Step 2)	95
Figure 7-9: Attack Scenario 2 Response (Step 3)	96
Figure 7-10: Attack Scenario 3 Response (Step 13)	96
Figure 7-11: Attack Scenario 4 Response (Step 2)	97
Figure 7-12: Attack Scenario 5 Response (Step 4)	97
Figure A-1: PC Beam Attack Scenario 1 Static Equivalent Joint Loads	109
Figure A-2: PC Beam Attack Scenario 2 Static Equivalent Joint Loads	109
Figure A-3: PC Beam Attack Scenario 3 Static Equivalent Joint Loads	110
Figure A-4: PC Beam Attack Scenario 4 Static Equivalent Joint Loads	110
Figure A-5: PC Beam Attack Scenario 5 Static Equivalent Joint Loads	111
Figure A-6: Plate Girder Elevation	112
Figure A-7: SG Bridge Attack Scenario 1 Static Equivalent Joint Loads	118
Figure A-8: SG Bridge Attack Scenario 2 Static Equivalent Joint Loads	118
Figure A-9: SG Bridge Attack Scenario 3 Static Equivalent Joint Loads	119
Figure A-10: SG Bridge Attack Scenario 4 Static Equivalent Joint Loads	119
Figure A-11: SG Bridge Attack Scenario 5 Static Equivalent Joint Loads	120
Figure A-12: DT Bridge Attack Scenario 1 Static Equivalent Joint Loads	123
Figure A-13: DT Bridge Attack Scenario 2 Static Equivalent Joint Loads	124
Figure A-14: DT Bridge Attack Scenario 3 Static Equivalent Joint Loads	124
Figure A-15: DT Bridge Attack Scenario 4 Static Equivalent Joint Loads	125
Figure A-16: DT Bridge Attack Scenario 5 Static Equivalent Joint Loads	125

1.0 INTRODUCTION

1.1 Background

Terrorism presents a real threat to all aspects of society. The terrorist attacks of September 11, 2001 have shown how devastating a successfully implemented attack can be. In the United States, homeland security has become a priority, one that government officials and civilians alike cannot take lightly.

In the past few years, the vulnerability of transportation infrastructure to terrorism has become evident. The casual observer might think that since most of the U.S. highway system has a natural redundancy, it is not susceptible to an attack. However, this is not the case. Transportation facilities are attractive targets for terrorists because they are easily accessible, and an attack could have considerable impact on human lives and economic activity. This is especially true for transportation assets such as bridges, which carry traffic through highway network meeting points and where alternate routes are not available because of geographic constraints.

Recent terrorist threats have targeted the Golden Gate Bridge and the Brooklyn Bridge. Bridges such as these not only provide transportation between two regions, but they also serve as national landmarks. A successful attack would disrupt regional traffic and have severe economic consequences, not to mention cause a blow to the United States' morale. It is imperative that homeland security procedures incorporate bridges, in order to prevent terrorist attacks, as well as minimize the impact if one should occur.

1.1.1 Risk and Consequence

Risk is defined as the potential of loss to a system due to the likelihood of an event and its consequences. Risk (R) is the multi-dimensional product of occurrence probability (L) and consequences given occurrence (C), as shown in Equation 1.1.

$$R = L \times C \quad (1.1)$$

In the homeland security field, Equation 1.1 is modified to include a vulnerability measure (V), which assesses the likelihood of an attack's success, given its occurrence.

$$R = L \times V \times C \quad (1.2)$$

The process of risk assessment answers three basic questions:

1. What could occur?
2. How likely is it to occur?
3. What are the consequences if it occurs?

Defining the probability of occurrence, or likelihood, is traditionally based on historical data and similar studies. In the case of natural hazards, such as earthquakes and hurricanes, thorough records are kept, so the probabilities of occurrence can be estimated for a certain location or geographical region. However, in the case of terrorism, data to estimate likelihood is virtually unavailable. A terrorist attack could occur anywhere, at any time. The nature of terrorist threats involves a human element that cannot be predicted. Therefore, man-made attacks are characterized as low probability, high consequence events. While an attack's probability of occurrence is very small, difficult to quantify and filled with uncertainty, the consequences in most

cases would be devastating. For these reasons, calculating the value of risk in Equation 1.1 or Equation 1.2 does not convey the significance of a terrorist attack and its effects. Instead, using conditional probability theory, more focus can be placed on the consequences of an attack, given its occurrence. That is, the probability of consequence, $P(C|I)$, where “C” is the consequences of an attack and “I” is the initiating event (e.g. attack scenario). Conditional probability theory states that $P(I) = 1$, and the expected value of consequence costs is denoted $E[C]$.

Many studies suggest that analyzing the consequences of terrorist attacks on bridges is a necessary area of future research. Only by having accurate knowledge of these consequences can risk management strategies be developed and implemented.

1.2 Purpose and Scope

This thesis proposes a method for evaluating the effects of a terrorist attack on highway bridges. The approach uses probability distributions to characterize the parameters of the vehicle-bound explosives attack scenario: magnitude and location. Applying Monte Carlo simulation, attack scenarios are randomly generated and the equivalent static loads are applied to the bridge’s structural model. Next, nonlinear static analysis is conducted using commercially available structural analysis software. Performance criteria, established in performance-based seismic design guidelines, are used to measure the structural damage to the bridge. Finally, the method estimates the costs associated with three consequences: structural damage, casualties, and bridge downtime. Probability distributions account for uncertainty in the consequences. Case studies demonstrate the proposed approach with three functional bridge types of an existing long-span bridge: prestressed concrete beam, continuous

steel plate girder, and deck cantilever truss. The case studies analyze attack scenarios to conventional explosives in a vehicle traveling on the bridge.

Knowing the effects of a terrorist attack is beneficial to bridge owners, who have limited funding for security-related issues. The bridge owner can use the proposed method to analyze one critical bridge or multiple bridges in their inventory. Examining the structural responses and consequences of an attack on different functional bridge types can shed light on which bridges are most vulnerable. The results of the proposed method can be valuable when bridge owners must decide among risk management or mitigation strategies.

1.3 Document Organization

This thesis has seven chapters and one supplemental appendix. Chapter 1 contains introductory information, which provides important background information, as well explains the purpose and scope of the study. Chapter 2 includes a literature review of existing works, including subject matter relating to transportation infrastructure vulnerability, terrorist attack scenarios, blast resistant bridge design, and performance-based design concepts. Chapter 3 is a general explanation of the proposed method. Chapter 4 describes the proposed method in more detail and demonstrates its application in the case studies. Chapters 5 - 7 carry out the case studies for three functional bridge types: prestressed concrete beam, continuous steel plate girder, and deck cantilever truss. Chapter 8 summarizes the case study results and recommends area of future research.

2.0 LITERATURE REVIEW

2.1 Introduction

Before describing this study's proposed method and demonstrating its application with three case studies, this chapter will review the existing literature with relevant subject matter. Section 2.2 summarizes the current body of knowledge related to transportation infrastructure vulnerability. These works use both qualitative and quantitative risk analysis methods to assess and manage risks to transportation facilities, such as bridges and tunnels. Special attention is paid to works that include consequence assessment. Section 2.3 describes possible terrorist threats, the most common involving conventional explosives. Section 2.4 presents recent studies in blast resistant bridge design, in order to get an idea of the structural response and reliability of bridges during blast events. In Section 2.5, performance-based design (PBD) is discussed. The current state-of-practice and "next generation" performance-based seismic design guidelines are summarized. Next, works that propose extending seismic PBD principles and practices to include other extreme events, such as blasts, are explained. The section closes with the potential application of performance-based methods to bridge design.

2.2 Transportation Infrastructure Vulnerability Analyses

2.2.1 Qualitative Risk Analysis Methods

In September 2003, the Blue Ribbon Panel (BRP) for Bridge and Tunnel Security issued *Recommendations for Bridge and Tunnel Security* [2]. This report was developed at the request of the Federal Highway Administration (FHWA) and the AASHTO Transportation Security Task Force. The BRP was made up of bridge and tunnel experts from academia, private practice and government agencies, who applied their collective knowledge “to examine bridge and tunnel security and to develop strategies and practices for deterring, disrupting, and mitigating potential attacks” [2]. The panel reports that of the 600,000 bridges and 500 tunnels in the United States, approximately 1,000 are deemed critical, meaning substantial casualties, economic and social consequences could occur if attacked. Terrorism imposes real threats that must be addressed in homeland security policy, and this should account for critical bridges and tunnels.

The report makes several “overarching recommendations” that will reduce bridge and tunnel vulnerability. Institutional recommendations include interagency coordination, outreach and communication strategies, and clarification of legal responsibility. The panel also makes fiscal recommendations, which includes finding new funding sources for bridge and tunnel security, as well as addressing funding eligibility. Technical recommendations include engineering new security solutions, and research, development, and implementation.

The BRP recognizes that a standardized and objective method for identifying the most vulnerable bridges and tunnels is needed. The panel recommends a two-step

process: prioritization and risk assessment. Prioritization, which could be based on subjective or empirical criteria, can identify the most likely targets. Risk assessment is applied to the high priority bridges and tunnels using this approach:

$$R = O * V * I \tag{2.1}$$

Where R = facility risk
 O = Occurrence likelihood of an attack
 V = Vulnerability of likely damage to the structure
 I = Importance of the facility with respect to the consequences of an attack

The factors can be calculated based on attributes shown in Figure 2-1. After collecting the necessary information, the decision makers come to a consensus on the facility's risk.

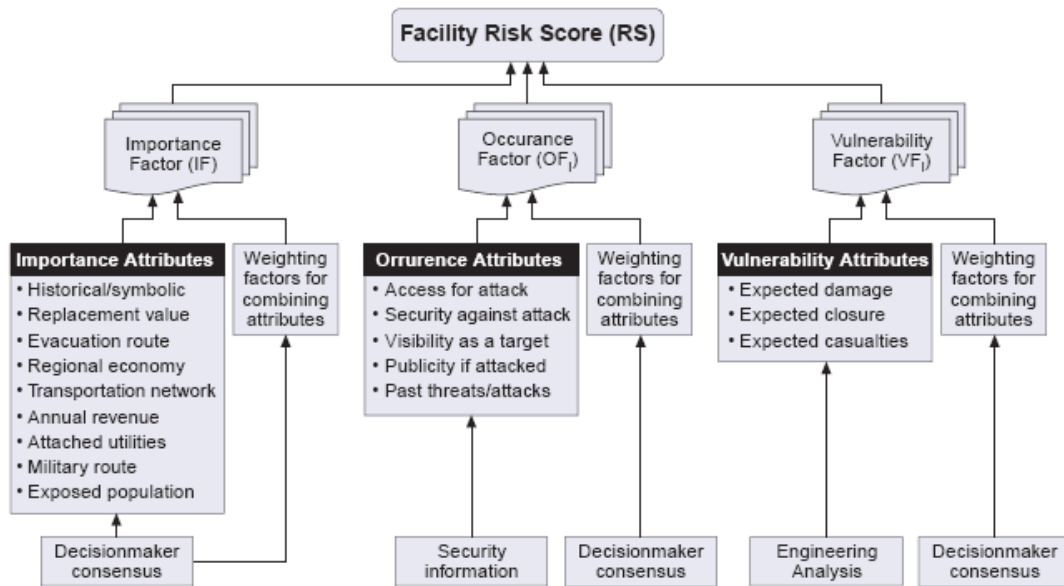


Figure 2-1: Components in Risk Assessment for an Individual Facility [2]

The Vulnerability Factor (V) is a consequence measure for the facility. The BRP recommends that the consequences analyzed should include expected damage to

the structure, expected closure or down-time to the facility, and expected number of casualties.

A Guide to Highway Vulnerability Assessment for Critical Asset Identification and Protection (Guide) [1] was prepared in May 2002 under the direction of the National Cooperative Highway Research Program (NCHRP) for AASHTO's Transportation Security Task Force. The *Guide* was developed for state departments of transportation to conduct vulnerability assessments of their transportation assets, develop countermeasures to possible terrorist threats, estimate the cost of these countermeasures, and improve security operational planning. The *Guide* recommends a six-step process for vulnerability analysis that can be applied to all forms of highway infrastructure:

Step 1: Critical Assets Identification

Step 2: Assess Vulnerabilities

Step 3: Assess Consequences

Step 4: Identify Countermeasures

Step 5: Estimate Countermeasures Cost

Step 6: Review Operational Security Planning

These steps are an iterative process, so each State DOT can adopt and adjust the procedure to its unique transportation assets. Step 3, the consequence assessment is of direct relevance to this thesis. The *Guide* recommends a two-step consequence assessment process. In the first step, “criticality (X) and vulnerability (Y) coordinates are calculated for each asset,” using the results from Step 1 and Step 2 of the *Guide's* methodology [1]. These coordinates can be plotted in a “Criticality and Vulnerability

Matrix,” as shown in Figure 2-2. This matrix prioritizes the assets with the highest consequence in Quadrant I.

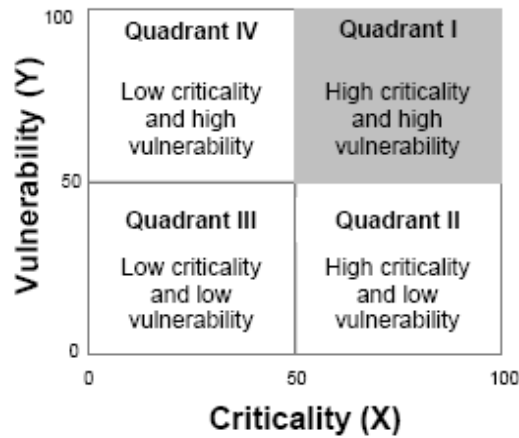


Figure 2-2: Criticality and Vulnerability Matrix [1]

The second step of consequence analysis is to consider the consequences of the critical assets in Quadrant I. The specific consequences are unique to the asset and the attack scenario. The *Guide* goes on to state that consequences can “vary from loss of life and property associated with the attack to loss of an important part of the transportation infrastructure needed to support economic activity, military deployment,” or the loss of an evacuation route [1].

In 2007, Adel Al-Weezer completed his Ph.D. dissertation at the University of Maryland entitled *Risk-Based Methodology for Bridge Maintenance Strategies* [4]. The study proposes a risk-based approach to aid in bridge maintenance decision making. Highway and bridge agencies are typically only concerned with costs, so adding a risk analysis procedure can increase the efficiency of traditional bridge maintenance strategies. The approach first assesses risks to a bridge, based on failure probabilities and failure consequences of the bridge elements. It also proposes strategies for managing these risks. Optimal maintenance actions can then be chosen

based on both benefit-cost analysis and the risks associated with the bridge elements. The study focuses on risks at the bridge element level, while also proposing bridge-level priority ranking. This allows state agencies to prioritize between bridges in their inventories and then between maintenance needs on an individual bridge.

Of direct relevance to this thesis, the author provides information on failure consequences of bridge elements. He summarizes the possible consequences to a bridge as the following:

1. Agency consequences related to the element,
2. Agency consequences related to the bridge,
3. Consequences related to the bridge users due to time delay, traffic diversion and/or bridge closure,
4. Consequences related to traffic accident,
5. Consequences related to health and safety in terms of injuries and/or deaths,
6. Consequences related to the environment,
7. Consequences to nearby businesses, and
8. Consequences to the general public [4].

The total consequence is the summation of all possible consequences to a bridge element. In addition, the author notes that uncertainty must be accounted for in consequence evaluation. Therefore, probability distributions can be used for each consequence type. The dissertation's appendix provides more details about possible bridge failure consequences and how to qualitatively estimate their severities.

2.2.2 Quantitative Risk Analysis Methods

Bensi, a University of Delaware student, completed her Master's thesis on vulnerability assessment of bridges to terrorist attacks [7]. Using a probabilistic, structural analysis based approach, the objective of the study is to guide bridge owners in deciding how to distribute their resources to protect the facilities in their

inventories from terrorist attack. A thorough literature review shows that “prescriptive” methodologies for vulnerability assessment are most common, and so the proposed methodology is less subjective and more technical.

The proposed method starts by simulating the “initiating events” (attack scenarios) using Monte Carlo simulation. Each initiating event is applied to the structure, and the structural response is analyzed. Next, the consequences for each simulated scenario must be determined and quantified as costs. Using the results, a distribution of the structural response is calculated, as well as a distribution of costs. Using the distribution of the structural response, a Vulnerability Index (I_v) is calculated. This index indicates the potential damage to the bridge, given that an attack occurs. The total costs of damage to the bridge can be used to calculate a Criticality Index (I_c). This index is based on the “costs associated with other bridges in the inventory relative to the individual bridge being assessed” [7]. This value aids the bridge owner in deciding how critical the loss of the bridge is in comparison with the other bridges in the inventory. Using both indices, a bridge owner can compare and contrast the structural reliability and expected loss of each bridge, which can aid decisions regarding risk mitigation strategies.

“Risk Analysis for Critical Asset Protection” by McGill et al. [21] proposes a quantitative risk assessment and management methodology in order to aid in security decision making for critical infrastructure resource allocations. This study applies an asset-driven approach, using a critical asset’s unique characteristics to develop all possible human-caused threat scenarios. The framework includes five phases:

Scenario Identification, Consequence and Criticality Assessment, Security Vulnerability Assessment, Threat Likelihood Assessment, and Benefit-Cost Analysis.

In the first phase, Scenario Identification, an “exhaustive set of plausible threat scenarios” is developed for a critical asset [21]. These threats can be mapped in a target susceptibility matrix in order to understand which threat types can affect each of the asset’s key elements.

Consequence and Criticality Assessment estimates the total amount of loss given that the threat scenario is successful. Five suggested dimensions of consequences are fatalities and injuries, asset repair costs, asset loss costs, recuperation time, and environmental damage. The loss for each threat scenario can be calculated as a function of the maximum possible loss, the physical vulnerability of the asset, and response and recovery effectiveness.

Security Vulnerability Assessment involves creating possible attack profiles, which are a combination of the threat delivery system and the intrusion path. Each threat delivery system has a range of possible threat intensities, which can be represented by a probability distribution or expert elicitation. The probability of the security system being successful is the product of the probability of threat detection and response engagement and the probability that the threat is neutralized, given that it is detected and engaged. The probability of threat success is the product of the probability of security system failure and the probability that the threat will be successful given that the security system fails. The conditional risk (in loss amount per threat event) can then be calculated as the probability of threat success multiplied by the expected loss (in Phase 3) given threat success.

The Threat Likelihood Analysis determines the annual rate of occurrence of each threat and takes into account that the threat might change when the adversary responds to security measures that are put in place. This idea is based on the adversary's expected utility of each attack profile. A target that is attractive to the adversary is more likely to be attacked than if the target is not as attractive as a result of security countermeasures or mitigation strategies.

The final phase of the methodology is a risk management strategy to evaluate the cost-effectiveness of proposed countermeasures and/or mitigation strategies. The goal is to maximize the benefit-cost ratio.







In "Critical Asset and Portfolio Risk Analysis (CAPRA) for Homeland Security: An All-Hazards Framework" [11] the authors expand the previous paper [21] to include both natural and man-made threats. The risk assessment and management approach follows the same procedure as in [21]. The method allows the implementer to take an asset-driven or portfolio-driven approach, depending on the assets in question. A region or owner's critical infrastructure can be grouped into a portfolio, and there can be interdependencies between assets. The study proposed a portfolio interdependency analysis to quantify consequences that account for this possibility.

The procedure calculates risk by using the model traditionally used in security studies, by finding the Cartesian product of threat, vulnerability, and consequence. As in the previous study, the parameters used in the model can be high-level, or a result of a detailed systems analysis.

2.3 Characterizing Terrorist Attack Scenarios

The *National Needs Assessment for Ensuring Transportation Infrastructure Security (NNA)* [3] was requested by AASHTO’s Transportation Security Task Force and completed in October 2002. The study focuses on three planning program areas: protecting critical mobility assets, enhancing traffic management capabilities, and improving state emergency response capabilities. Protecting critical mobility assets is of relevance to this thesis, so only this planning program area will be discussed further. The *NNA* states that the “principal threat against highway physical assets is explosive attacks on key links such as bridges, interchanges, and tunnels” [3]. The report characterizes terrorist attacks as having “high concept/low tech” approaches. Explosive attacks are the most common, and the most likely explosive attack scenarios and their impacts are shown in Table 2-1, taken from the Federal Alcohol, Tobacco and Firearms (ATF) Agency web site.

Table 2-1: Vehicle Bomb Explosion Effects [3]

ATF	VEHICLE DESCRIPTION	MAXIMUM EXPLOSIVES CAPACITY	LETHAL AIR BLAST RANGE	MINIMUM EVACUATION DISTANCE	FALLING GLASS HAZARD
	COMPACT SEDAN	500 Pounds 227 Kilos <i>(In Trunk)</i>	100 Feet 30 Meters	1,500 Feet 457 Meters	1,250 Feet 381 Meters
	FULL SIZE SEDAN	1,000 Pounds 455 Kilos <i>(In Trunk)</i>	125 Feet 38 Meters	1,750 Feet 534 Meters	1,750 Feet 534 Meters
	PASSENGER VAN OR CARGO VAN	4,000 Pounds 1,818 Kilos	200 Feet 61 Meters	2,750 Feet 838 Meters	2,750 Feet 838 Meters
	SMALL BOX VAN <i>(14 FT BOX)</i>	10,000 Pounds 4,545 Kilos	300 Feet 91 Meters	3,750 Feet 1,143 Meters	3,750 Feet 1,143 Meters
	BOX VAN OR WATER/FUEL TRUCK	30,000 Pounds 13,636 Kilos	450 Feet 137 Meters	6,500 Feet 1,982 Meters	6,500 Feet 1,982 Meters
	SEMI-TRAILER	60,000 Pounds 27,273 Kilos	600 Feet 183 Meters	7,000 Feet 2,134 Meters	7,000 Feet 2,134 Meters

The report goes on to estimate that approximately 450 bridges and 50 tunnels meet criteria to be deemed “critical” facilities. These critical assets can be protected

by deterring terrorist attacks, which can be done in two ways: by adding new security features to reduce the vulnerability and by minimizing the potential damage, given that an attack occurs.

2.4 Blast Resistant Bridge Design

Islam, a Ph.D. student at Florida State University completed his dissertation on the *Performance of AASHTO Girders Bridges under Blast Loading* [18]. The purpose of the study is to assess the performance of a concrete girder bridge to typical blast loads, in the hope that blast-resistant design guidelines for such bridges will be developed in the future. The study begins by reviewing bridges in Florida's highway system in order to choose a bridge type to model. Then, the author reviews some well-known explosive attacks and bridge failures of the past.

For the bridge model, the author designs a typical two-span, two-lane concrete Type III girder bridge using AASHTO Load and Resistance Factor Design (LRFD) methods. The bridge model is characteristic of concrete bridges in Florida, where some 90% of highway bridges use AASHTO girders. The author uses AT-Blast, a software program that estimates blast loadings in open-air explosion, to convert a 500-pound TNT explosion into equivalent static loads that could be easily applied to the bridge model. Using STAAD.Pro software, the bridge is modeled with five blast loading cases: under the bridge at mid-span, over the bridge at mid-span, over the bridge at the pier cap, over the bridge at end span, and under the bridge at four feet away from the column. The program output gave moments and shear forces for critical bridge elements, which are compared to the respective elements capacity to determine failure. In all five loading cases, the girder bridge fails, leaving the author

to conclude that Type III AASHTO girder bridges cannot withstand a 500-pound TNT explosion. The study then uses a trial and error approach to find the amount of blast loads and the minimum standoff distance that the girders and columns/pier cap could resist.

In August 2005, an article entitled “Analysis and Design of Critical Bridges Subjected to Blast Loads” appeared in ASCE’s *Journal of Structural Engineering* [28]. Blast-resistant design standards are usually reserved for important buildings, such as essential government, military and petrochemical structures. Security has not been a consideration for bridge designers, but recent terrorist threats and activity has brought attention to the vulnerability of transportation infrastructure, especially bridges. This study summarizes the results of current research to develop performance-based blast design standards for bridges. Physical security techniques and site layout principles must be integrated into the bridge design process.

This paper makes some observations about a bridge’s structural response to a blast load. One point that is relevant to this thesis is that military operations have suggested that a bridge’s substructure can generally withstand “modest above deck explosive loads” [28]. In the analysis, bomb sizes are considered ranging from 100 lbs to 4,000 lbs of TNT equivalent explosives. A large hand-placed explosion is about 100 lbs of TNT, while a typical car bomb can hold 220 lbs of TNT. A light, single rear-axle delivery vehicle can hold 4,000 lbs of explosives. The authors note that “individual charges greater than 4,000 lbs are very difficult to achieve when using improvised explosives” [28]. The explosion is difficult to initiate so that the

entire amount reacts at once, which means that higher charge weights may not have an impact much greater than 4,000 pounds of explosives.

Suthar, another student of Dr. Chung Fu at the University of Maryland, completed his Master's thesis entitled *The Effect of Dead, Live and Blast Loads on a Suspension Bridge* [24]. After creating a 3D finite element analysis model of the westbound Chesapeake Bay Bridge's suspension span, nonlinear analysis with dead, live and blast loads is carried out. For the live load, the author uses the design truck (HS-20) dynamic loading. The results obtained closely align with data from the State Roads Commission, which shows the validity of the software used, Visual Bridge Design System (VBDS). For the blast load, the suspension bridge was modeled in SAP2000, and the static-equivalent of a charge weight of 500 pounds TNT is applied. The author uses the progressive collapse approach, which includes the formation of plastic hinges. The software's output displayed moments, axial loads, and deformations of the structural members, and the study concludes that the suspension bridge experiences local failure in response to the blast load. The author hopes that his work can provide a guideline for blast load analysis on a suspension bridge, since there are currently no standardized criteria.

2.5 Performance-Based Design

Traditional structural design codes use prescriptive methodologies. These codes focus on designing individual structural members to a certain strength or capacity, without addressing the overall performance of the structure in response to the applied loading. Performance-based design (PBD) is a process that allows the design of new structures (or upgrade of existing structures) to meet performance

objectives that are acceptable to the designer, owner, and/or other stakeholders. It is a systematic process that has four basic steps:

1. Select performance objective.
2. Design the structure.
3. Assess performance of structure using acceptance criteria.
4. Revise design if performance objectives not met.

This process can be repeated until the desired performance level is achieved.

At this point in time, the performance-based approach is most widely applied in building design for earthquakes. However, these performance-based building codes can be applied to other structures, such as highway bridges, and extended to account for events other than earthquakes, such as hurricanes, fires, or in the case of this thesis, terrorist attacks.

2.5.1 Performance-Based Earthquake Engineering (PBEE)

The 1989 Loma Prieta and 1994 Northridge earthquakes caused substantial economic losses and structural damage in California. These events stimulated the development of performance-based design procedures in order to minimize the losses triggered by earthquakes. The Federal Emergency Management Agency (FEMA) funded the Applied Technology Council (ATC) and Building Seismic Safety Council (BSSC) to produce the *NEHRP Guidelines and Commentary for the Seismic Rehabilitation of Buildings*, also known as FEMA 273 [13]. An important feature of FEMA 273 is that it introduced “standard performance levels, which quantified levels of structural and nonstructural damage, based on values of standard structural response parameters” [26]. These performance levels describe the degree to which

the building or structure is able to withstand the chosen design earthquake. The three performance levels are Immediate Occupancy (IO), Life Safety (LS), and Collapse Prevention (CP), which are described in Table 2-2 and in the following paragraphs.

Table 2-2: Building Performance Levels per FEMA 273 [26]

<i>Performance level</i>	<i>Damage description</i>	<i>Downtime</i>
Immediate occupancy	Negligible structural damage; essential systems operational; minor overall damage	24 hours
Life safety	Probable structural damage; no collapse; minimal falling hazards; adequate emergency egress	Possible total loss
Collapse prevention	Severe structural damage; incipient collapse; probable falling hazards; possible restricted access	Probable total loss

The Immediate Occupancy performance level means that the building or structure can be occupied immediately following the earthquake. There is negligible structural damage, no threat to occupants’ safety, and the building can function normally while any minor damage is being repaired.

At the Life Safety performance level, significant damage to the structure has occurred, “but some margin against either partial or total structure collapse remains” [13]. It is possible that some structural elements are severely damaged, but there is no falling debris hazard. The overall risk to life as a result of structural damage is low. However, the structure is not safe for re-occupancy until repairs are made. The repairs necessary are possible, but for economic reasons may not be practical.

At the Collapse Prevention performance level, the building is on the verge of partial or total collapse. There is severe structural damage, and the structure has experienced a significant decrease in stiffness and strength. Large permanent lateral deformations are probable. There are significant risks of injury or death as a result of

falling structural debris. The structure is unsafe for occupancy, and total replacement is probably more practical than repairing the damage.

In 2000, the American Society of Civil Engineers (ASCE) converted the FEMA 273 and 274 reports into FEMA 356, the *Prestandard and Commentary for Seismic Rehabilitation of Buildings* [14]. FEMA 356 represents the current state-of-practice for performance-based earthquake engineering.

2.5.2 Recent Developments in PBEE

In 2001, FEMA awarded a contract to the Applied Technology Council to produce the “next-generation” performance-based seismic design guidelines for new and existing buildings, called the ATC-58 project [6]. “First generation” procedures, such as FEMA 273/274 [13], do not include direct quantitative information on possible consequences at the different performance levels. ATC-58 addresses this concern and will express structural performance directly in terms of three quantified risks: direct losses (cost of structural damage and repair/replacement), downtime associated with structural damage, and casualties. These measures are most important to stakeholders, as was decided in a workshop. In addition to seismic effects, ATC-58 seeks to incorporate effects from blast, fire, and wind to performance-based design.

The ATC-58 project will use the procedures developed by the Pacific Earthquake Engineering Research (PEER) Center, headquartered at the University of California, Berkeley. Over the past 10 years, PEER has developed a performance-based earthquake engineering (PBEE) approach, “aimed at improving decision-making about seismic risk by making the choice of performance goals and the

tradeoffs that they entail apparent to facility owners and society at large” [22]. The procedure is a probabilistic, performance-based method that accounts for the many sources of uncertainty in seismic design. It is the first approach to date that incorporates loss modeling and takes an economic standpoint in evaluating structural performance during and after an earthquake event.

PEER’s performance-based method has four sequential steps. The result of each step is a generalized variable: intensity measure (IM), engineering demand parameter (EDP), damage measure (DM), and decision variable (DV), as shown in Figure 2-3.

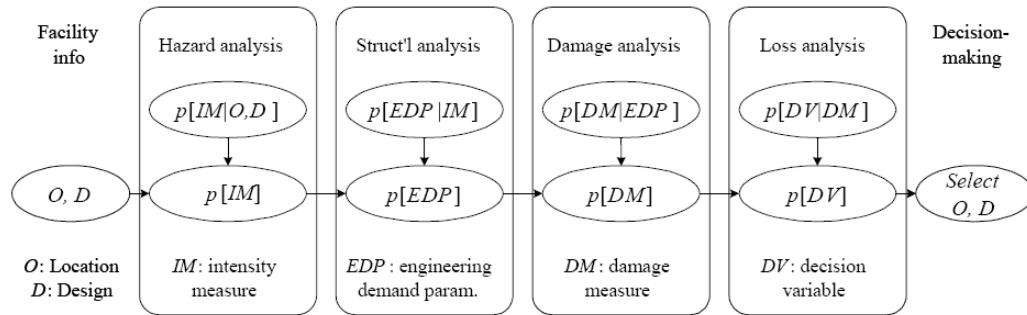


Figure 2-3: PEER Framework [19]

In the first step, Hazard Analysis, the ground motion intensity for the design earthquake is decided on, which yields the IM. During Step 2, a structural analysis is performed on the structure, and the seismic demand is characterized by structural response measures, or EDPs. Examples of EDPs could be stresses, forces, or plastic deformation. The outcome of this step is a conditional probability distribution; that is, the probability of the structural response measure given that the IM occurs. During the third step, Damage Analysis, response measure in Step 2 is converted to a quantifiable damage state. In the PEER framework, damage states are expressed as fragility functions, which are cumulative distribution functions of the damage

measure (DM). The fourth and final step of the PEER methodology calculates the loss-modeling measure, or decision variable. Possible DVs include economic losses, such as replacement costs or duration of facility closure. Each step is based on a conditional probability with the previous step's generalized variable.

It should be noted that PEER's PBEE framework depends on three mathematical models [20]. First, a probabilistic seismic demand model is needed to relate earthquake intensities to structural response parameters (IMs to EDPs). A probabilistic damage model is needed to relate the engineering demand parameters to the damage states for structural components (EDPs to DMs). Finally, a cost model is necessary to relate the damage state of a structural component to the estimated costs or material quantities that repair or replacement would require (DMs to DVs).

In 2007, Sashi Kunnath applied and evaluated the PEER performance-based method to a viaduct in California [19]. The study is part of several "testbed" studies with the purpose of testing the PEER framework on existing facilities. To account for uncertainty in structural modeling, a lognormal probability distribution is used for the structural response measures, or EDPs. The EDP chosen is the maximum column drift ratio, which must be related to the chosen damage measure (DM), the onset of cover concrete spalling and longitudinal bar buckling. The PEER Structure Performance Database provides the information necessary to quantitatively link these two parameters, and the fragility functions for the damage measures could be derived. Next, conducting the loss analysis presents a challenge, since "limited research has been conducted on the relationship between bridge damage and bridge performance" [19]. The study attempts to use the traditional performance levels outlined in FEMA

273/274 (Immediate Occupancy, Life Safety, and Collapse Prevention) to create the decision variable, which is the probability of bridge closure.

In “Method for Post-Earthquake Highway Bridge Repair Cost Estimation” [20], three researchers from the University of California, Berkeley demonstrate the PEER PBEE framework by estimating highway bridge repair costs. The study quantifies the expected repair cost and variance of a representative reinforced concrete highway overpass bridge after applying an earthquake event. Repair cost data for the different bridge elements were taken from the California Department of Transportation’s Construction Statistics *Bridge Design Aids* [9] and used to formulate repair costs models as a function of earthquake intensity. The approach uses a graphical tool called Fourway, and it is based on first and second central probabilistic moments. The study finds that the expected repair cost of the bridge after an earthquake is significantly lower than the expected bridge replacement cost.

2.5.3 Performance-Based Blast Engineering (PBBE)

Although performance-based design has been mostly applied to earthquake engineering, the concepts can be extended to other extreme loadings, such as blasts. In “Performance-Based Engineering of Buildings and Infrastructure for Extreme Loadings” [27], Whittaker recommends applying the wealth of knowledge developed for PBEE to blast loadings on structures. Prior to the 1990’s, blast resistance was a concern of only a small group of professionals: consulting specialists who worked to protect “high exposure” facilities, such as government buildings, military and energy facilities. However, recent terrorist attacks have increased awareness of the importance of blast resistant design. Unlike in seismic design, “there has been no

national effort” to publish guidelines for the design and analysis of blast-resistant structures [27].

The author compares and contrasts seismic and blast loadings in order to identify how PEER’s PBEE framework would have to be adjusted to extend to blasts. Overall, it can be said that inelastic structural response can be expected in any extreme loading case. However, characterizing a blast load is deterministic and uses a scenario event composed of a charge weight and location, while seismic events are characterized probabilistically using a hazard curve. The blast intensity measure (IM) would have to be converted into a loading function, such as a pressure-impulse curve. Also, the response of the individual structural components would differ (EDPs).

The author recommends using the performance levels established in FEMA 273/274 [13] and FEMA 356 [14] for blast analysis, as shown in Table 2-3. It should be noted that the damage descriptions and downtime estimates are changeable and only proposed to “foster discussion” [27].

Table 2-3: Possible Performance Levels for Blast-Type Loadings [27]

<i>Performance level</i>	<i>Damage description</i>	<i>Downtime</i>
Immediate occupancy	Negligible structural and nonstructural damage	24 hours
Life safety	Nonstructural and glazing damage; probable structural damage to beams and columns over a limited area; no collapse; adequate emergency egress; no loss of life due to structural damage	Several months to a year
Collapse prevention	Severe structural and nonstructural damage; structural damage over a wide area; incipient collapse; possible restricted egress; minimal loss of life due to structural damage	Possible total loss

In “Risk Perception in Performance-Based Building Design and Applications to Terrorism-Resistant Design” [25], the authors note that the public’s perception of risk has increased dramatically in recent years as a result of terrorist attacks, natural

disasters, and fires. As technology and structural design methods advance, buildings and structures are becoming taller, larger, and more complex, which can cause their occupants to feel anxiety about their safety. The article discusses the current applications of performance-based design in earthquake engineering and suggests applying PBD to terrorist-resistant design, such as blasts. Since terrorist attacks are difficult to characterize and predict (e.g. they can occur anywhere at any time), traditional prescriptive codes are insufficient. Performance-based methods can adapt and change based on the hazard identified.

2.5.4 Performance-Based Approach to Bridges

In “Performance-Based Design Approach in Seismic Analysis of Bridges” [16], the authors discuss the relevance of performance-based design criteria to highway bridges. The article begins by summarizing and evaluating the current body of knowledge relating to performance-based seismic analysis. The authors then discuss how the existing guidelines are relevant to highway bridges and include example bridge applications. Next, the article discusses the findings of “The Working Group on Bridge Design Issues” [23]. Since bridges contain less nonstructural elements than buildings, the inclusion of nonstructural elements in performance-based seismic analysis of bridges is not necessary. Three performance levels are proposed: operational without traffic interruption, operational with minor damage, and near collapse. ATC-18 recommends two service levels for bridges in seismic events: immediate and limited. ATC-32 proposes three damage levels: minimal, repairable, and significant. The authors combine the performance, service,

and damage criteria to propose three bridge performance levels: immediate service, limited service, and collapse prevention.

The article closes by discussing the barriers to widespread implementation of the performance-based method to bridge design. First of all, the initial investment for the bridge will be higher, in order to meet the desired performance levels. Designers and bridge owners must be able to work together and absorb these higher costs, keeping in mind that the bridge will perform better in an earthquake event. In addition, the design process becomes “more complex and time consuming” when performance-based methods are applied [16].

2.6 Closing Remarks

This chapter has presented an overview of existing literature that is relevant to this thesis. An important concept to take away from this chapter is that risk analysis is a useful tool for assessing the vulnerability of bridges to terrorist threats. Consequence assessment, one aspect of risk analysis, can be qualitative or quantitative. Qualitative studies are simpler and more straightforward to conduct; however, they sometimes can be too subjective. The analyzer’s own judgments and bias can skew the results. Quantitative analyses with a mathematical basis can yield more accurate results. However, quantitative studies require far more input data than their qualitative counterparts, which can increase computational time and effort. In addition, sometimes there is not enough input data to complete an acceptable quantitative study.

This chapter also describes performance-based design guidelines and their establishment in the seismic community. It is clear that performance-based concepts

can be adapted for blast events on bridges. The performance level criteria will be used in this thesis to characterize the structural response of bridges to an explosive attack. It is the hope of the author that future research will build on current performance-based practices and stimulate the development of official guidelines (similar to FEMA 356 and ATC-58) for blast loads.

3.0 PROPOSED METHOD

3.1 Introduction

This study proposes a method to evaluate the structural response and consequences of a terrorist attack on a highway bridge. The procedure is based on structural analysis and uses probability distributions to account for uncertainty. Performance level criteria, well established in the seismic community, can be adapted to blast loads and used to measure the bridge structural response. The consequences of an attack, in monetary terms, are estimated based on the response's performance levels. By analyzing the different bridge functional types separately, the bridge owner or operating agency can compare the expected consequences, to help make decisions regarding risk mitigation or countermeasures.

3.2 Proposed Method

This study seeks to estimate the expected consequence costs of a terrorist attack, using three functional bridge types of an existing long-span bridge as case studies. The proposed method is illustrated in a flowchart in Figure 3-1. The procedure can be adapted and modified as needed to fit the user's purpose and scope. Following Figure 3-1 is a general description of each step. Details of the method unique to this study will be explained in Chapters 4-7, where three case studies demonstrate the procedure.

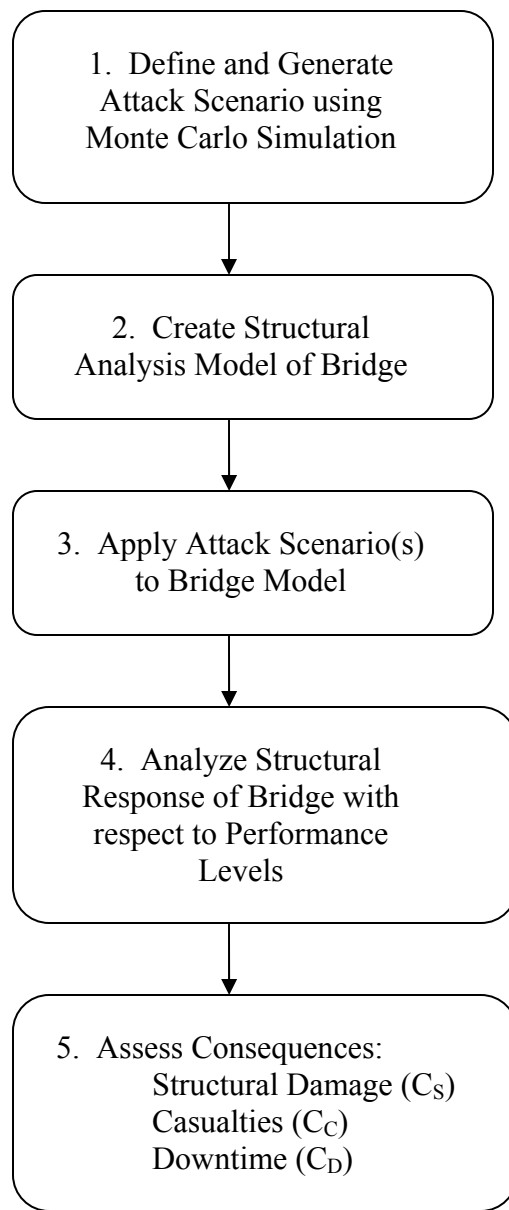


Figure 3-1: Proposed Method

The first step of the method is defining the attack scenario. This includes the location of the attack, delivery method, and magnitude. The *National Needs Assessment* [3] characterizes possible weapons used by terrorists to include: conventional explosives, chemical, biological, radiological, and nuclear. Another type of attack is described as “novel concept,” such as an unusual delivery system

(i.e. aircraft or boat) [3]. This study will limit the attack scenarios to vehicle-bound conventional explosives, measured in TNT charge weight. After deciding which attack type will be analyzed, the location and magnitude of the scenario must be defined. These parameters can be characterized by appropriate probability distributions to account for uncertainty. Monte Carlo simulation is used to randomly generate the attack scenarios. The user determines how many simulations are necessary for the analysis, based on the purposes of the study.

The second step of the procedure is creating a structural analysis model of the bridge(s) in question. If the study includes an inventory of facilities, representative spans of each functional type should be chosen to model. This method can also be used to study a long-span bridge with different functional bridge types. Again, representative spans of each functional type can be modeled. The use of commercial structural analysis software is suggested (e.g. ANSYS, SAP2000, STAADPro). The complexity of the structural model can vary in conjunction with the level of detail necessary in the analysis.

Next, the randomly generated attack scenarios are applied to the modeled bridge(s) and structural analysis is performed. Analyzing the structural response involves designating a damage measure. This study proposes that the performance levels established in performance-based seismic design guidelines (Immediate Occupancy, Life Safety, and Collapse Prevention) are used to describe the level of damage the structure experiences.

The final step of the procedure involves estimating the consequences of the attacks. Possible consequences include cost of structural repair or replacement,

casualties and injuries, costs associated with downtime of the structure, environmental costs, costs to society, and so on. It is important to acquire reliable data and cost information before completing a consequence analysis. Often, consequences are estimated based on historical data, expert opinion, or quantitative models. This study proposes estimating the consequences suggested by ATC-58 [6], discussed in the literature review: cost of structural damage (repair or replacement), downtime associated with structural damage, and loss of life. The BRP report [2] also recommends analyzing these three consequences. The consequences are estimated for each attack scenario and then averaged for each bridge type in order to find the expected value of consequence costs.

Chapter 4 demonstrates the proposed method in more detail. Case studies for three bridge functional types follow in Chapter 5, 6 and 7.

4.0 METHOD DEMONSTRATION

The proposed method will be demonstrated for three functional bridge types of an existing long-span bridge. For security reasons, the bridge's name and location cannot be identified. The case studies will analyze representative spans of three bridge types: 60' prestressed concrete (PC) beam bridge, 606' continuous steel plate girder (SG) bridge, and 1350' deck cantilever truss (DT) bridge.

This chapter describes the proposed method as applied to the three case studies. Chapters 5 -7 will describe each bridge as well as items unique to the modeling of that particular bridge type. Chapters 5-7 will also summarize the applied attack scenarios, structural responses, and consequences for each bridge type.

4.1 Define Attack Scenarios

4.1.1 Introduction

The Federal Highway Administration estimates that 60% of terrorist attacks use conventional explosives. In this study, the attack scenarios are limited to TNT-equivalent blasts that occur over the bridge deck (e.g. carried in a vehicle traveling on the bridge). Winget et al. states that a height of four feet is "considered the standard center of mass for most vehicle explosions" [28]. This value is used in the case studies.

This study's analysis is completed with the assumption that an attack has occurred on the bridge. A probabilistic method is used to generate random attack scenarios using Monte Carlo simulation. The attack scenarios are based on

probability distributions for the explosion's centroid location on the bridge deck, as well as the charge weight of the blast. Five attack scenarios are randomly generated in this study. Although some might say this violates small sample properties, the case studies are included for the purpose of demonstrating how to apply the proposed method. Therefore, more attack scenarios are not needed.

4.1.2 Attack Location

The location of an explosive attack can be represented by a uniform probability distribution along the bridge's length; that is, there is an equal probability of the attack occurring at any one point on the bridge. The bridge in question has three lanes of traffic, so it is assumed that the explosives are carried in a vehicle traveling along the centerline of the middle lane of traffic, as shown in Figure 4-1.

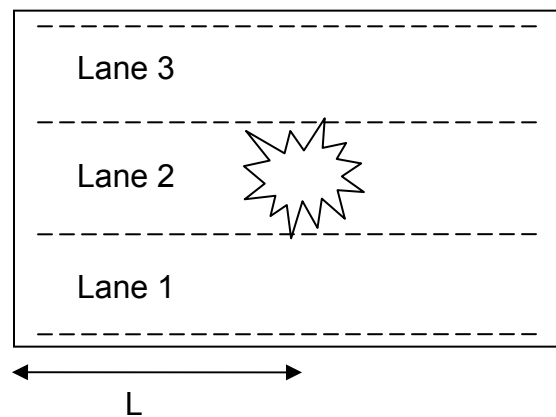


Figure 4-1: Attack Location in Center Lane

Since the three bridge types vary in length, the randomly generated value is a relative location along the bridge length, characterized by a uniform distribution from 0 to 1. The uniform distribution is illustrated in Figure 4-2. This relative location is multiplied by the bridge type's length to calculate the location. Table 4-1 shows the

randomly generated relative location value for the five simulations. Table 4-2 displays the associated blast location for each bridge type.

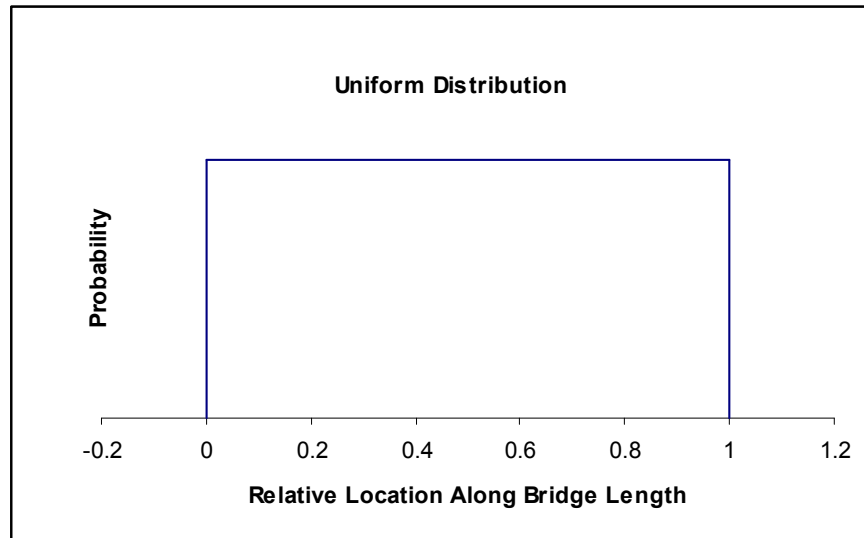


Figure 4-2: Relative Location of Blast Centroid

Table 4-1: Randomly Generated Attack Locations

Attack Scenario	Relative Blast Location Along Bridge Length
1	0.57
2	0.73
3	0.21
4	0.60
5	0.34

Table 4-2: Attack Location along Bridge Length for Bridge Types

Attack Scenario	Blast Location Along Bridge Length (feet)		
	Pre-Stressed Concrete Beam Bridge	Continuous Plate Girder Bridge	Cantilever Deck Truss Bridge
1	34	347	773
2	44	444	990
3	13	130	290
4	36	361	803
5	21	209	465

4.1.3 Attack Magnitude

Chapter 2’s literature review is helpful in defining the explosion magnitude. The BRP report notes that the “highest probability” threat of a conventional explosive attack is a car bomb carrying 500 pounds of TNT explosives [2]. Winget et al. recommends setting an upper limit charge weight of 4,000 pounds and a lower limit of 100 pounds [28]. A triangular probability distribution is assigned to the blast magnitude, as shown in Figure 4-3. Triangular distributions are best suited when the lower and upper limits are known, as well as the most likely case.

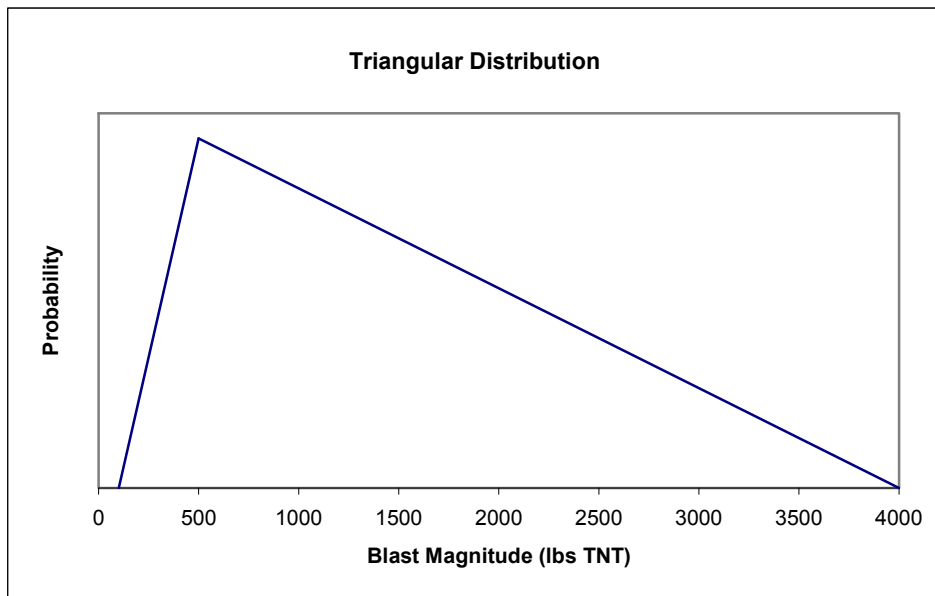


Figure 4-3: Blast Magnitude Probability Distribution

Table 4-3 presents the randomly generated blast charge weights for the five simulations. These charge weights apply to all three bridge types in the case studies.

Table 4-3: Randomly Generated Blast Magnitudes

Attack Scenario	Charge Weight (lbs TNT)
1	674
2	1009
3	437
4	2911
5	1821

4.2 Create Bridge Model

4.2.1 Structural Analysis Software

The three bridge models are using SAP2000 [10], a commercially available structural analysis and design software package. SAP2000 was created over 30 years ago, by Computers and Structures, Inc. (CSI), in Berkeley, California. The software's 3D object-based graphical modeling interface has countless analysis and design options: from simple linear elastic analyses to complex nonlinear dynamic analyses. Add-on modules are available for modeling bridges, offshore/wave structures, or structures with staged construction.

For this thesis, SAP2000 Advanced Version 11 is used. The "Bridge Wizard" module was found to be helpful for modeling the prestressed concrete beam and steel plate girder bridges. For the deck truss bridge, the element geometry was entered into a formatted Microsoft Excel spreadsheet and then imported into SAP. The specific details related to each bridge's structural model is discussed at the beginning of Chapters 5, 6 and 7.

4.3 Apply Attack Scenarios to Bridge Model

4.3.1 Blast Loads

When explosives are detonated, substantial amounts of energy are released. The blast wave contains high pressure/high temperature gas that expands spherically outward from the blast origin, at speeds faster than the speed of sound. As the wave expands, pressures decrease at a high rate, approximately the cube root of distance. The positive pressure wave is followed by a negative pressure wave, as shown in Figure 4-4. However, the effects of the negative pressure wave can usually be ignored. A typical blast wave only lasts a few milliseconds.

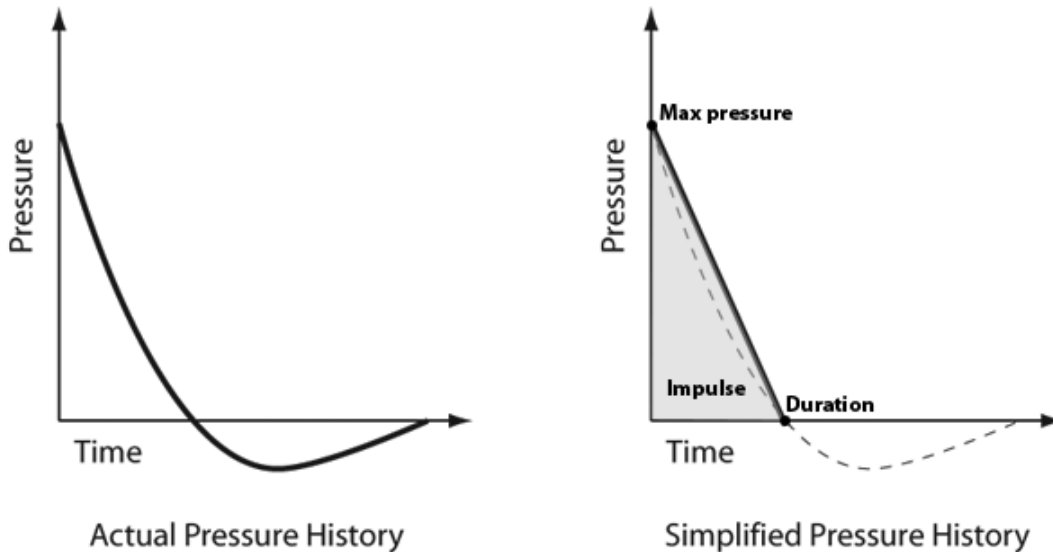


Figure 4-4: Blast Pressure vs. Time

When the shock front of the blast wave comes in contact with a structure, it reflects back, causing an increase in pressure. Reflected pressure is always greater than the incident pressure. Surface faces that are perpendicular to the blast wave experience higher reflected pressures than surfaces that are parallel to the blast wave.

4.3.2 Equivalent Static Loads

This thesis uses nonlinear static analysis to analyze the bridge structures with blast loading. Therefore, the blast pressures must be converted to equivalent static loads. In 1990, the Department of Defense published the TM 5-1300 Manual, *Structures to Resist the Effects of Accidental Explosions*. The manual contains an empirical formula to find the scaled distance (Z) of a blast wave.

$$Z = \frac{R}{W^{1/3}} \quad (4.1)$$

In Equation 4.1, R is the standoff distance of an object from the blast centroid, measured in feet, and W is the charge weight of TNT in pounds. The TM 5-1300 Manual contains a chart using this empirical formula.

With this formula, Applied Research Associates, Inc. created AT-Blast [5], a software program that estimates the equivalent blast loads that occur during an open-air explosion. The program allows the user to input explosion characteristics, such as minimum and maximum distance from the explosion centroid to a surface, explosive charge weight of TNT, and angle of incidence. The program then calculates shock front velocity, time of arrival, pressure, impulse, and duration. These values are displayed in a tabular and graphical format. Figure 4-5 displays a screenshot from AT-Blast with the following inputs: a minimum range of 5 feet, a maximum range of 25 feet, a 500-pound TNT charge weight, and a 0° angle of incidence.

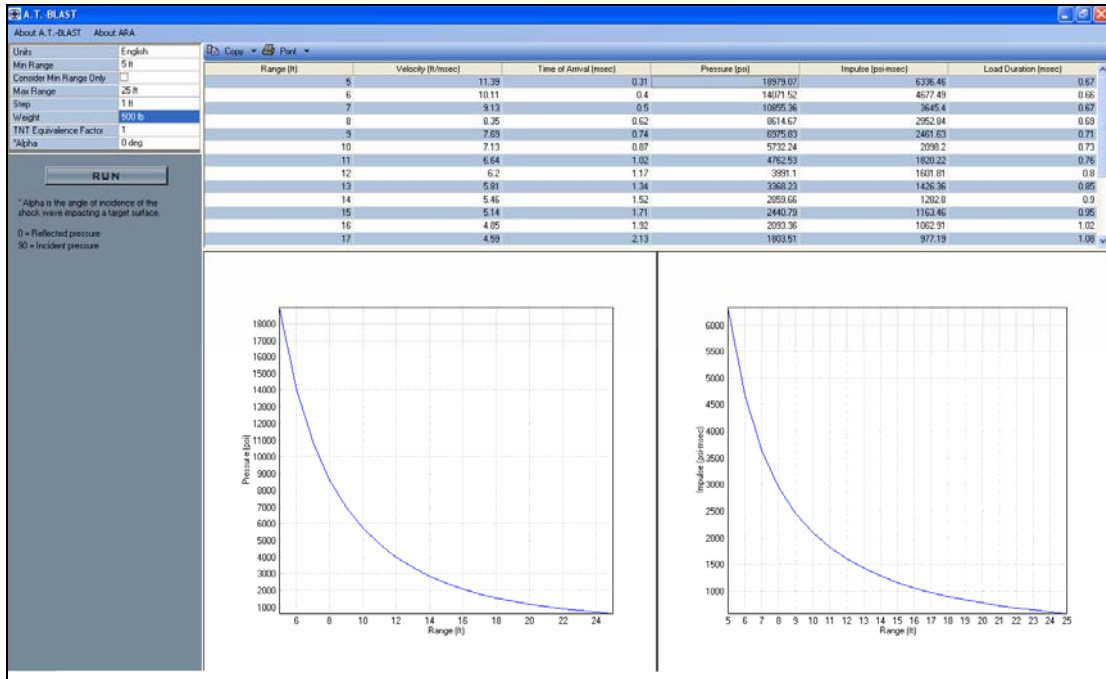


Figure 4-5: AT-Blast Screenshot

AT-Blast’s pressure outputs are used to apply static equivalent loads to this study’s bridge models. The equivalent static loads are applied to the automatically generated joints along the beams and girders. In order to calculate the distance from the explosion to the bridge surface, the height of the blast centroid must be defined. Assuming the bomb is carried in a car trunk or on a truck bed, it is approximated that the explosion centroid occurs four feet¹ above the bridge deck, which is designated as Z. The distance in the plane of the bridge deck of the point of interest from the explosion centroid is designated as X. Using the Pythagorean Theorem, the distance (D) from the explosion centroid to the point on the bridge deck surface is calculated. The angle alpha (α) is calculated, which then gives the angle of incidence (θ_i). The angle of incidence is defined as the angle measured from a ray to the surface normal to the surface at the point of intersection. This means that: $\theta_i = 90^\circ - \alpha$. If the point

¹ Four feet is the accepted distance of an explosion centroid carried by a vehicle above a bridge deck [28].

of interest on the bridge deck is exactly perpendicular to the blast wave, then the angle of incidence is 0° . If the point of interest is parallel to the blast wave, then the angle of incidence is 90° . These relationships are shown below in Figure 4-6.

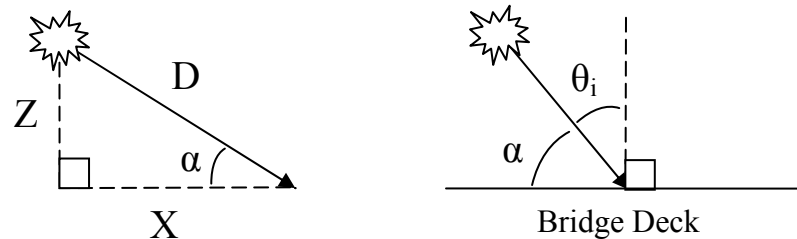


Figure 4-6: Explosion Incidence Orientation

For each joint coordinate that falls on the centerline of beams or girders, the distance from the explosion centroid (D) and the angle of incidence (θ_i) is calculated. Entering these parameters into AT-Blast yields the static equivalent pressure at that joint coordinate. Using the tributary area method, the load in kips on each joint is resolved.

Since this study uses varying charge weights, the influence surface of the blast will differ for each attack scenarios. The influence surface is the surface area expanding radially from the explosion centroid. As the blast magnitude increases, the influence surface increases. This idea must be balanced with the fact that after a certain distance, the blast wave has little effect. In addition, since the blast loads in this study are manually applied on each joint, reasonable cutoff criteria is necessary. Trial and error aided in deciding that the blast loads will be cutoff at pressures less than 200 psi.

4.4 Analyze Structural Response

4.4.1 Nonlinear Analysis

After applying each attack scenario's blast loads to the bridge models, the structural responses are analyzed. Blast loads, as well as other extreme loads (e.g. earthquakes) cause nonlinear response in structures. Linear elastic analysis cannot sufficiently exhibit the bridge's behavior to a blast load. Therefore, nonlinear static analysis is performed.

This study accounts for material nonlinearity by applying plastic² hinges to SAP2000 frame elements. Hinge properties characterize the rigid-plastic behavior of a given member. The nonlinear hinges plastify after reaching their strength or deformation capacities. When the hinge can no longer support the load, the load is dropped and redistributed to other members. FEMA 356 provides default hinge properties for use in seismic design, and SAP2000 incorporates these nonlinear values in its own hinge definitions. One study notes that “use of this implementation is very common among the structural engineering profession and researchers” [17]. Figure 4-7 shows a force vs. deformation diagram of a plastic hinge, used for force degrees of freedom such as axial and shear. The same relationship applies to moment degrees of freedom, such as bending and torsion. In that case, the axes would read moment vs. rotation.

² In this study, “plastic” hinges will be used synonymously with “nonlinear” hinges.

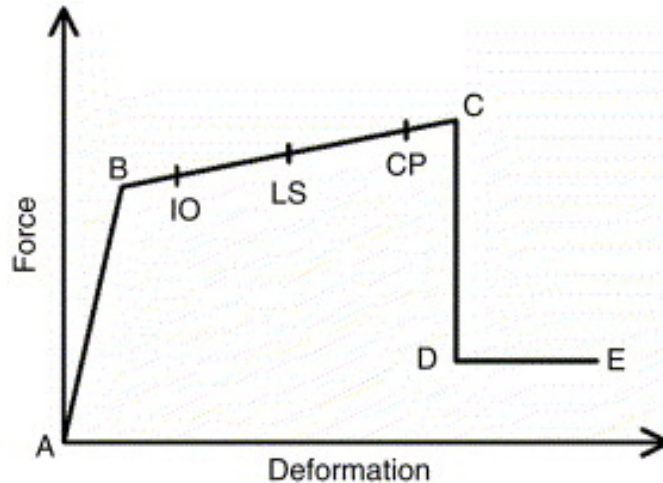


Figure 4-7: Typical Plastic Hinge [17]

On the force-deformation (moment-rotation) curve, Point A is always at the origin. Point B represents the yield strength of the material. After Point B, the hinge will only experience plastic behavior. Point C represents the ultimate strength, while Point D represents the residual strength. At Point E, total failure occurs as a result of the plastic hinge being unable to support the load.

This study use deformation controlled “M3” hinges on the bridge frame elements³, which include the beam, stringer, and deck elements for the prestressed concrete beam and steel plate girder bridges. The M3 hinge type is used for beam elements that experience flexure. For the deck truss bridge, M3 hinges are applied to the deck elements, stringers and floorbeams, while axial force “P” hinges are applied to the truss elements and bracing. Hinges are applied at both ends of an element.

4.4.2 Performance Levels

In the default nonlinear hinge properties, SAP2000 incorporates the three performance levels outlined in performance-based seismic design guidelines, FEMA

³ SAP2000 calls beam members “frame” elements.

273 [13] and FEMA 356 [14]. Discussed in the literature review, the performance criteria represent the level of performance that a structure exhibits in response to a loading event. This thesis proposes that these performance levels be adapted for blasts and utilized to express the structural response of bridges to blast loadings. These performance levels can be helpful in estimating the direct consequences of the blast attack, such as the cost of repairing or replacing the structural damage. The definitions of the three performance levels will remain consistent with the FEMA studies; however, wording will be changed to apply to bridges experiencing a blast event.

The first performance level, Immediate Occupancy (IO), is characterized by minor damage. The structure is safe for vehicles immediately following the blast event. The bridge is stable and repairs can be completed while the bridge is in service.

At the second performance level, Life Safety (LS), there is significant damage to the bridge; however, the bridge is not near collapse. Inspections and repairs will be necessary before the bridge can carry traffic again.

The third performance level, Collapse Prevention (CP), represents a structure that is on the verge of collapse. The bridge's strength and deformation capacity is reached. Structural damage is extensive, and repairs are most likely not economically feasible. Instead, replacement of the bridge is necessary. Since the structure is unstable, there is risk to life at this performance level.

SAP2000 uses the FEMA guidelines to locate the performance levels on the nonlinear hinge force-deformation or moment-rotation graphs. Figure 4-8 shows SAP2000's deformation-controlled, M3 hinge property data.

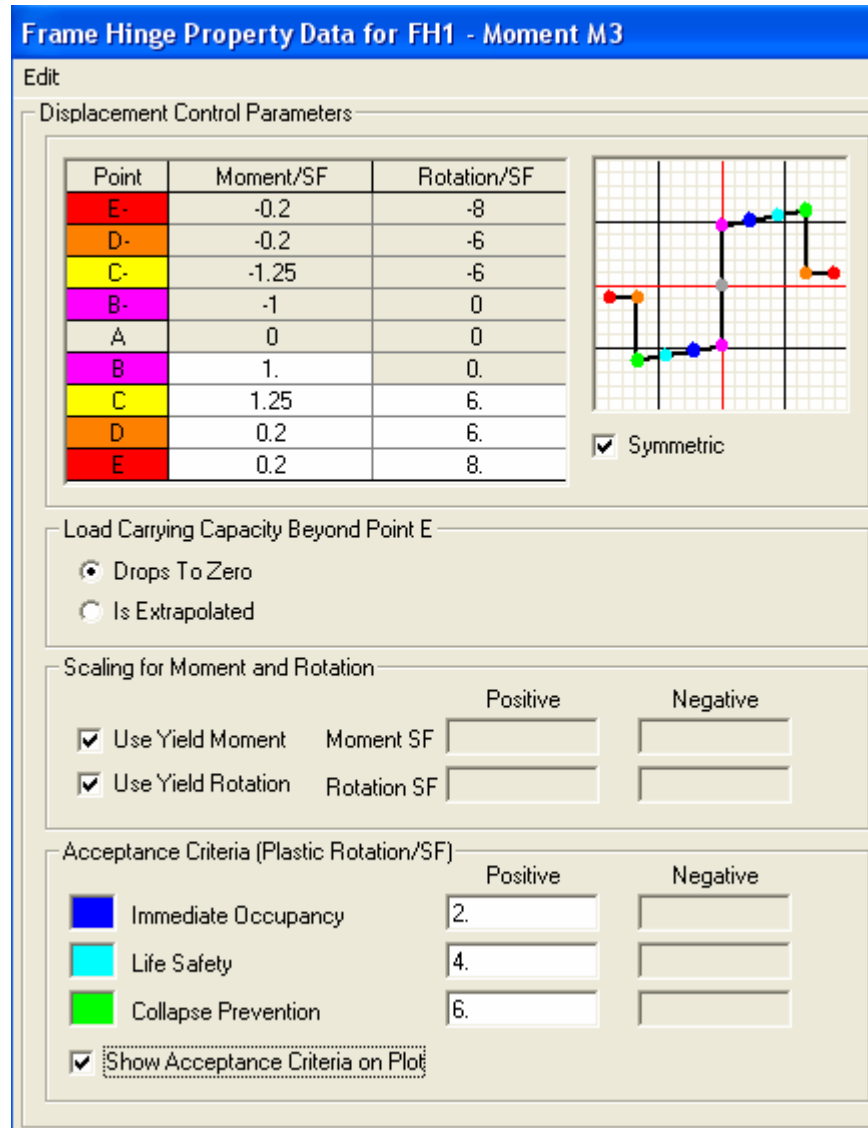


Figure 4-8: Deformation-Controlled M3 Hinge Data

The points A-B-C-D-E are color-coded and valued as a ratio of the yield moment and yield rotation of the structural material. For instance, Point B has a value of 1, since it represents the yield moment. The performance acceptance criteria is shown at the bottom of the window. The Immediate Occupancy performance level

occurs at one-third the distance between the yield moment (Point B) and the ultimate moment (Point C), or two times the yield rotation. The Life Safety Performance Level occurs at two-thirds the distance between Point B and Point C, or four times the yield rotation. The Collapse Prevention performance level occurs at Point C, the ultimate strength, or at six times the yield rotation. Point E is colored in red and denotes collapse of the structure.

The nonlinear analysis output uses these color-coded nodes to represent hinge performance. This study will use this information in order to estimate possible consequences of a blast attack occurring above the bridge deck.

4.5 Consequence Assessment

After analyzing the bridge responses to the blast loading, the consequences of the attack can be estimated. By knowing the possible consequences and their associated costs, the bridge owner can make informed decisions regarding how to allocate risk mitigation and countermeasure funding and efforts. Comparing the results for different bridge functional types can be beneficial, whether the bridge owner is concerned with one long-span bridge with multiple bridge types, or an inventory of bridge facilities.

Before describing the procedure, it should be noted that the author of this thesis is in no way an expert in consequence assessment. The proposed method for estimating the consequences of an attack is a way to present the results of the structural analysis. Using performance levels is a rational means of measuring structural damage; however, the author hopes that the proposed application will stimulate future research. More research is needed to develop the relationship

between performance levels and structural damage, number of casualties, and bridge downtime.

In order to estimate consequences, reliable data sources are needed. Sources of information include in-house databases and historical records, similar studies, analytical or probabilistic analyses, or expert elicitation. The seismic community has used these resources to develop probabilistic models to quantify the economic effects of earthquakes [20]. However, a study involving terrorist attacks has limited sources of data. There is not a database with the damage records of bridges that have experienced an explosive attack. Compared to weather-related and natural disasters, terrorist attacks are few and far between, and the data necessary to create sound analytical models does not exist. For these reasons, the approach proposed in this thesis uses a performance-based structural analysis and probabilistic-based method to assess the consequences of a terrorist attack on a bridge.

There are many possible consequences of a blast attack on a bridge. This study quantifies the monetary costs of the three consequences proposed in the next generation seismic performance guidelines [6] and the BRP Report [2]: structural damage, casualties, and downtime. The cost of structural damage includes the cost to repair or replace the bridge structure. The cost of casualties includes the value of any loss of life. The costs of bridge downtime include monetary losses associated with the bridge being closed for repair or replacement. In this study, downtime costs quantified are losses in toll revenue and user detour costs.

The consequences are expressed by a uniform probability distribution with a lower and upper limit. A uniform distribution is used as a means of demonstration.

Other probability distributions can be applied if more information about the consequences is known.

4.5.1 Structural Damage

The most apparent consequence of an attack on a bridge is physical damage to the structure. Using a relationship between performance levels and replacement cost, the cost of the structural damage is quantified. At an IRCC-PEER workshop on performance-based seismic design, a presentation estimated the percent of structure replacement cost at each of the three performance levels: Immediate Occupancy, Life Safety, and Collapse Prevention [22]. The relationship is shown in Table 4-4.

Table 4-4: Replacement Cost by Performance Level

Performance Level	% of Replacement Cost
Immediate Occupancy (IO)	25%
Life Safety (LS)	50%
Collapse Prevention (CP)	100%




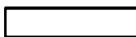

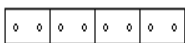
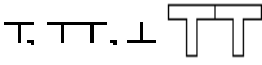



At the CP performance level, the structure requires approximately 100% replacement. This means that for this study, any structural performance equal to or greater than the Collapse Prevention performance level (e.g. Points C, D and E in Figure 4-8) is characterized as total failure. Using Table 4-4's percentages, SAP2000's structural analysis output and bridge cost information, the cost of structural damage can be quantified for each attack scenario and bridge type.

The California Department of Transportation (CALTRANS) has estimated comparative bridge costs⁴ for different bridge types [8], as shown in Table 4-5.

⁴ "These costs are the 'bridge costs' only and do not include items such as: bridge removal, approach slabs, slope paving, soundwalls or retaining walls" [8].

CALTRANS provides a cost range based on common span lengths. The costs are recommended to be used as “general guidelines for structure type selection and its relative cost” [8]. This information is used to estimate the replacement costs of the prestressed concrete beam and steel plate girder bridges.

Table 4-5: CALTRANS Comparative Bridge Costs [8]

STRUCTURAL SECTION	COMMON SPAN RANGE (feet)	COST RANGE (\$ / Square foot)
RC SLAB 	16 - 44	130 - 210
RC T-BEAM 	40 - 60	150 - 275
RC BOX 	50 - 120	160 - 270
CIP/PS SLAB 	40 - 65	160 - 205
CIP/PS BOX 	100 - 250	150 - 230
PC/PS SLAB 	20 - 50	195 - 270
PC/PS 	30 - 120	200 - 270
BULB T GIRDER	90 - 145	180 - 280
PC/PS I GIRDER 	50 - 120	200 - 260
PC/PS BOX 	120 - 200	220 - 395
STRUCT STEEL I GIRDER 	60 - 300	240 - 370

For the steel deck cantilever truss bridge, CALTRANS does not provide an estimated cost. However, other data sources can be used. Construction contract data was obtained from the agency responsible for the bridge used in the case studies, in order to estimate the replacement cost. Table 4-6 shows a range of possible bridge costs for each bridge type, measured in square feet of bridge deck.

Table 4-6: Replacement Bridge Costs

Bridge Type	Spans (ft)	Estimated Replacement Cost (\$/ft ²)	
		Lower Bound	Upper Bound
Pre-stressed Concrete Beam (PC)	60	200	260
Steel Plate Girder (SG)	3@202	240	370
Deck Cantilever Truss (DT)	1350	350	510

Using SAP2000's output, the amount of damaged area, in square feet, for each performance level is estimated for each bridge type and attack scenario. The damaged area is multiplied by the values in Table 4-4 to yield the lower and upper limits of structural damage cost, $(C_{i,S})^B_{low}$ and $(C_{i,S})^B_{high}$, respectively. Equations 4.2 and 4.3 calculate these values for each attack scenario and bridge type. In order to account for uncertainty in these costs, a uniform probability distribution is assigned to this cost range.

$$(C_{i,S})^B_{low} = (25\%)(R_1)^B(A_{i,IO})^B + (50\%)(R_1)^B(A_{i,LS})^B + (100\%)(R_1)^B(A_{i,CP})^B \quad (4.2)$$

$$(C_{i,S})^B_{high} = (25\%)(R_2)^B(A_{i,IO})^B + (50\%)(R_2)^B(A_{i,LS})^B + (100\%)(R_2)^B(A_{i,CP})^B \quad (4.3)$$

Where i = attack scenario number

B = bridge type: PC, SG, or DT

R_1 = lower limit of replacement cost (from Table 4-6)

R_2 = upper limit of replacement cost (from Table 4-6)

A = damaged area by performance level: IO, LS, or CP

The mean and standard deviation of the uniform distribution can be calculated as $(C_{i,S})^B$ and $(\sigma_{i,S})^B$, respectively, for each attack scenario and bridge type. These are the expected costs associated with structural damage.

4.5.2 Casualties

As with any explosion, there are risks to human lives if an attack occurs on a bridge deck. Quantifying the number of casualties and converting this number to a monetary loss is a challenge in any consequence analysis. The first step in doing so is to assign value of a human life, which is a difficult task, as it is subjective. Different organizations assign different values to a human life, depending on the situation. However, for this study, the U.S. Department of Transportation's value of life will be used, since this is an incident occurring on the national highway system. In 2002, the Office of the Secretary of Transportation issued a memorandum to revise a DOT published guide entitled "Treatment of Value of Life and Injuries in Preparing Economic Evaluations" [26]. The memo recommends that the value of life used in all DOT analyses be raised from \$2.7 million to \$3 million. This \$3 million figure is used in this study.

The structural response in terms of performance levels are used quantify the number of casualties. Since any structural response greater than or equal to the Collapse Prevention performance level is considered total failure, any vehicles in this damaged area are in jeopardy. Peak hour traffic data or field surveys can aid in estimating how many vehicles could possibly be on the bridge at any one time. Assuming the vehicles are uniformly distributed across the bridge's deck area, the percent of failed bridge area is proportional to the number of cars in that area. The ratio of failed bridge area for attack scenario can be calculated by dividing the damaged area in or above the Collapse Prevention performance level ($A_{i,CP}$) by the

total surface area of that bridge type (A). This value is designated as the Failure Ratio and is calculated in Equation 4.4

$$\text{Failure Ratio} = (F_i)^B = \left(\frac{A_{i,CP}}{A} \right)^B \times 100\% \quad (4.4)$$

The Failure Ratio is multiplied by maximum number of vehicles on the bridge at any one time (V_{peak}) in order to estimate the maximum number of vehicles in the failed area. Using transportation study estimates of 1.2 persons per vehicle (n), the cost of casualties is calculated. Again, to account for uncertainty, a uniform distribution is applied to this situation, with zero casualties as the lower limit (since it is possible that no vehicles are in the failed area). Equation 4.6 calculates the upper limit of casualty cost.

$$(C_{i,C})^B_{\text{low}} = 0 \quad (4.5)$$

$$(C_{i,C})^B_{\text{high}} = (F_i)^B \times V_{\text{peak}} \times n \times \frac{\$3\text{M}}{\text{person}} \quad (4.6)$$

The mean and standard deviation of the uniform distribution can be calculated as $(C_{i,C})^B$ and $(\sigma_{i,C})^B$, respectively, for each attack scenario (i) and bridge type (B). These values represent the expected costs of casualties as a result of the attack.

4.5.3 Downtime

There are indirect consequences associated with the time that the bridge remains closed to traffic for structural repairs or replacement. Examples include losses in toll revenue (if the bridge is a toll facility), user delay costs, user detour costs, and economic impacts on surrounding businesses. This study will quantify toll revenue losses and user detour costs as a means of demonstration.

Before assessing these consequences, the bridge downtime is estimated. First, one must know the amount of time necessary for full bridge replacement. In the aftermath of a terrorist attack, it is assumed that design and construction of repairs would have an accelerated schedule. Keeping this in mind, Table 4-7 displays a range of bridge replacement times (T_1 and T_2) for each bridge type and span length.

Table 4-7: Bridge Replacement Times

Bridge Type and Length	Replacement Time (months)		Replacement Time (days)	
	Lower Bound	Upper Bound	Lower Bound	Upper Bound
60' PC Beam	2	4	60	120
606' Steel Girder	6	8	180	240
1350' Deck Truss	14	16	420	480

The time needed to complete repairs on the bridge will depend on how much of the bridge needs replacement. The percent of bridge replacement is calculated using the Failure Ratio in Equation 4.4, based on the amount of damaged area in or above the Collapse Prevention performance level. Then, the Failure Ratio is multiplied by the range of replacement time, yielding a lower and upper bound of downtime.

$$(D_i)_{\text{low}}^B = (F_i)^B \times (T_1)^B \quad (4.7)$$

$$(D_i)_{\text{high}}^B = (F_i)^B \times (T_2)^B \quad (4.8)$$

This procedure uses the assumption that downtime depends solely on the portion of bridge that requires replacement (damaged area greater than or equal to the CP performance level). This means that other parts of the bridge that fall in the Immediate Occupancy or Life Safety performance levels, and need more minor repairs, will be repaired during time allotted to replace the failed area.

4.5.3.1 Toll Revenue Losses

The bridge used in the case studies is a toll facility. Any amount of time that the bridge remains closed, the agency responsible loses toll revenue. This could have a significant impact on the agency, depending on how many facilities are in the agency's inventory, as well as how important the particular bridge facility is to its revenue. The total loss in toll revenue for each attack scenario (i) and bridge type (B), designated $(C_{i,D1})^B$, can be found by multiplying the bridge's average annual daily traffic (AADT) by the toll rate per vehicle (r) and downtime $(D_i)^B$. Equations 4.9 and 4.10 calculate the lower and upper limit of the toll revenue loss range. A uniform distribution is applied to this range to account for uncertainty.

$$(C_{i,D1})^B_{\text{low}} = \text{AADT} \times r \times (D_i)^B_{\text{low}} \quad (4.9)$$

$$(C_{i,D1})^B_{\text{high}} = \text{AADT} \times r \times (D_i)^B_{\text{high}} \quad (4.10)$$

For the case studies in Chapters 5-7, the AADT is 30,000 vehicles per day and the toll rate is \$2.00 per vehicle.⁵

4.5.3.2 User Detour Cost

While the bridge remains closed, vehicles are forced to use an alternate route. The user detour cost, denoted C_{D2} , can be calculated by multiplying the bridge's AADT by the user value of time (u), detour time, and bridge downtime. The detour time is defined as two times the distance from the bridge to the nearest alternate route (d), divided by the average speed on the detour (v). The user value of time is based on the average annual income in the area, which can be broken down into an hourly

⁵ Toll facilities often collect different toll rates for different vehicle classes. This can be taken into account by apportioning the AADT by vehicle class and multiplying by the appropriate toll rate. For simplicity and so as not to indicate the actual facility used for the case studies, a \$2.00 toll rate is used for all vehicles.

rate. For the purposes of this study, the average user's value of time will be used synonymously with the average vehicle's value of time.

$$(C_{i,D2})^B_{\text{low}} = \text{AADT} \times u \times \frac{2d}{v} \times (D_i)^B_{\text{low}} \quad (4.11)$$

$$(C_{i,D2})^B_{\text{high}} = \text{AADT} \times u \times \frac{2d}{v} \times (D_i)^B_{\text{high}} \quad (4.12)$$

For the case studies in Chapters 5-7, the AADT is 30,000 vehicles per day. The user value of time (u) is \$22.50 per hour. The distance from the bridge to the nearest alternate route (d) is 50 miles, and the average speed (v) on the detour is 60 mph.

4.5.3.3 Total Downtime Cost

The total cost of bridge downtime is the sum of the individual downtime consequence costs. To find the lower and upper limit for the downtime cost range, use Equations 4.13 and 4.14.

$$(C_{i,D})^B_{\text{low}} = (C_{i,D1})^B_{\text{low}} + (C_{i,D2})^B_{\text{low}} \quad (4.13)$$

$$(C_{i,D})^B_{\text{high}} = (C_{i,D1})^B_{\text{high}} + (C_{i,D2})^B_{\text{high}} \quad (4.14)$$

The mean and standard deviation of the uniform distribution can be calculated as $(C_{i,D})^B$ and $(\sigma_{i,D})^B$, respectively, for each attack scenario (i) and bridge type (B). These values represent the expected costs of the bridge downtime after the attack.

4.5.4 Total Consequence Cost

After quantifying the costs of structural damage $(C_{i,S})^B$, casualties $(C_{i,C})^B$, and bridge downtime $(C_{i,D})^B$, the expected cost of the consequences $E[(C_i)^B]$ and standard deviation $(\sigma_i)^B$ can be calculated for each attack scenario (i) and bridge type (B).

$$E[(C_i)^B] = (C_{i,S})^B + (C_{i,C})^B + (C_{i,D})^B \quad (4.15)$$

$$(\sigma_i)^B = \sqrt{[(\sigma_{i,S})^B]^2 + [(\sigma_{i,C})^B]^2 + [(\sigma_{i,D})^B]^2} \quad (4.16)$$

The expected consequence cost $E[C^B]$ and standard deviation σ^B for each bridge type can then be estimated. Equations 4.17 and 4.18 show these calculations, where N is the number of attack scenarios.

$$E[C^B] = \frac{1}{N} \sum_{i=1}^N E[(C_i)^B] \quad (4.17)$$

$$\sigma^B = \sqrt{\frac{1}{N} \sum_{i=1}^N \{E[(C_i)^B] - E[C^B]\}^2} \quad (4.18)$$

5.0 CASE STUDY 1: PRESTRESSED CONCRETE (PC) BEAM BRIDGE

Case Study 1 demonstrates the proposed method on a prestressed concrete beam bridge. First, general information about the span's geometry and material properties is provided.

5.1 Geometry and Material Properties

The bridge plans were obtained by the agency responsible for the long-span bridge used in this study. The bridge was designed using AASHTO's *Standard Specifications for Highway Bridges* for an HS20-44 live load. A representative prestressed concrete beam span is simply supported, 60' in length and 39'8" wide. There are six AASHTO Type III beams, spaced 7'2" center-to-center. Figure 5-1 shows bridge's typical half section, with symmetry occurring at the center line.

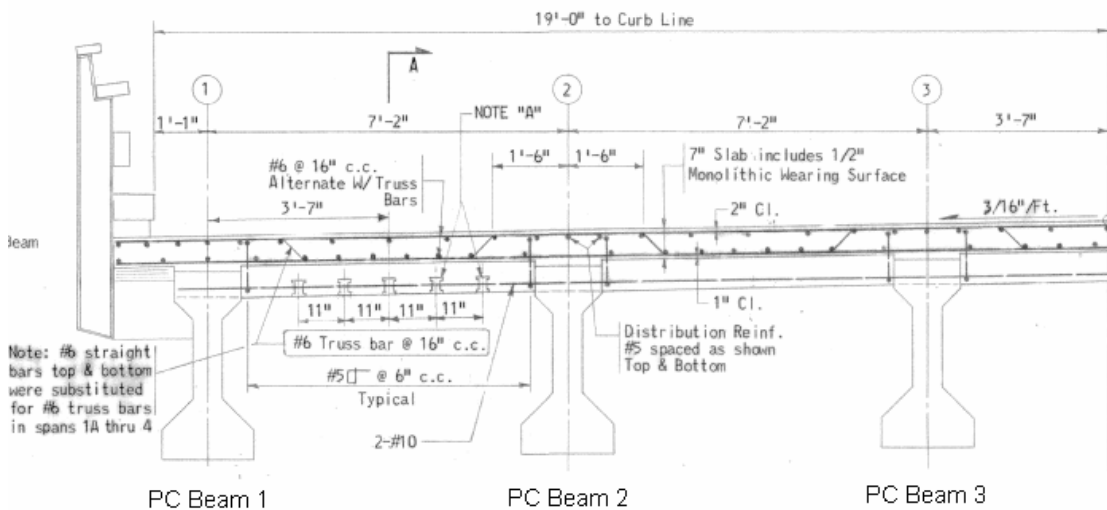


Figure 5-1: Prestressed Concrete Beam Typical Half Section

The bridge deck is 7" thick, which includes a 1/2" monolithic wearing surface. The AASHTO Type III beam cross-section dimensions and prestressing tendon layout is shown in Figure 5-2. Section A-A corresponds the end of the bridge, while Section B-B is the beam cross-section at the bridge midspan.

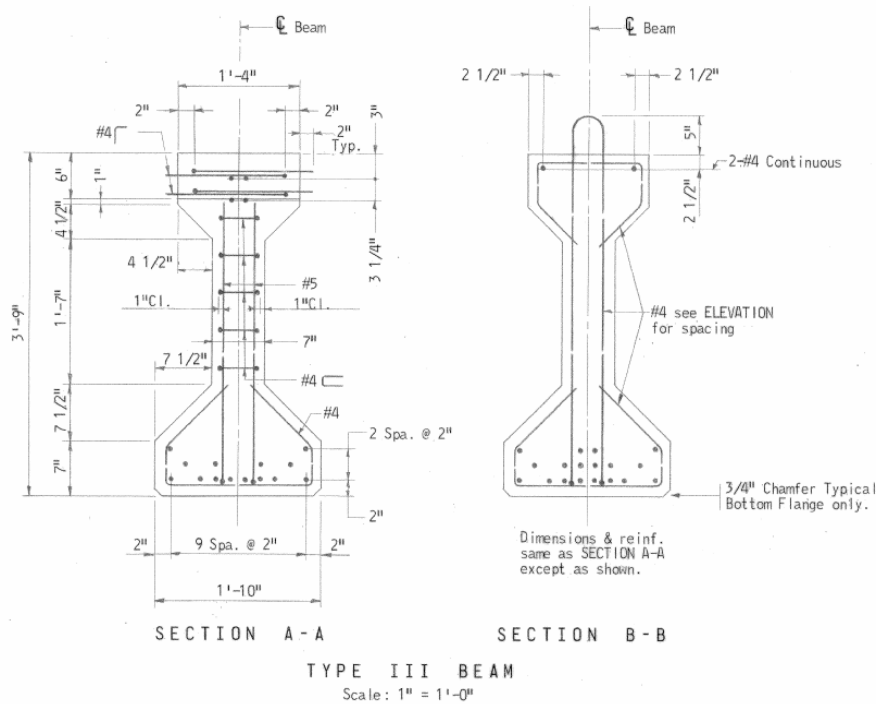


Figure 5-2: AASHTO Type III Beam Cross-sections

The prestressed beam concrete has a minimum 28-day compressive strength of 5,000 psi and a minimum compressive strength of 4,000 psi at transfer of stressing force. The prestressing tendons are number 7 wire, with 1/2" diameter and a cross-sectional area of 0.153 in². The capacity of the wire is 270 ksi.

5.2 Attack Scenarios

The five attack scenarios for the PC beam bridge are restated in Table 5-1. Each scenario is characterized by a charge weight of TNT and location along the

bridge's 60' length. As explained in Chapter 4, the charge weight and locations were assigned probability distributions and randomly generated.

Table 5-1: Attack Scenarios for PC Beam Bridge

Attack Scenario	Charge Weight (lbs TNT)	Blast Location Along Bridge Length (ft)
1	674	34
2	1009	44
3	437	13
4	2911	36
5	1821	21

5.3 Bridge Model

SAP2000 is used to create a model of the prestressed concrete beam bridge. The "Bridge Wizard" module is used to create the typical section and layout of the bridge. The Bridge Wizard's step by step guide allows the user to choose a section and input the geometry and materials of the bridge. The module automatically meshes the elements and creates a finite element model. Joints are automatically created along the centerlines of the PC beams.

5.3.1 Bridge Deck

Since this study is concerned with the response of the deck as well as the beams, the deck is also modeled using frame elements. By defining the deck as frame elements, nonlinear hinges can be assigned, so the deck will exhibit nonlinear plastic behavior. In order to properly model the bridge deck and account for transverse and longitudinal stiffness, a grid of frame elements is created. The deck frame elements are connected to the automatically generated joints along the prestressed concrete beam centerlines. Four frame elements are defined, two in the transverse direction

and two in the longitudinal direction. Deck Sections 1 and 2 are in the transverse direction, while Deck Sections 3 and 4 are in the longitudinal direction. Figure 5-3 shows a cross section of the deck frame elements.

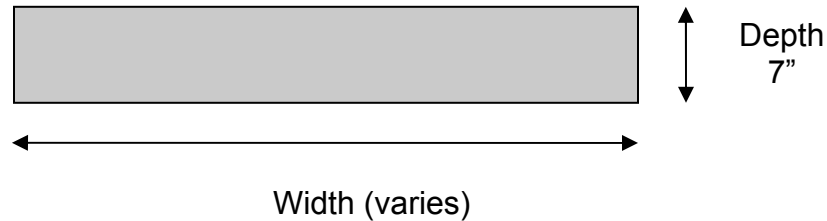


Figure 5-3: Prestressed Concrete Beam Bridge Deck Section

The width of the deck sections are calculated via the beam tributary area concept. First, a few distances must be defined. The distance between joints along the centerline of the concrete beams in the longitudinal direction is designated as “b” and equal to 10’ (120”). The spacing between the concrete beams in the transverse direction is designated as “s” and equal to 7’2” (86”). The overhang distance between the exterior concrete beams and the edge of the bridge is designated as “o” and equal to 1’11” (23”).

Deck Section 1 falls along the end of the bridge in the transverse direction. The width of this section is equal to half the distance between joints along the concrete beams, or $b/2$. Deck Section 2 is also in the transverse direction, with a width equal to the spacing between joints, or b . Deck Section 3 falls in the longitudinal direction along the exterior concrete beams, so the width is defined as the overhang distance plus half the beam spacing, or $o + s/2$. Deck Section 4 elements, also in the longitudinal direction, are along the interior beams with a width equal to

the beam spacing, s . Table 5-2 summarizes the deck frame elements used to model the bridge deck, and Figure 5-4 shows the deck “grid.”

Table 5-2: Prestressed Concrete Beam Bridge Deck Elements

Deck Section	Direction	Depth (in)	Width (in)	
1	Transverse	7	$b/2$	60
2	Transverse	7	b	120
3	Longitudinal	7	$o + s/2$	66
4	Longitudinal	7	s	86

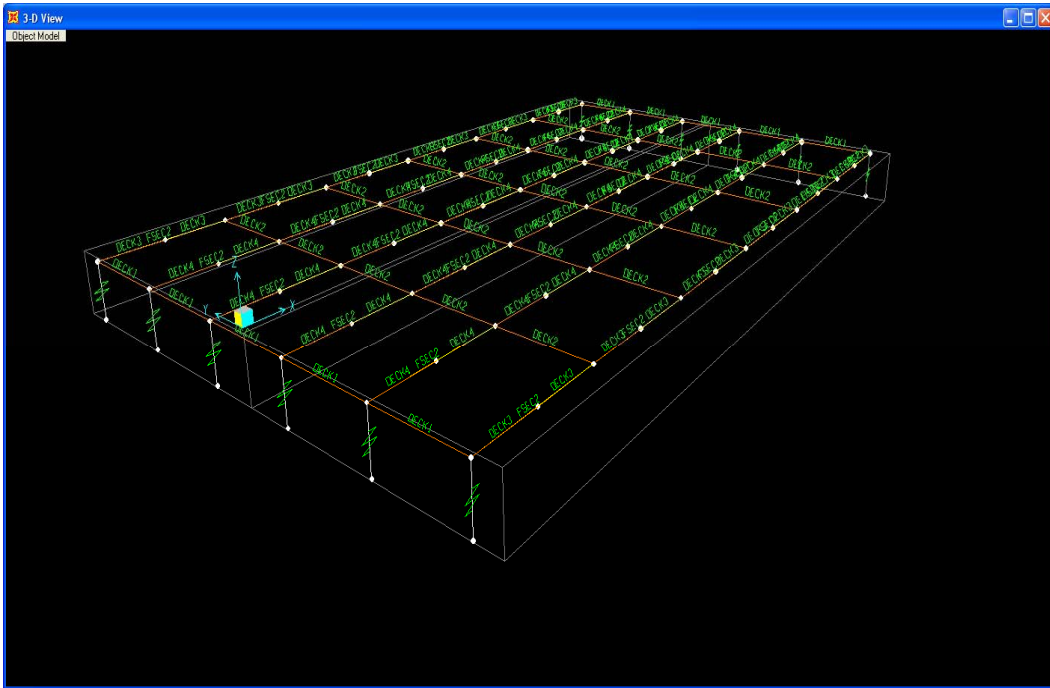


Figure 5-4: Grid of Deck Frame Elements for PC Beam Bridge

5.3.2 Tendons

As Figure 5-2 shows, AASHTO Type III beams have 20 prestressing tendons. SAP2000 allows prestressed tendons to be modeled as forces or elements. For the purposes of this study, the tendons are modeled as frame elements. Four of these tendons are deflected strands that vary along the beam length. The remaining 16 strands are linear along the beam length. Using the center of mass, the four deflected tendons are modeled together, with a cross-sectional area equal to four times the area

of one tendon, or 0.612 in^2 . The straight tendons are also modeled as one tendon, with a cross-sectional area equal to 2.448 in^2 . Figure 5-5 illustrates the tendon layout.

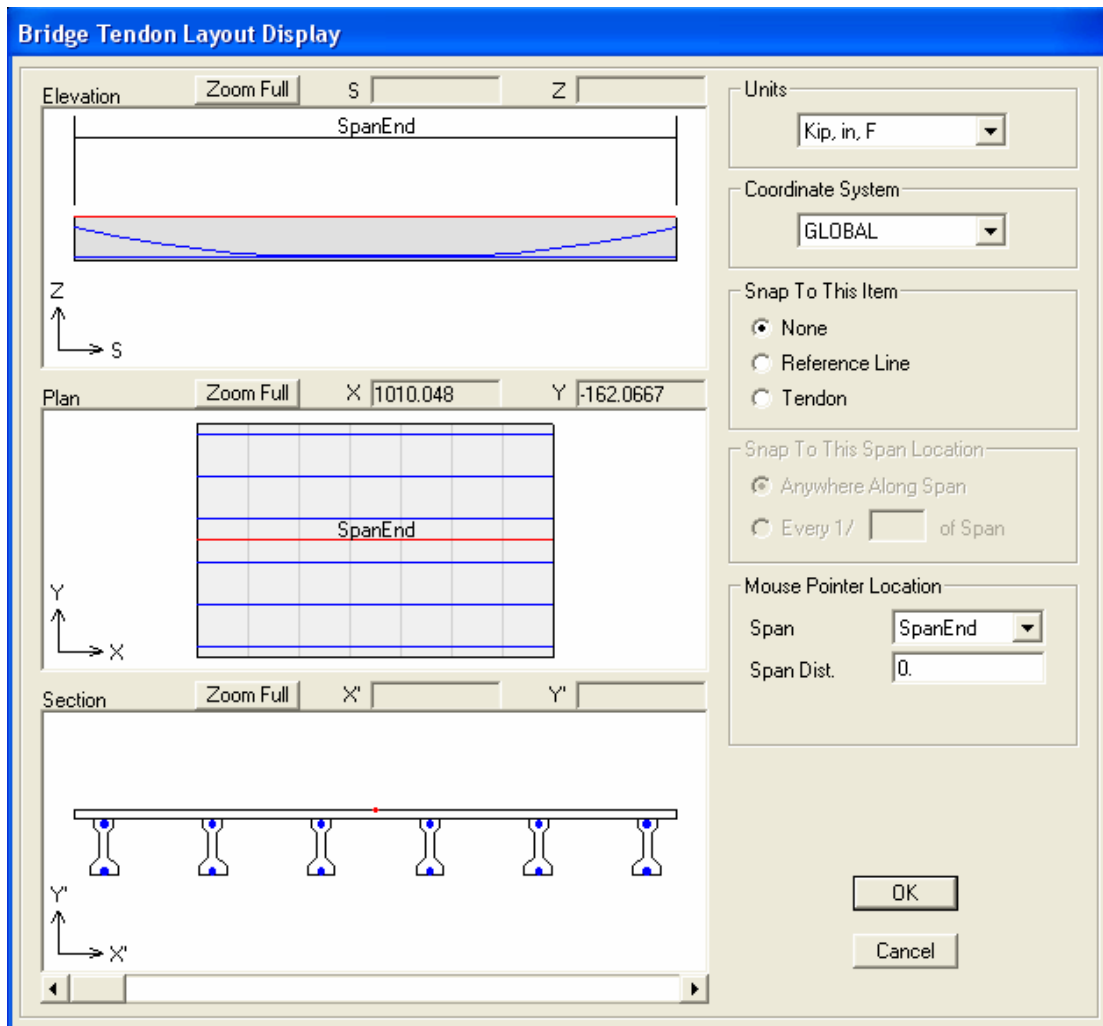


Figure 5-5: Prestressing Tendon Layout

5.3.3 Completed Model

Figure 5-6 shows the SAP2000 model for the 60' prestressed concrete beam bridge, in a 3D view of the cross-section.

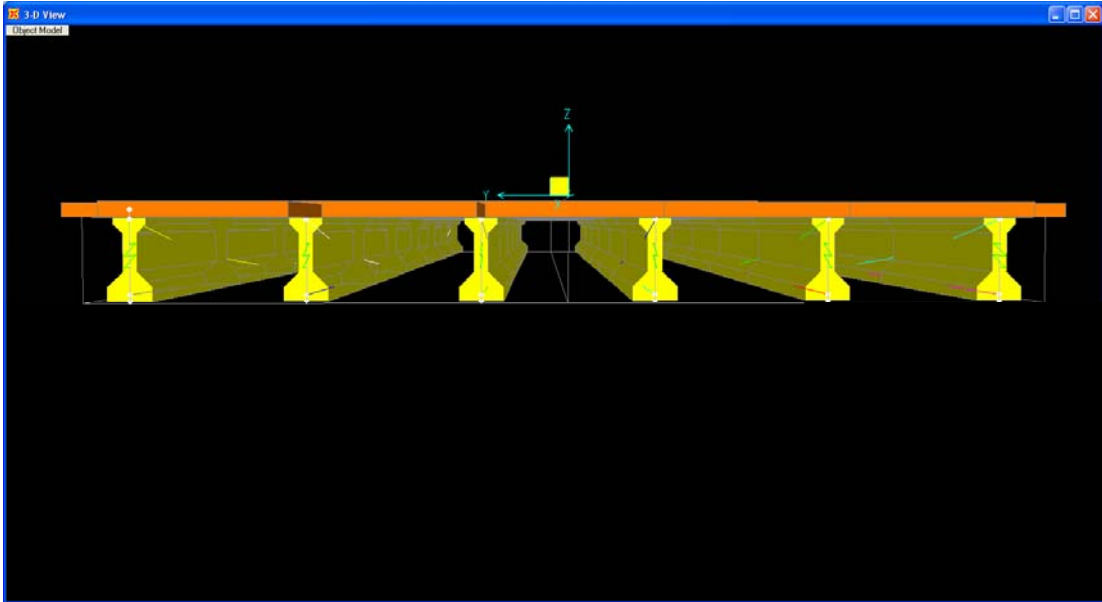


Figure 5-6: SAP2000 Model of Prestressed Concrete Beam Bridge

5.4 Apply Attack Scenarios to PC Beam Bridge Model

Using the procedure outlined in Chapter 4, the static equivalent loads of each attack scenario are calculated. Table 5-3 displays these calculations for Attack Scenario 1 as an example. All five attack scenario's calculations can be found in the Appendix. First, the coordinates of the automatically generated joints along the concrete beams are entered. Next, the distance in the plane of the bridge deck is found between the blast centroid and each bridge joint, denoted as X . Using X and the height of the blast (Z), the distance from the blast centroid to each joint (D) and the angle of incidence (θ_i) is calculated. Entering the values of D and θ_i into AT-Blast yields the static pressure at each joint. Using the tributary area method, the pressure is resolved into joint loads. In the tables below, the pressures highlighted in yellow are greater than or equal to 200 psi, so these pressures' corresponding joint loads are applied to the PC beam bridge model.

Table 5-3: Attack Scenario 1 (674 lbs TNT) Static Equivalent Load Calculations

	Joint No.	Coord. Relative to Origin		X (ft)	Z (ft)	D (ft)	θ_i (°)	Pressure (psi)	Tributary Area (ft ²)	Load on Joint (K)
		x	y							
PC Beam 1	1	0	17.92	38	4	39	84	59.19	27.50	234
	2	10	17.92	30	4	30	82	119.43	55.00	946
	3	20	17.92	23	4	23	80	233.64	55.00	1850
	4	30	17.92	18	4	19	78	312.75	55.00	2477
	5	40	17.92	19	4	19	78	312.75	55.00	2477
	6	50	17.92	24	4	24	81	197.09	55.00	1561
	7	60	17.92	32	4	32	83	100.12	27.50	396
PC Beam 2	1	0	10.75	36	4	36	84	73.51	35.83	379
	2	10	10.75	26	4	27	81	150.43	71.67	1552
	3	20	10.75	18	4	18	77	321.06	71.67	3313
	4	30	10.75	11	4	12	71	784.48	71.67	8096
	5	40	10.75	12	4	13	72	668.49	71.67	6899
	6	50	10.75	19	4	20	78	306.30	71.67	3161
	7	60	10.75	28	4	28	82	137.49	35.83	709
PC Beam 3	1	0	3.58	34	4	34	83	86.82	35.83	448
	2	10	3.58	24	4	25	81	173.95	71.67	1795
	3	20	3.58	14	4	15	75	472.39	71.67	4875
	4	30	3.58	5	4	7	53	7869.88	71.67	81217
	5	40	3.58	7	4	8	60	3487.37	71.67	35990
	6	50	3.58	16	4	17	76	365.83	71.67	3775
	7	60	3.58	26	4	27	81	150.43	35.83	776
PC Beam 4	1	0	-3.58	34	4	34	83	86.82	35.83	448
	2	10	-3.58	24	4	25	81	173.95	71.67	1795
	3	20	-3.58	14	4	15	75	472.39	71.67	4875
	4	30	-3.58	5	4	7	53	7869.88	71.67	81217
	5	40	-3.58	7	4	8	60	3487.37	71.67	35990
	6	50	-3.58	16	4	17	76	365.83	71.67	3775
	7	60	-3.53	26	4	27	81	150.43	35.83	776
PC Beam 5	1	0	-10.75	36	4	36	84	73.51	35.83	379
	2	10	-10.75	26	4	27	81	150.43	71.67	1552
	3	20	-10.75	18	4	18	77	321.06	71.67	3313
	4	30	-10.75	11	4	12	71	784.48	71.67	8096
	5	40	-10.75	12	4	13	72	668.49	71.67	6899
	6	50	-10.75	19	4	20	78	306.30	71.67	3161
	7	60	-10.75	28	4	28	82	137.49	35.83	709
PC Beam 6	1	0	-17.92	38	4	39	84	59.19	27.50	234
	2	10	-17.92	30	4	30	82	119.43	55.00	946
	3	20	-17.92	23	4	23	80	233.64	55.00	1850
	4	30	-17.92	18	4	19	78	312.75	55.00	2477
	5	40	-17.92	19	4	19	78	312.75	55.00	2477
	6	50	-17.92	24	4	24	81	197.09	55.00	1561
	7	60	-17.92	32	4	32	83	100.12	27.50	396

Figure 5-7 shows the static equivalent joint loads for Attack Scenario 1 applied to the prestressed concrete beam bridge model in SAP2000.

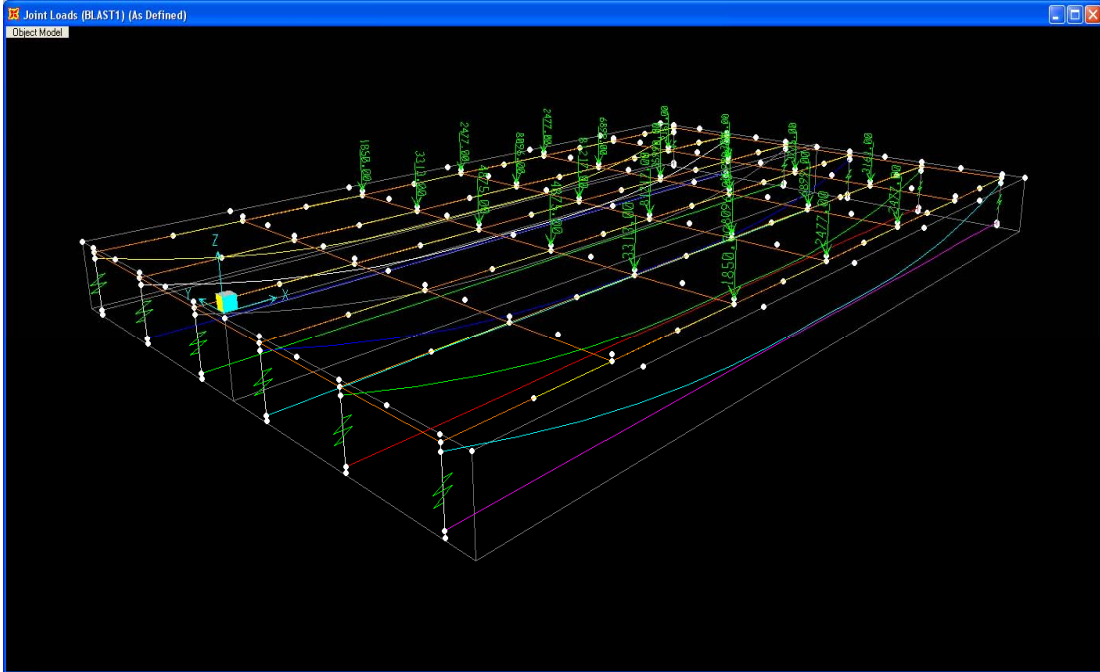


Figure 5-7: Attack Scenario 1 (674 lbs TNT) Static Equivalent Joint Loads

5.5 Analyze Structural Response

Now that the equivalent static loads of the blast are applied to the bridge model, the analysis is run. SAP2000's nonlinear static analysis output shows the performance of structural members' plastic hinges. The nodes are color-coded, as shown in Figure 4-8, to represent the hinge's state on the moment-rotation or force-deformation curve.

The analysis saves multiple response steps. Figures 5-8 through 5-12 show the final response steps for each attack scenario.

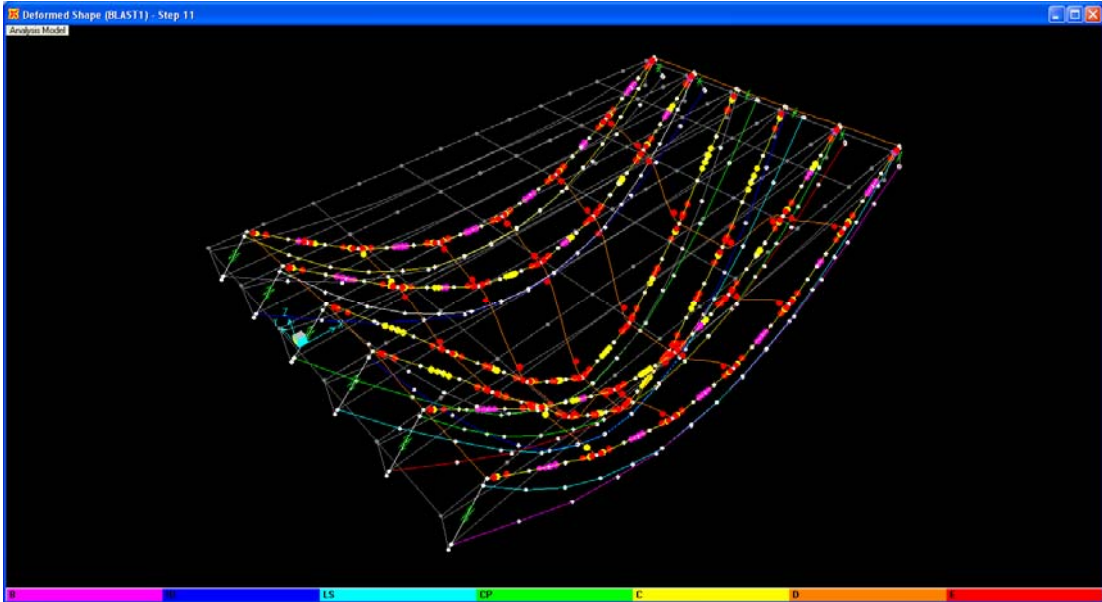


Figure 5-8: Attack Scenario 1 Response (Step 11)

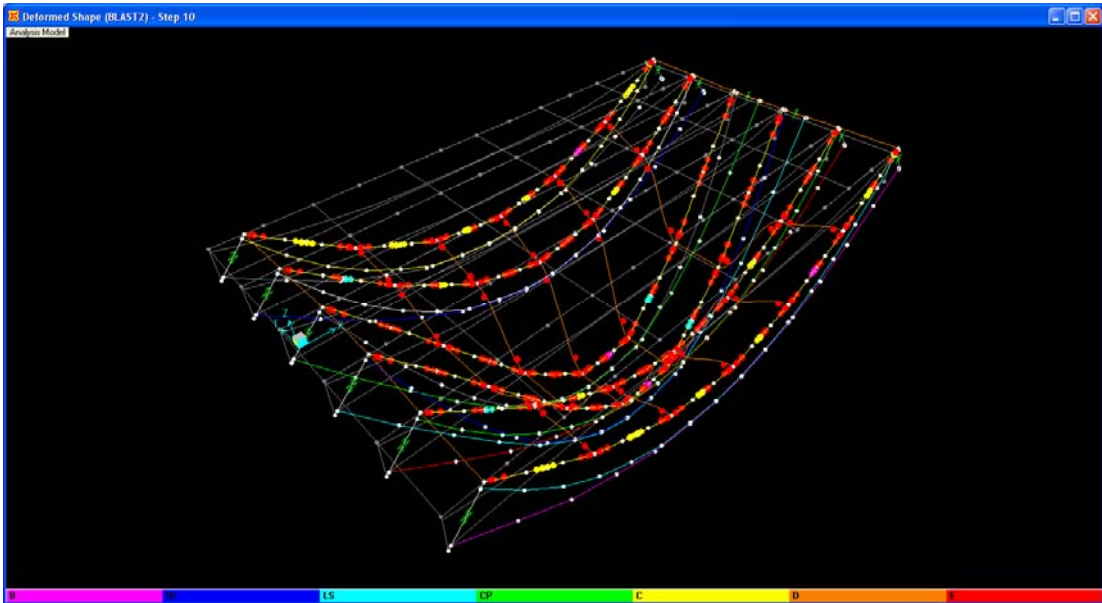


Figure 5-9: Attack Scenario 2 Response (Step 11)

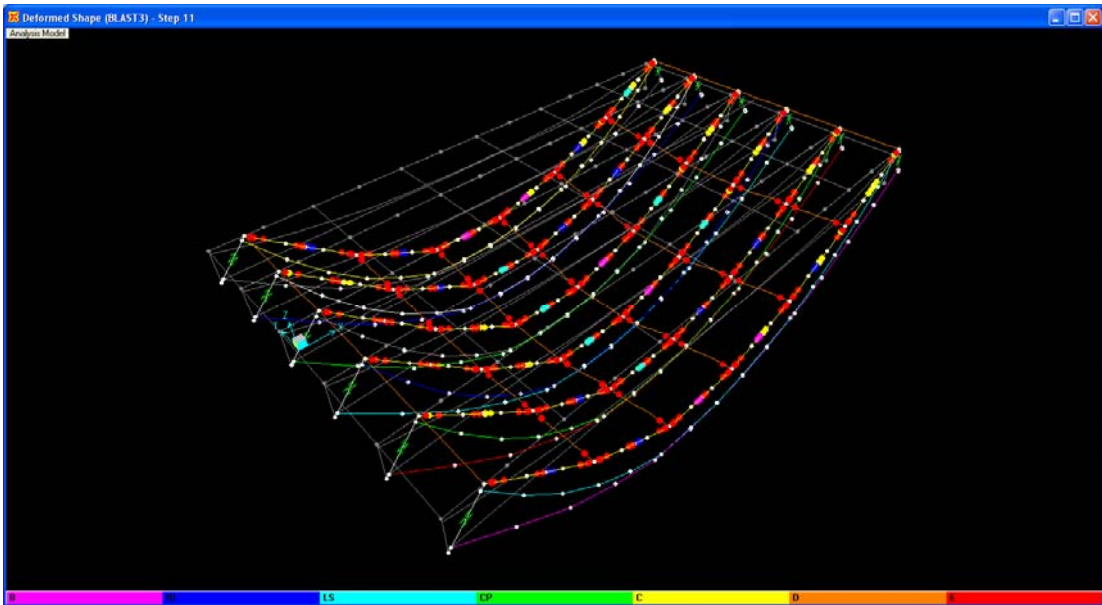


Figure 5-10: Attack Scenario 3 Response (Step 11)

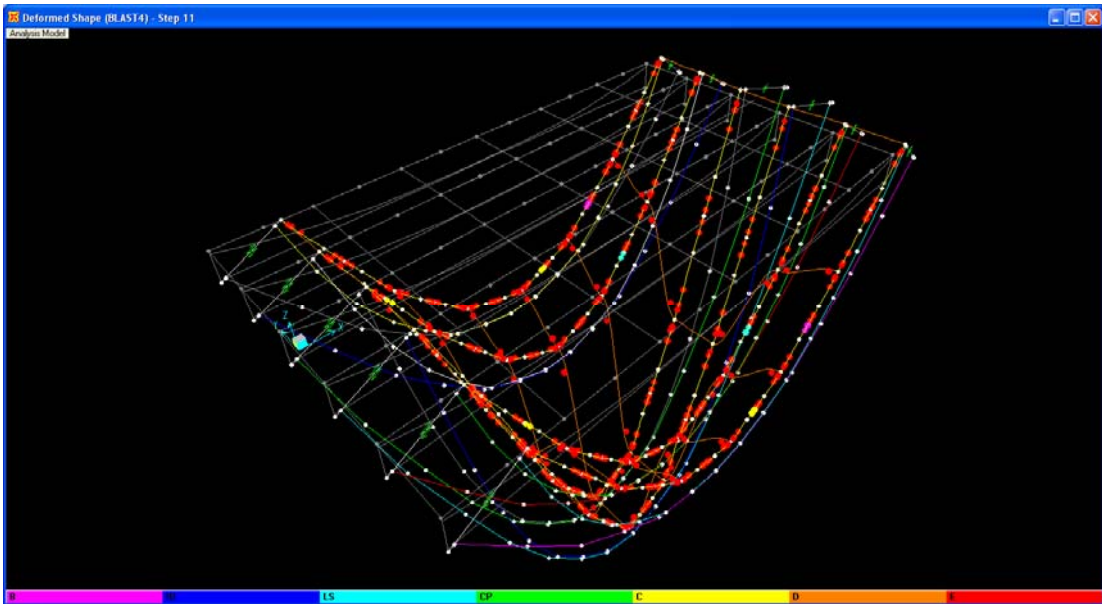


Figure 5-11: Attack Scenario 4 Response (Step 11)

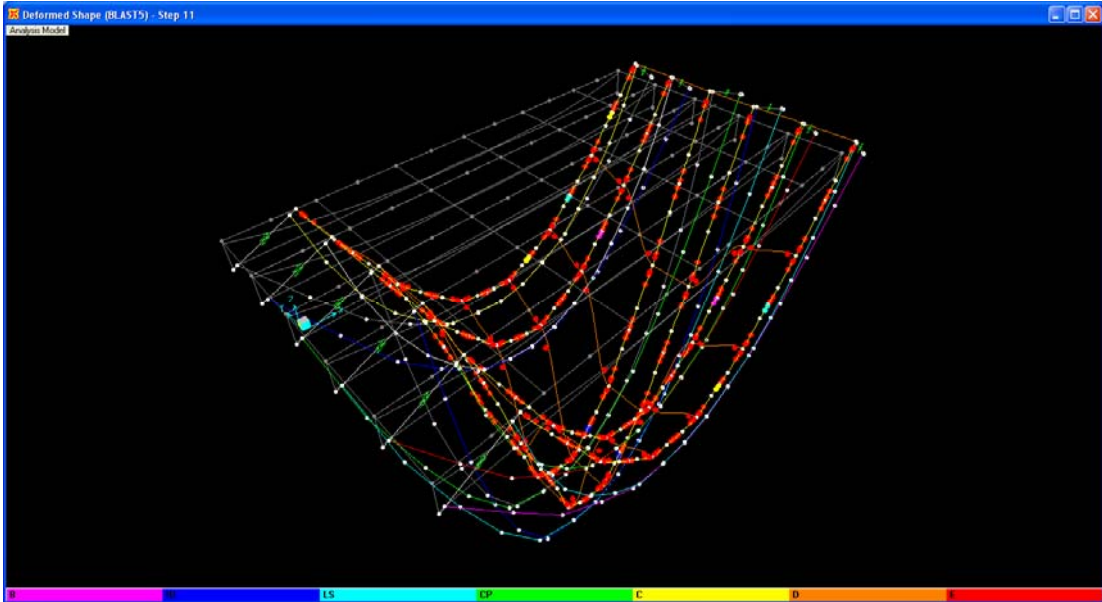


Figure 5-12: Attack Scenario 5 Response (Step 11)

5.6 Consequence Assessment

For the prestressed concrete beam bridge, the consequences are estimated using the method described in Chapter 4.5.

5.6.1 Structural Damage

Figures 5-8 through 5-12 reveal that the PC beam bridge experiences total failure in every attack scenario. Therefore, the bridge will have to be replaced. This simplifies the quantification of damaged areas by performance levels. Table 5-4 summarizes the structural damage and associated costs.

Table 5-4: PC Beam Bridge Structural Damage Costs

Attack Scenario (i)	Damaged Area by Performance Level (ft ²)			Structural Damage Cost (\$) (C _{i,s}) ^{PC}	
	≥ IO	≥ LS	≥ CP	Lower Bound	Upper Bound
1	-	-	2,380	476,000	618,800
2	-	-	2,380	476,000	618,800
3	-	-	2,380	476,000	618,800
4	-	-	2,380	476,000	618,800
5	-	-	2,380	476,000	618,800

5.6.2 Casualties

Based on the peak hour traffic data, the number of vehicles on the 60' bridge at any time (V_{peak}) is four vehicles. Equations 4.5 and 4.6 yield the estimated cost of casualties, as shown in Table 5-5.

Table 5-5: Cost of Casualties for PC Beam Bridge

Attack Scenario (i)	Failure Ratio (F _i) ^{PC}	(F _i)*V _{peak} (vehicles)	Cost of Casualties (\$) (C _{i,c}) ^{PC}	
			Lower Bound	Upper Bound
1	100%	4	0	14,400,000
2	100%	4	0	14,400,000
3	100%	4	0	14,400,000
4	100%	4	0	14,400,000
5	100%	4	0	14,400,000

5.6.3 Downtime

Using the Failure Ratio and bridge replacement times, Equations 4.7 and 4.8 are used to calculate upper and lower limit of bridge downtime for each attack scenario, as Table 5-6 displays. Equations 4.9 - 4.12 calculate the cost ranges for toll revenue loss and user delay. The results are shown in Table 5-7.

Table 5-6: PC Beam Bridge Downtime

Attack Scenario (i)	Failure Ratio $(F_i)^{PC}$	Downtime (days) $(D_i)^{PC}$	
		Lower Bound	Upper Bound
1	100%	60	120
2	100%	60	120
3	100%	60	120
4	100%	60	120
5	100%	60	120

Table 5-7: PC Beam Bridge Downtime Costs

Attack Scenario (i)	Lost Toll Revenue (\$) $(C_{i,D1})^{PC}$		User Detour Cost (\$) $(C_{i,D2})^{PC}$	
	Lower Bound	Upper Bound	Lower Bound	Upper Bound
1	3,600,000	7,200,000	67,500,000	135,000,000
2	3,600,000	7,200,000	67,500,000	135,000,000
3	3,600,000	7,200,000	67,500,000	135,000,000
4	3,600,000	7,200,000	67,500,000	135,000,000
5	3,600,000	7,200,000	67,500,000	135,000,000

5.6.4 Total Consequences for PC Beam Bridge

Equations 4.15 and 4.16 calculate the expected cost of the consequences $E[(C_i)^{PC}]$ and standard deviation $(\sigma_i)^{PC}$ for each attack scenario. Finally, the expected consequence cost, $E[C^{PC}]$, and standard deviation (σ^{PC}) for the prestressed concrete beam bridge type is estimated using Equations 4.17 and 4.18. Table 5-8 summarizes these consequence costs.

Table 5-8: PC Beam Bridge Consequence Costs

i	Consequence	Cost (\$)		Mean (\$) (C _i) ^{PC}	Std Dev (\$) (σ _i) ^{PC}
		Lower Bound	Upper Bound		
1	Structural Damage	476,000	618,800	547,400	41,223
	Casualties	0	14,400,000	7,200,000	4,156,922
	Downtime	71,100,000	142,200,000	106,650,000	20,524,802
	E[(C₁)^{PC}]			114,397,400	20,941,566
2	Structural Damage	476,000	618,800	547,400	41,223
	Casualties	0	14,400,000	7,200,000	4,156,922
	Downtime	71,100,000	142,200,000	106,650,000	20,524,802
	E[(C₂)^{PC}]			114,397,400	20,941,566
3	Structural Damage	476,000	618,800	547,400	41,223
	Casualties	0	14,400,000	7,200,000	4,156,922
	Downtime	71,100,000	142,200,000	106,650,000	20,524,802
	E[(C₃)^{PC}]			114,397,400	20,941,566
4	Structural Damage	476,000	618,800	547,400	41,223
	Casualties	0	14,400,000	7,200,000	4,156,922
	Downtime	71,100,000	142,200,000	106,650,000	20,524,802
	E[(C₄)^{PC}]			114,397,400	20,941,566
5	Structural Damage	476,000	618,800	547,400	41,223
	Casualties	0	14,400,000	7,200,000	4,156,922
	Downtime	71,100,000	142,200,000	106,650,000	20,524,802
	E[(C₅)^{PC}]			114,397,400	20,941,566
Expected Consequence Costs, E[C^{PC}]				\$114,397,400	-

6.0 CASE STUDY 2: STEEL PLATE GIRDER (SG) BRIDGE

Case Study 2 demonstrates the proposed method outlined in Chapters 3 and 4 on a three-span continuous steel plate girder (SG) bridge. Before the method is demonstrated, general information about the span's geometry and material properties is provided.

6.1 Geometry and Material Properties

The bridge plans were obtained by the agency responsible for the long-span bridge used in this study. The bridge was designed using AASHTO's *Standard Specifications for Highway Bridges* for an HS20-44 live load. The SG bridge is a continuous three-span bridge. Each span is 202' long, totaling 606'. The 6.5'' concrete deck slab is 38'4'' wide. There are two steel built-up plate girders and five rolled beam stringers. The plate girders are spaced 28' center-to-center. Between the plate girders, the interior stringers are spaced 7' apart. The exterior stringers are 4'7'' center-to-center from the plate girders. Figure 6-1 shows the bridge's typical section and girder/stringer numbering scheme.

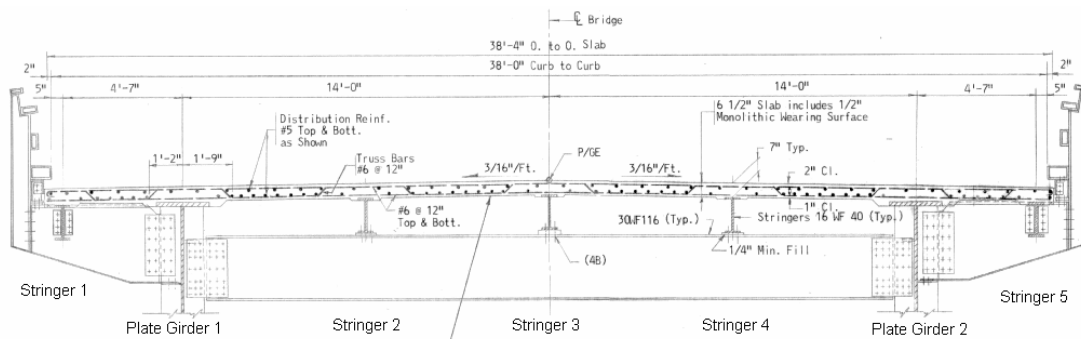


Figure 6-1: Continuous Steel Plate Girder Bridge Typical Section

6.1.1 Steel Plate Girders and Stringers

All structural steel sections are A36 carbon steel, and the concrete deck lightweight concrete. The stringers are W16x40 rolled beams, and the plate girder sections vary along the bridge length. There are three different plate girder sections, each having a constant web plate depth of 120". The web thickness varies along the plate girder from $\frac{3}{8}$ " to $\frac{7}{16}$ ". The plate girder flange plates are 30" wide, with a thickness that ranges from $1\frac{5}{16}$ " to $2\frac{1}{4}$ ". The Appendix also contains a girder elevation view that displays the plate girder dimension variations.

6.2 Attack Scenarios

The five attack scenarios for the steel plate girder bridge are restated in Table 6-1. Each scenario is characterized by a charge weight of TNT and location along the bridge's 606' length. As explained in Chapter 4, the charge weight and location were assigned probability distributions and randomly generated.

Table 6-1: Attack Scenarios for Steel PG Bridge

Attack Scenario	Charge Weight (lbs TNT)	Blast Location Along Bridge Length (ft)
1	674	347
2	1009	444
3	437	130
4	2911	361
5	1821	209

6.3 Bridge Model

A model of the three-span continuous plate girder bridge is created in SAP2000. The "Bridge Wizard" module aided in defining the typical section and materials of the bridge. The Bridge Wizard's step by step guide allows the user to

choose a section and input the geometry and materials of the bridge. At a minimum, a bridge layout line, deck section, and bridge object must be defined. The module automatically meshes the elements and creates a finite element model. Joints are automatically created along the centerlines of the plate girders and stringers.

6.3.1 Bridge Deck

Since this study is concerned with the response of the major structural elements (e.g. plate girders, stringers, deck), the deck is modeled using frame elements. By defining the deck as frame elements, nonlinear hinges can be assigned, so the deck will exhibit nonlinear plastic behavior. In order to properly model the bridge deck and show transverse and longitudinal stiffness, a grid of frame elements is created. The deck frame elements are connected to the automatically generated joints along the plate girder and stringer centerlines. Four frame elements were defined, two in the transverse direction and three in the longitudinal direction. Deck Sections 1 and 2 are in the transverse direction, while Deck Sections 3 - 5 are in the longitudinal direction. Figure 6-2 shows a cross section of the deck frame elements.

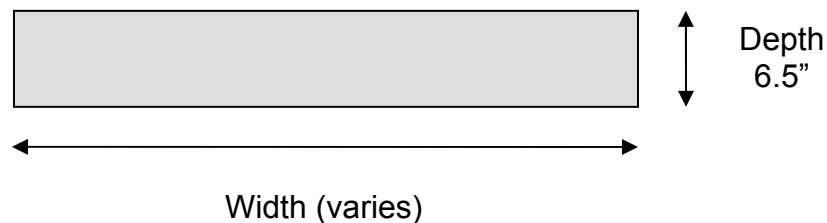


Figure 6-2: Plate Girder Bridge Deck Section

The width of the deck sections are calculated via the girder tributary area concept. First, a few distances must be defined. The distance between joints along the centerline of the plate girders and stringers in the longitudinal direction is

designated as “b” and equal to 8.5’ (102”). The distance between the plate girders and exterior stringers is designated as “s₁” and equal to 4’7” (55”). The spacing between the plate girders and interior stringers in the transverse direction is designated as “s₂” and equal to 7’ (84”). The overhang distance between the exterior stringers and the bridge edge is designated as “o” and equal to 7”.

Deck Section 1 is along the end of the bridge in the transverse direction. The width of this section is equal to half the distance between joints along the plate girders and stringers, or b/2. Deck Section 2 is also in the transverse direction, with a width equal to the spacing between joints, or b. Deck Section 3 falls in the longitudinal direction along the exterior stringers, so the width is defined as the overhang distance plus half the beam spacing, or (o + s₁/2). Deck Section 4 elements, also in the longitudinal direction, are along the plate girders with a width equal to (s₁+s₂)/2. Finally, Deck Section 5 elements are in the longitudinal direction along the interior stringers, with a width equal to their center-to-center spacing, or s₂. Table 6-2 summarizes the deck frame elements used to model the bridge deck, and Figure 6-3 shows a plan view of the deck “grid” at the left end of the bridge model.

Table 6-2: Continuous Steel Plate Girder Bridge Deck Elements

Deck Section	Direction	Depth (in)	Width (in)	
1	Transverse	6.5	b/2	51
2	Transverse	6.5	b	102
3	Longitudinal	6.5	o + (s ₁ /2)	34.5
4	Longitudinal	6.5	(s ₁ +s ₂)/2	69.5
5	Longitudinal	6.5	s ₂	84

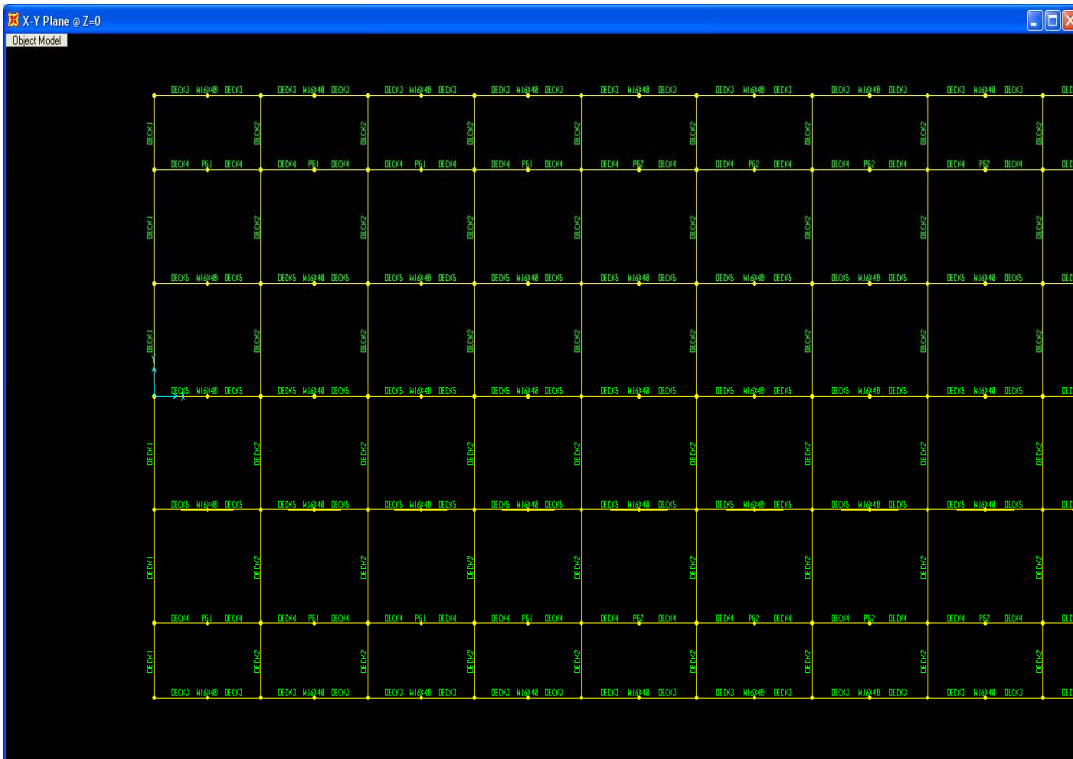


Figure 6-3: Grid of Deck Frame Elements for PG Bridge

6.3.2 Abutments and Bents

The bridge is modeled with abutments at both ends and two intermediate bents. Each bent consists of a concrete cap beam and two concrete columns, all having a rectangular cross-section. The cap beam is 34' long with a 6' depth and 7' width. The columns are approximately 70' in height, spaced 28' feet apart. They each have a depth of 7' and a width of 6'. Figure 6-4 shows a plan view of the bent cap.

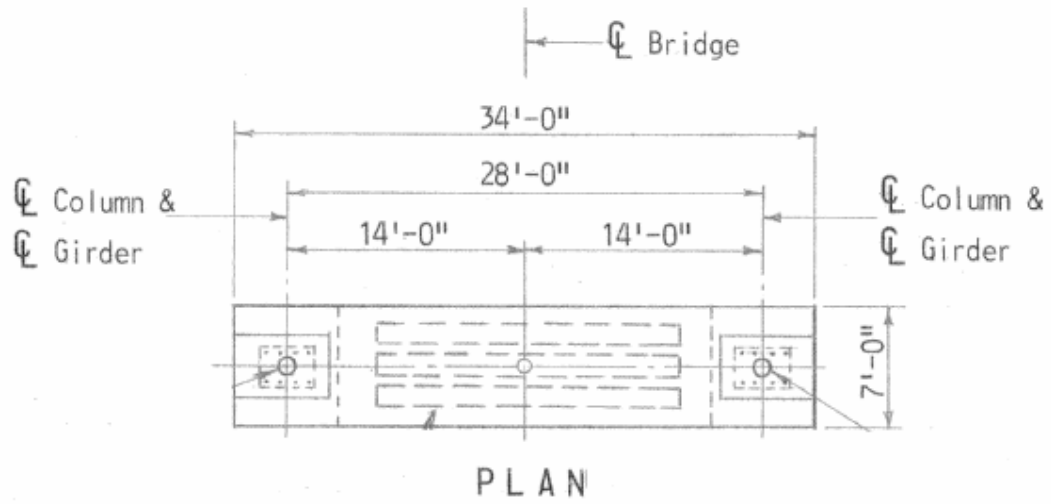


Figure 6-4: Bent Cap Beam

6.3.3 Completed Model

Figure 6-5 shows a 3D view of the model for the 606' continuous plate girder bridge.

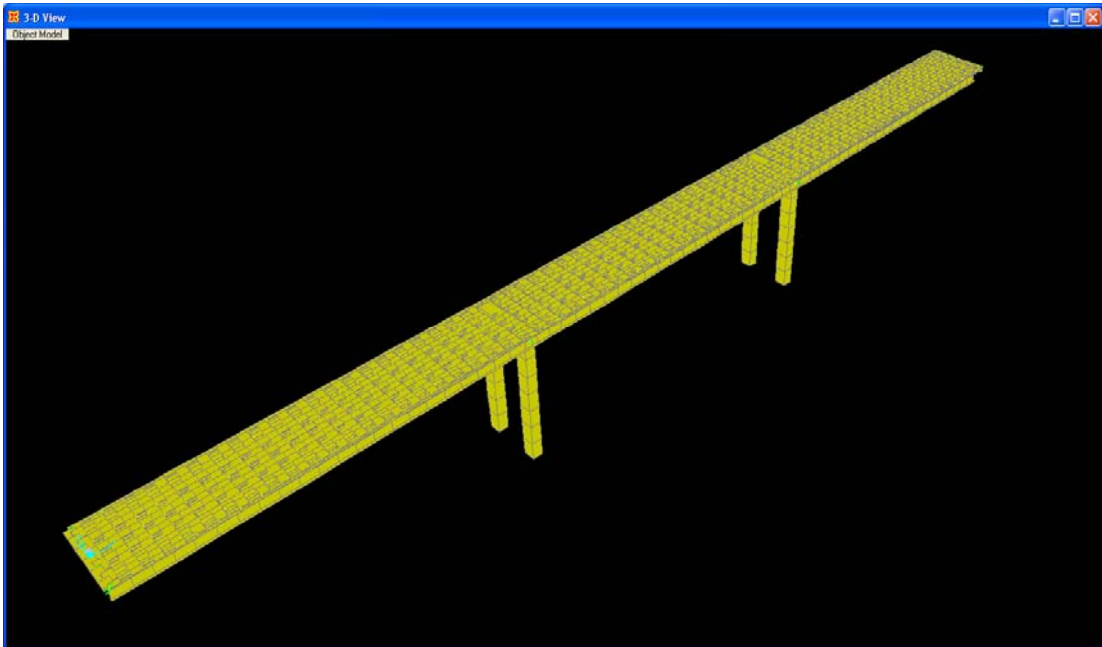


Figure 6-5: SAP2000 Model of Continuous Steel PG Bridge

6.4 Apply Attack Scenarios to SG Bridge Model

Using the procedure outlined in Chapter 4, the static equivalent loads of each attack scenario are calculated. Table 6-3 displays these calculations for Attack Scenario 1 as an example. All five attack scenario's calculations can be found in the Appendix. First, the coordinates of the automatically generated joints along the plate girders and stringers are entered. Next, the distance (in the plane of the bridge deck) is found between the blast centroid and each bridge joint, denoted as X . Using X and the height of the blast (Z) the distance from the blast centroid to each joint (D) and the angle of incidence (θ_i) is calculated. Entering the values of D and θ_i into AT-Blast yields the static pressure at each joint. Using the tributary area method, the pressure is resolved into joint loads. In the tables below, the pressures highlighted in yellow are greater than or equal to 200 psi, so these pressures' corresponding joint loads are applied to the PG bridge model.

Table 6-3: Attack Scenario 1 (674 lbs TNT) Static Equivalent Load Calculations⁶

	Joint No.	Coord. Relative to Origin		X (ft)	Z (ft)	D (ft)	θ_i (°)	Pressure (psi)	Tributary Area (ft ²)	Load on Joint (K)
		x	y							
Stringer 1	35	312.75	18.58	39	4	39	84	59.19	27.98	239
	36	322.5	18.58	31	4	31	83	107.86	27.98	435
	37	332.25	18.58	24	4	24	80	205.34	27.98	827
	38	342	18.58	19	4	20	78	306.30	27.98	1234
	39	351.75	18.58	19	4	20	78	306.30	27.98	1234
	40	361.5	18.58	24	4	24	80	205.34	27.98	827
	41	371.25	18.58	31	4	31	83	107.86	27.98	435
	42	381	18.58	39	4	39	84	59.19	25.00	213
Plate Girder 1	35	312.75	14	37	4	37	84	68.22	56.45	555
	36	322.5	14	28	4	29	82	128.05	56.45	1041
	37	332.25	14	20	4	21	79	290.81	56.45	2364
	38	342	14	15	4	15	75	472.39	56.45	3840
	39	351.75	14	15	4	15	75	472.39	56.45	3840
	40	361.5	14	20	4	21	79	290.81	56.45	2364
	41	371.25	14	28	4	28	82	137.49	56.45	1118
	42	381	14	37	4	37	84	68.22	50.43	495
Stringer 2	35	312.75	7	35	4	35	83	81.09	68.25	797
	36	322.5	7	25	4	26	81	161.43	68.25	1587
	37	332.25	7	16	4	17	76	365.83	68.25	3595
	38	342	7	9	4	9	65	1833.63	68.25	18021
	39	351.75	7	8	4	9	65	1833.63	68.25	18021
	40	361.5	7	16	4	17	76	365.83	68.25	3595
	41	371.25	7	25	4	26	81	161.43	68.25	1587
	42	381	7	35	4	35	83	81.09	60.97	712
Stringer 3	35	312.75	0	34	4	34	83	86.82	68.25	853
	36	322.5	0	25	4	25	81	173.85	68.25	1709
	37	332.25	0	15	4	15	75	472.39	68.25	4643
	38	342	0	5	4	6	51	11320.26	68.25	111256
	39	351.75	0	5	4	6	50	12000.89	68.25	117945
	40	361.5	0	15	4	15	75	472.39	68.25	4643
	41	371.25	0	24	4	25	81	173.95	68.25	1710
	42	381	0	34	4	34	83	86.82	60.97	762

Figure 6-6 shows Attack Scenario 1’s static equivalent joint loads applied to the plate girder bridge model. Figures for all five attack scenario’s loading can be found in the Appendix.

⁶ Because of the symmetry of the bridge’s typical section, the load calculations for Stringer 1, Plate Girder 1, and Stringer 2 also apply to Stringer 5, Plate Girder 2, and Stringer 4, respectively.

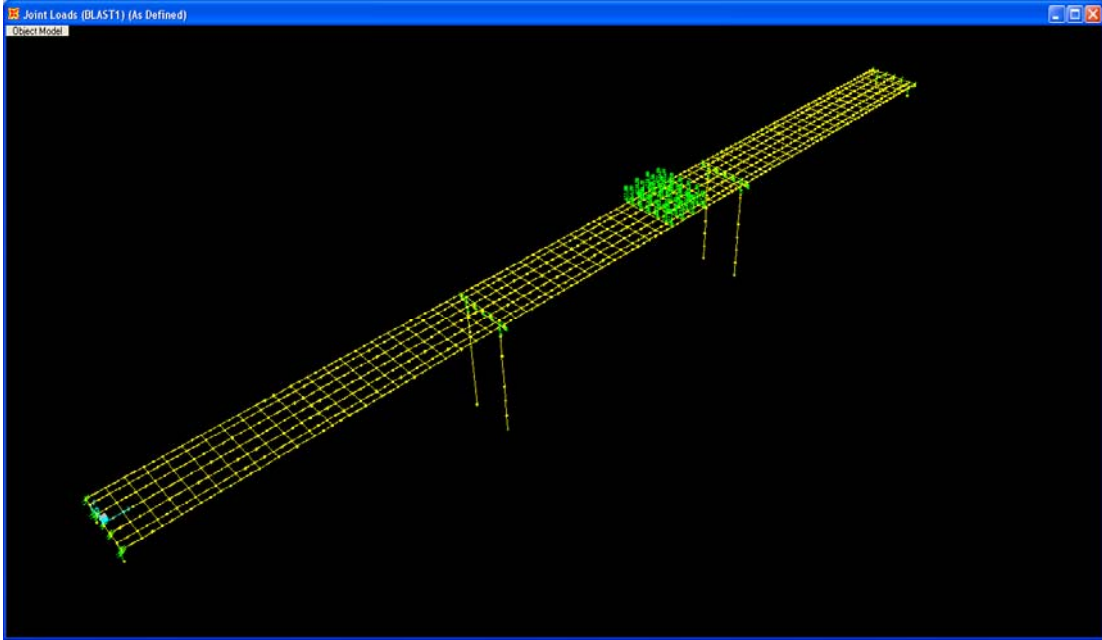


Figure 6-6: Attack Scenario 1 (674 lbs TNT) Static Equivalent Joint Loads

6.5 Analyze Structural Response

Now that the equivalent static loads of the blast are applied to the bridge model, the analysis can run. SAP2000's nonlinear static analysis output shows the performance of the structural members' plastic hinges. The nodes are color-coded, as shown in Figure 4-8, to represent the hinge's state on the moment-rotation or force-deformation curve. The analysis saves multiple response steps. Figures 6-6 through 6-10 show the final response steps for each attack scenario.

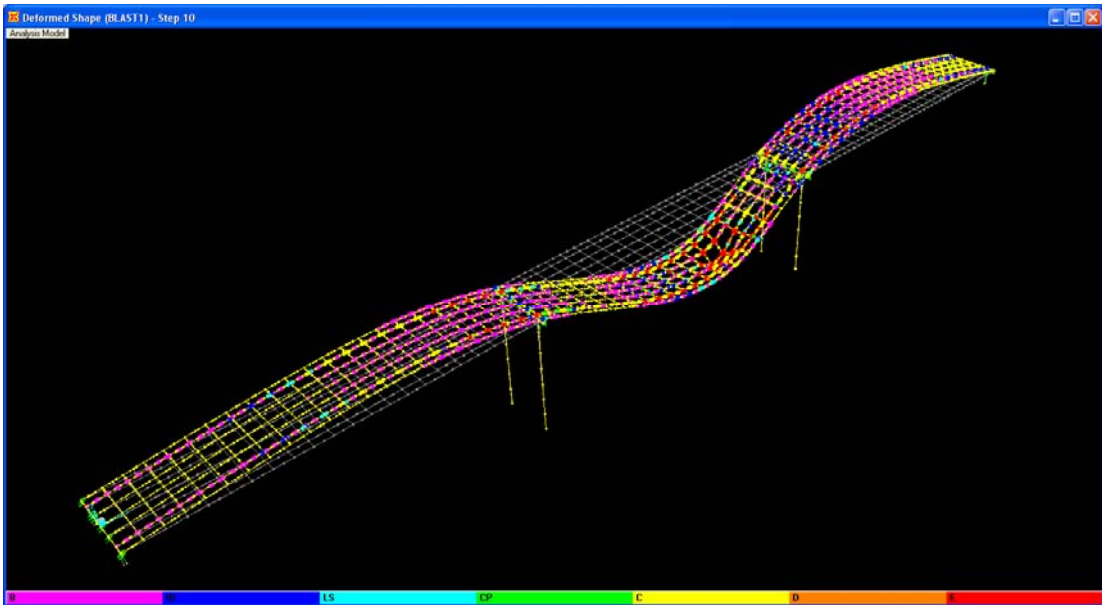


Figure 6-6: Attack Scenario 1 Response (Step 10)

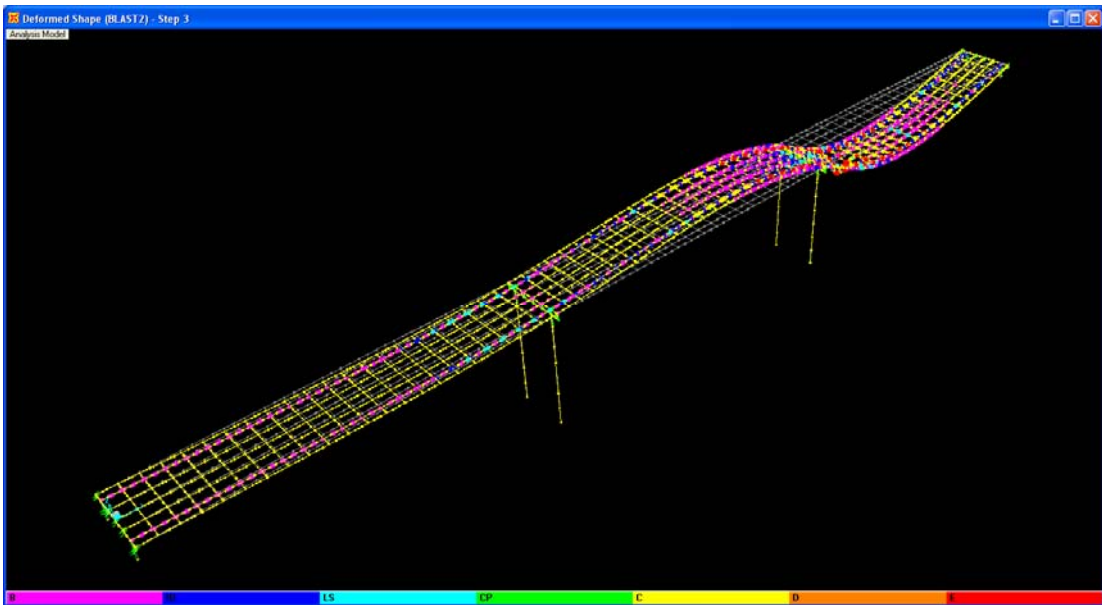


Figure 6-7: Attack Scenario 2 Response (Step 3)

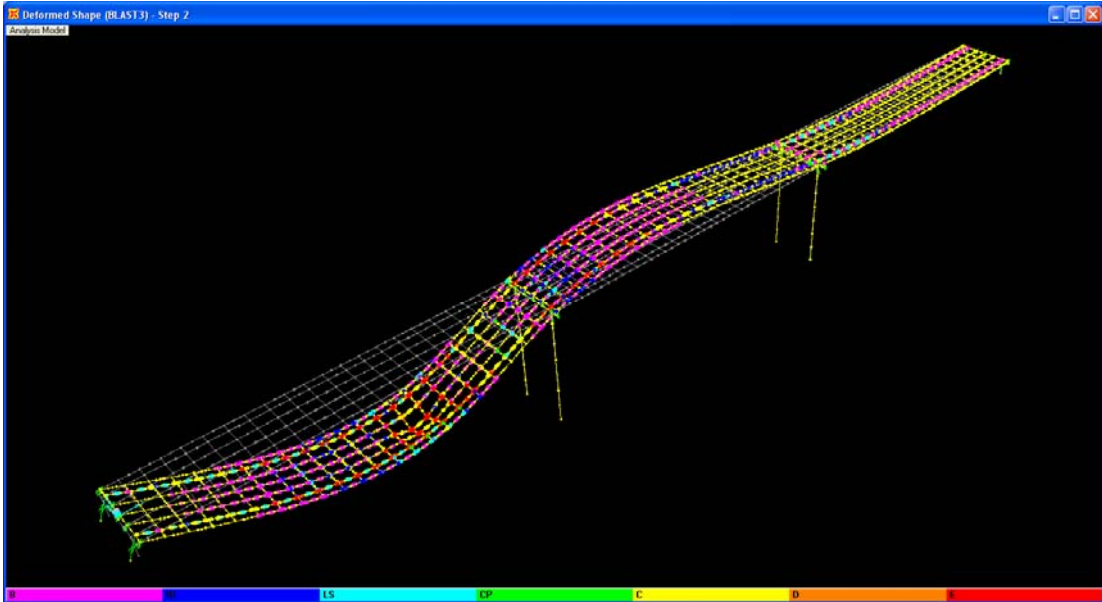


Figure 6-8: Attack Scenario 3 Response (Step 2)

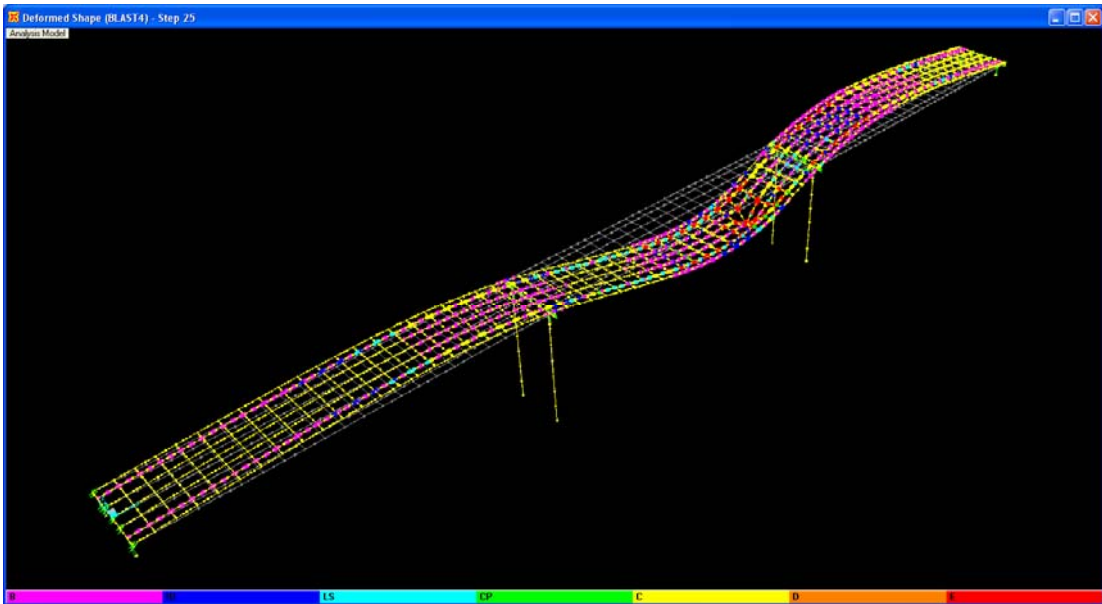


Figure 6-9: Attack Scenario 4 Response (Step 25)

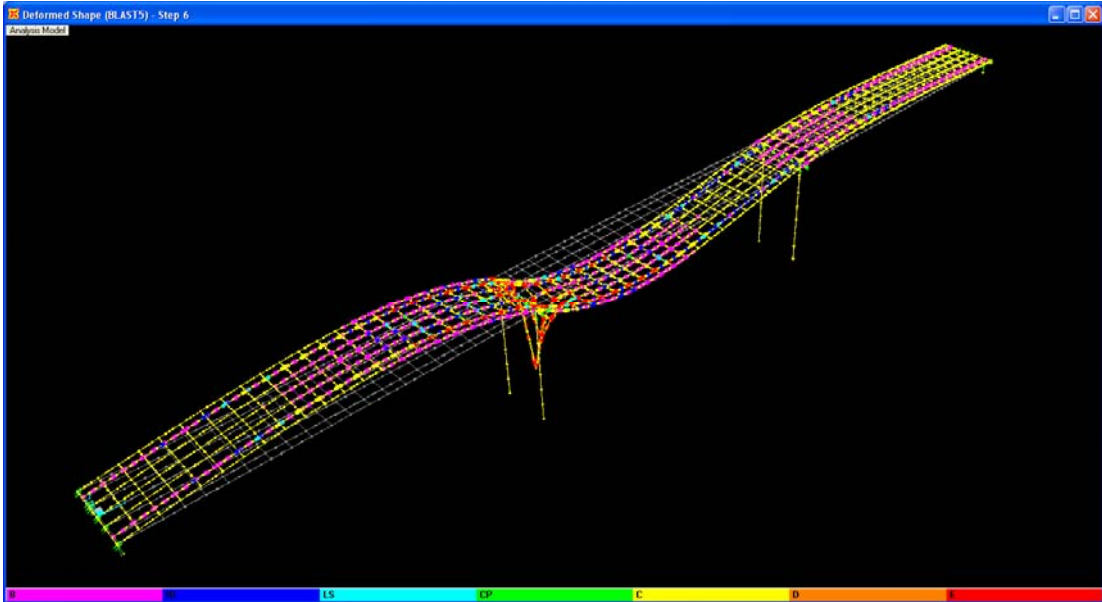


Figure 6-10: Attack Scenario 5 Response (Step 6)

6.6 Consequence Assessment

For the continuous steel plate girder bridge, the consequences are estimated using the method described in Section 4.5.

6.6.1 Structural Damage

Figures 6-6 through 6-10 reveal that SG bridge experiences damage in all three performance levels. Table 6-4 summarizes the structural damage and associated costs, calculated using Equations 4.2 and 4.3.

Table 6-4: SG Bridge Structural Damage Costs

Attack Scenario (i)	Damaged Area by Performance Level (ft ²)			Structural Damage Cost (\$) (C _{i,s}) ^{SG}	
	≥ IO	≥ LS	≥ CP	Lower Bound	Upper Bound
1	3,310	540	3,930	\$1,206,720	\$1,860,360
2	2,861	1,962	4,303	\$1,439,804	\$2,219,698
3	2,902	1,353	4,273	\$1,362,000	\$2,099,750
4	1,926	1,341	3,578	\$1,135,170	\$1,750,054
5	2,041	930	4,439	\$1,299,420	\$2,003,273

6.6.2 Casualties

Based on the peak hour traffic data, the number of vehicles on the 606' bridge at any time (V_{peak}) is 40 vehicles. Equations 4.5 and 4.6 yield the estimated cost of casualties, as shown in Table 6-5.

Table 6-5: Cost of Casualties for SG Bridge

Attack Scenario (i)	Failure Ratio (F_i) ^{SG}	$(F_i) * V_{\text{peak}}$ (vehicles)	Cost of Casualties (\$) ($C_{i,c}$) ^{SG}	
			Lower Bound	Upper Bound
1	17%	7	0	25,200,000
2	19%	7	0	25,200,000
3	18%	7	0	25,200,000
4	15%	6	0	21,600,000
5	19%	8	0	28,800,000

6.6.3 Downtime

Using the Failure Ratio and bridge replacement times, Equations 4.7 and 4.8 are used to calculate upper and lower limit of bridge downtime for each attack scenario, as Table 6-6 displays. Equations 4.9 - 4.12 calculate the cost ranges for toll revenue loss and user delay. The results are shown in Table 6-7.

Table 6-6: SG Bridge Downtime

Attack Scenario (i)	Failure Ratio (F_i) ^{SG}	Downtime (days) (D_i) ^{SG}	
		Lower Bound	Upper Bound
1	17%	31	41
2	19%	33	45
3	18%	33	44
4	15%	28	37
5	19%	34	46

Table 6-7: SG Bridge Downtime Costs

Attack Scenario (i)	Lost Toll Revenue (\$) $(C_{i,D1})^{SG}$		User Detour Cost (\$) $(C_{i,D2})^{SG}$	
	Lower Bound	Upper Bound	Lower Bound	Upper Bound
1	1,860,000	2,460,000	34,875,000	46,125,000
2	1,980,000	2,700,000	37,125,000	50,625,000
3	1,980,000	2,640,000	37,125,000	49,500,000
4	1,680,000	2,220,000	31,500,000	41,625,000
5	2,040,000	2,760,000	38,250,000	51,750,000

6.6.4 Total Consequences for Steel Plate Girder Bridge

Equations 4.15 and 4.16 calculate the expected cost of the consequences $E[(C_i)^{SG}]$ and standard deviation $(\sigma_i)^{SG}$ for each attack scenario. Finally, the expected consequence cost, $E[C^{SG}]$, and standard deviation (σ^{SG}) for the steel girder bridge type is estimated using Equations 4.17 and 4.18. Table 6-8 summarizes these consequence costs.

Table 6-8: SG Bridge Consequence Costs

i	Consequence	Cost (\$)		Mean (\$) $(C_i)^{SG}$	Std Dev (\$) $(\sigma_i)^{SG}$
		Lower Bound	Upper Bound		
1	Structural Damage	1,206,720	1,860,360	1,533,540	188,690
	Casualties	0	25,200,000	12,600,000	7,274,613
	Downtime	36,735,000	48,585,000	42,660,000	3,420,800
	$E[(C_1)^{SG}]$			56,793,540	8,040,987
2	Structural Damage	1,439,804	2,219,698	1,829,751	225,136
	Casualties	0	25,200,000	12,600,000	7,274,613
	Downtime	39,105,000	53,325,000	46,215,000	4,104,960
	$E[(C_2)^{SG}]$			60,644,751	8,355,919
3	Structural Damage	1,362,000	2,099,750	1,730,875	212,970
	Casualties	0	25,200,000	12,600,000	7,274,613
	Downtime	39,105,000	52,140,000	45,622,500	3,762,880
	$E[(C_3)^{SG}]$			59,953,375	8,192,962
4	Structural Damage	1,135,170	1,750,054	1,442,612	177,502
	Casualties	0	21,600,000	10,800,000	6,235,383
	Downtime	33,180,000	43,845,000	38,512,500	3,078,720
	$E[(C_4)^{SG}]$			50,755,112	6,956,294
5	Structural Damage	1,299,420	2,003,273	1,651,346	203,185
	Casualties	0	28,800,000	14,400,000	8,313,844
	Downtime	40,290,000	54,510,000	47,400,000	4,104,960
	$E[(C_5)^{SG}]$			63,451,346	9,274,265
Expected Consequence Costs, $E[C^{SG}]$				\$58,319,625	\$4,334,990

7.0 CASE STUDY 3: DECK CANTILEVER TRUSS (DT) BRIDGE

Case Study 3 demonstrates the proposed method outlined in Chapters 3 and 4 on a three-span deck cantilever truss (DT) bridge. Before the method's application, general information about the span's geometry, material properties, and bridge model is provided.

7.1 Geometry and Material Properties

The bridge plans were obtained by the agency responsible for the long-span bridge used in this study. The bridge was designed using AASHTO's *Standard Specifications for Highway Bridges* for an HS20-44 live load. The representative DT bridge in this case study has three spans totaling 1350' in length. There are three span arrangements that follow a repeating pattern: suspended, cantilever, anchor, and cantilever, which are shown in Figure 7-1.

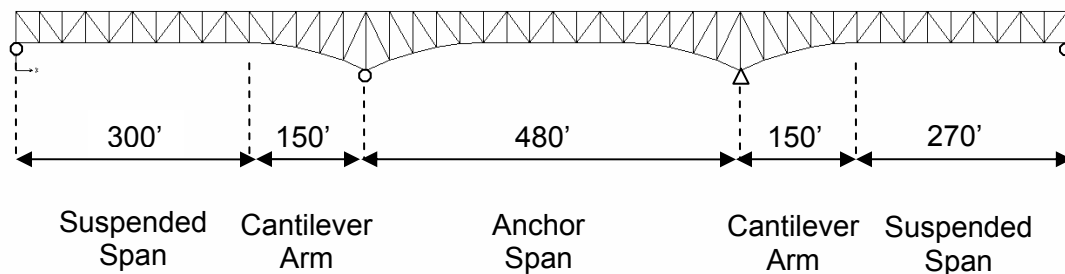


Figure 7-1: Deck Cantilever Truss Configuration

7.1.1 Truss Members

Two parallel truss structures are spaced at 28' center-to-center, one on each side of the bridge's typical section. Within each truss, the chords, vertical members, and diagonals are connected at each panel point, spaced 30' apart. The depth of the truss varies from 40' at the end of the bridge to 75' at the interior supports. All truss members are built-up plate sections, constructed of A36 carbon structural steel or high-strength low alloy structural steel. The section depths and plate thicknesses vary from member to member. The chords and vertical members consist of two web plates and two cover plates. The diagonal and some vertical members have two flange plates and one web plate. These truss member shapes are shown in Figure 7-2.

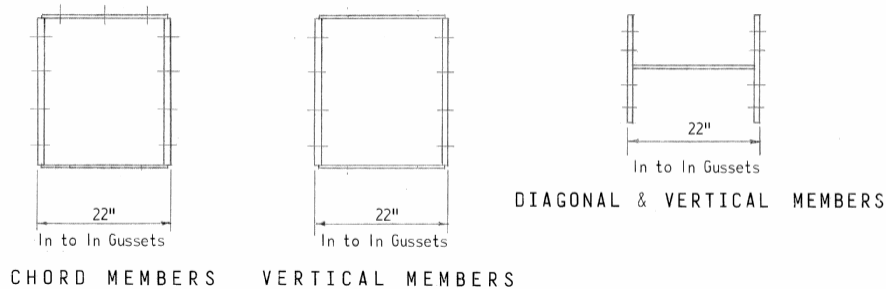


Figure 7-2: Truss Member Cross Sections

The lateral bracings and sway frames between trusses are constructed of A36 carbon steel. These members are rolled W-shape beams. The top and bottom lateral bracing members are arranged in an X-shaped pattern and connected to each panel point of the main truss. The sway frames provide further lateral stiffness by connecting the two main truss structures at every other panel point.

7.1.2 Floorbeams and Stringers

Intermediate floorbeams connect the two parallel truss structures at each panel point, which is every 30'. Six stringers are connected to the floorbeams and support the 6.5" lightweight concrete deck. The stringers are spaced 7' center-to center, which Figure 7-3 illustrates. The floorbeams are W36x160 rolled beams, while the stringers are W24x76. All floorbeams and stringers are constructed of A36 carbon structural steel.

7.2 Attack Scenarios

The five attack scenarios for the deck cantilever truss bridge are restated in Table 7-1. Each scenario is characterized by a charge weight of TNT and location along the bridge's 1350' length. As explained in Chapter 4, the charge weight and locations were assigned probability distributions and randomly generated.

Table 7-1: Attack Scenarios for DT Bridge

Attack Scenario	Charge Weight (lbs TNT)	Blast Location Along Bridge Length (ft)
1	674	773
2	1009	990
3	437	290
4	2911	803
5	1821	465

7.3 Bridge Model

A model of the deck cantilever truss bridge is created in SAP2000. A pre-formatted excel spreadsheet is used to enter the 2D truss member geometry. Then the spreadsheet is imported into the software to create the bridge model. After replicating the imported truss panel, the member sections can be defined. Then, the lateral bracing/sway frames, floor beams, and stringers are added, based on the bridge plans. All members are designated as frame elements.

7.3.1 Bridge Deck

Since this study is concerned with the response of the major structural elements (e.g. truss members, floorbeams, stringers, deck), the deck is also modeled using SAP2000 frame elements. By defining the deck as frame elements, nonlinear hinges can be assigned, so the deck will exhibit nonlinear plastic behavior. In order

to properly model the bridge deck and account for transverse and longitudinal stiffness, a grid of frame elements is created. The deck frame elements are connected to the automatically generated joints along the plate girder and stringer centerlines. Four frame elements are defined, two in the transverse direction and two in the longitudinal direction. Deck Sections 1 and 2 are in the transverse direction, while Deck Sections 3 and 4 are in the longitudinal direction. Figure 7-4 shows a cross section of the deck frame elements.

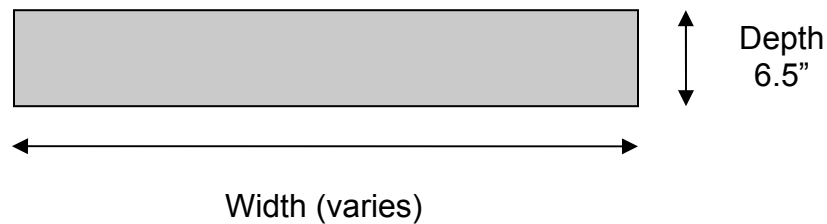


Figure 7-4: Deck Cantilever Truss Bridge Deck Section

The width of the deck sections are calculated via the tributary area method. First, a few distances must be defined. The distance between stringers in the longitudinal direction is designated as “b” and equal to 30’ (360”). The spacing between stringers is designated as “s” and equal to 7’ (84”). The overhang distance between the exterior stringers and the edge of the bridge is designated as “o” and equal to 2’4” (28”).

Deck Section 1 is along the end of the bridge in the transverse direction. The width of this section is equal to half the distance between stringers, or $b/2$. Deck Section 2 is also in the transverse direction, with a width equal to the spacing between panel points, or b . Deck Section 3 falls in the longitudinal direction along the exterior stringers, so the width is defined as the overhang distance plus half the beam spacing, or $(o + s/2)$. Finally, Deck Section 4 elements are in the longitudinal direction along

the interior stringers, with a width equal to their center-to-center spacing, or s . Table 7-2 summarizes the deck frame elements used to model the bridge deck.

Table 7-2: DT Bridge Deck Elements

Deck Section	Direction	Depth (in)	Width (in)	
1	Transverse	7	$b/2$	180
2	Transverse	7	b	360
3	Longitudinal	7	$o + s/2$	70
4	Longitudinal	7	s	84

7.3.2 Completed Model

Figure 7-5 displays a 3D view of the model for the 1350' deck cantilever truss bridge. Figure 7-6 is a zoomed-in view without extruded sections.

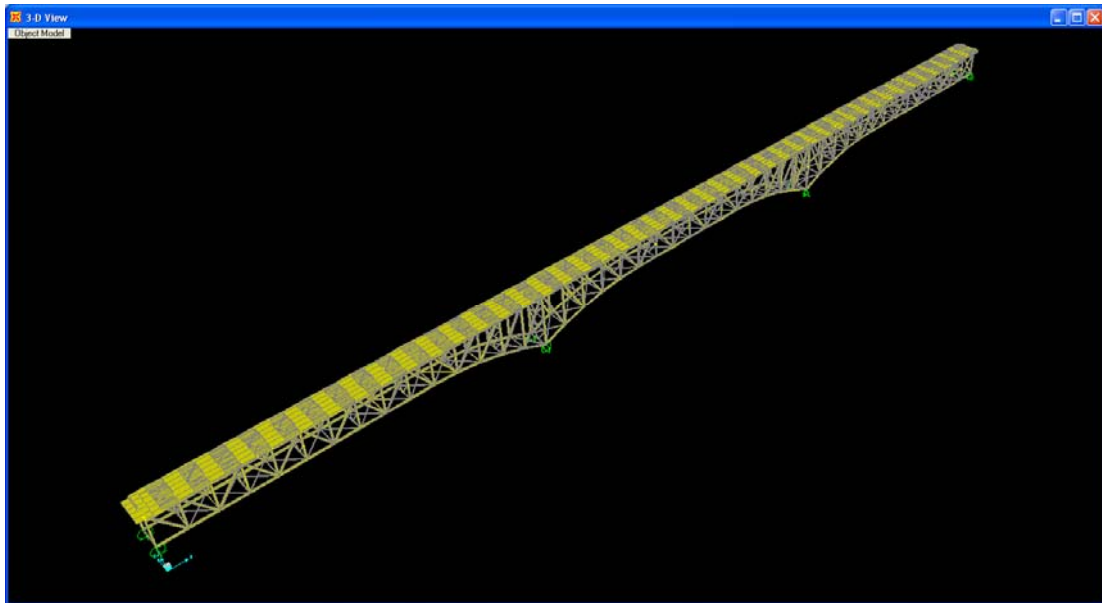


Figure 7-5: SAP2000 Model of Deck Cantilever Truss Bridge

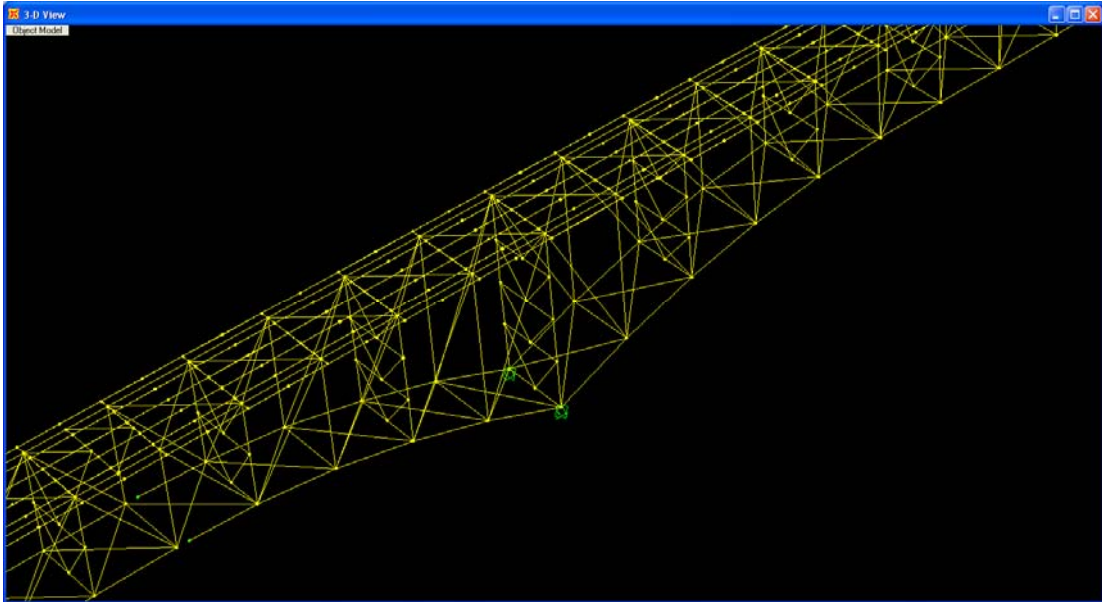


Figure 7-6: SAP2000 Model of Deck Cantilever Truss Bridge (Zoomed In)

7.4 Apply Attack Scenarios to DT Bridge Model

Using the procedure outlined in Chapter 4, the static equivalent loads of each attack scenario are calculated. Table 7-3 displays these calculations for Attack Scenario 1 as an example. All five attack scenario's calculations can be found in the Appendix. First, the coordinates of the joints between deck elements are entered. Next, the distance (in the plane of the bridge deck) is found between the blast centroid and each bridge joint, denoted as X . Using X and the height of the blast (Z) the distance from the blast centroid to each joint (D) and the angle of incidence (θ_i) is calculated. Entering the values of D and θ_i into AT-Blast yields the static pressure at each joint. Using the tributary area method, the pressure is resolved into joint loads. In Table 7-3, the pressures highlighted in yellow are greater than or equal to 200 psi, so these pressures' corresponding joint loads will be applied to the DT bridge model.

Table 7-3: Attack Scenario 1 (674 lbs TNT) Static Equivalent Load Calculations⁷

	Joint No.	Coord. Relative to Origin		X (ft)	Z (ft)	D (ft)	θ_i (°)	Pressure (psi)	Tributary Area (ft ²)	Load on Joint (K)
		x	y							
Stringer 1	1	750	17.5	29	4	29	82	128.05	87.45	1613
	2	765	17.5	19	4	20	78	312.75	87.45	3938
	3	780	17.5	19	4	19	78	306.30	87.45	3857
	4	795	17.5	28	4	28	82	137.49	87.45	1731
Stringer 2	1	750	10.5	25	4	26	81	161.43	105.00	2441
	2	765	10.5	13	4	14	73	572.36	105.00	8654
	3	780	10.5	13	4	13	72	668.49	105.00	10108
	4	795	10.5	24	4	25	81	173.95	105.00	2630
Stringer 3	1	750	3.5	23	4	24	80	205.34	105.00	3105
	2	765	3.5	9	4	10	65	1567.80	105.00	23705
	3	780	3.5	8	4	9	63	2123.15	105.00	32102
	4	795	3.5	22	4	23	80	233.64	105.00	3533

Figure 7-7 shows the static equivalent joint loads for Attack Scenario 1 applied to the deck cantilever truss model. Figures for all five attack scenario's loading can be found in the Appendix.

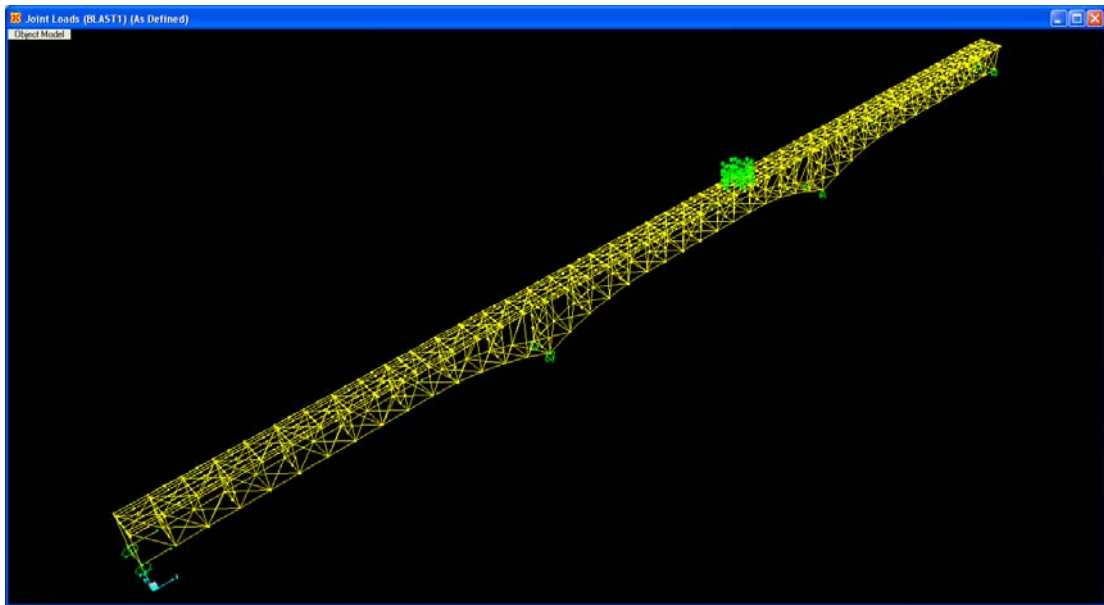


Figure 7-7: Attack Scenario 1 (674 lbs TNT) Static Equivalent Joint Loads

⁷ Because of the bridge's typical section symmetry, the load calculations for Stringer 1, Stringer 2, and Stringer 3 also apply to Stringer 4, Stringer 5, and Stringer 6, respectively.

7.5 Analyze Structural Response

Now that the equivalent static loads of the blast are applied to the bridge model, the analysis is run. SAP2000's nonlinear static analysis output shows the performance of the structural members' plastic hinges. The nodes are color-coded, as shown in Figure 4-8, to represent the hinge's state on the moment-rotation or force-deformation curve. The analysis saved multiple response steps. Figures 7-8 through 7-12 show the final response steps for each attack scenario on the deck truss bridge.

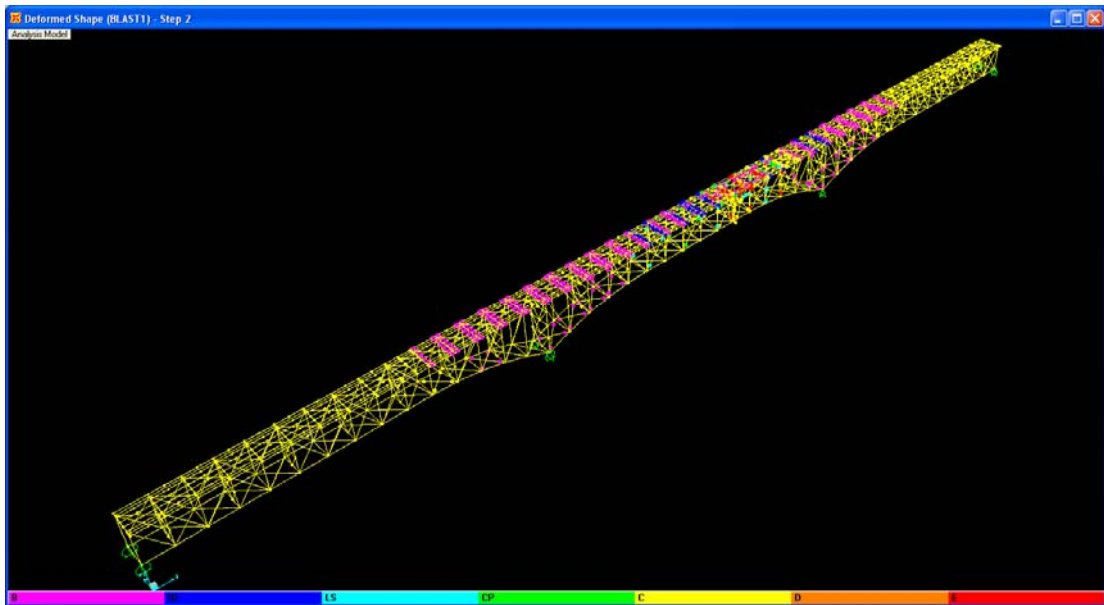


Figure 7-8: Attack Scenario 1 Response (Step 2)

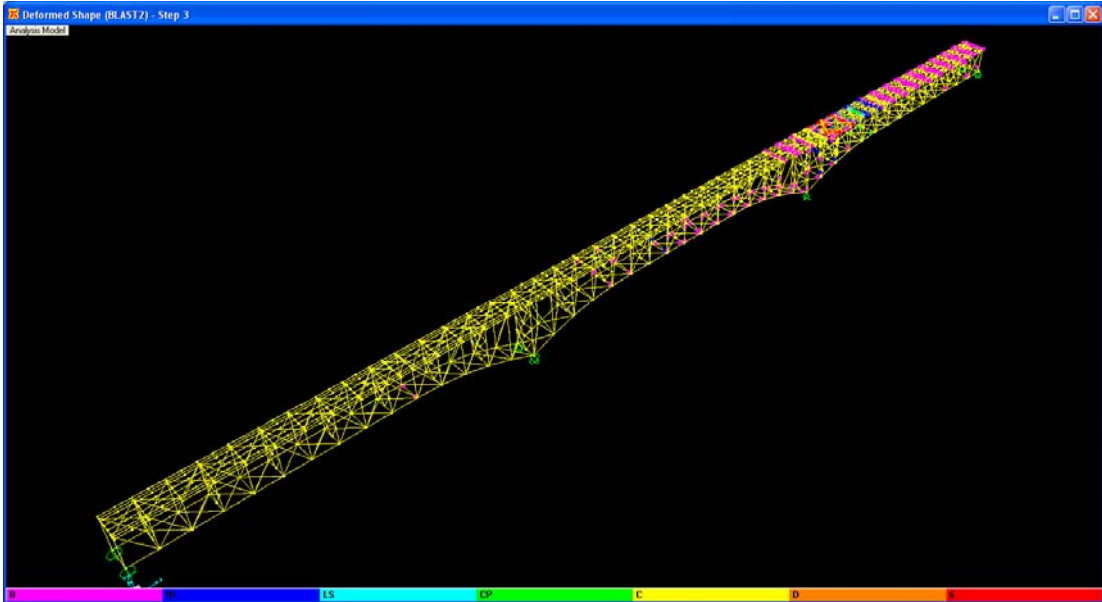


Figure 7-9: Attack Scenario 2 Response (Step 3)

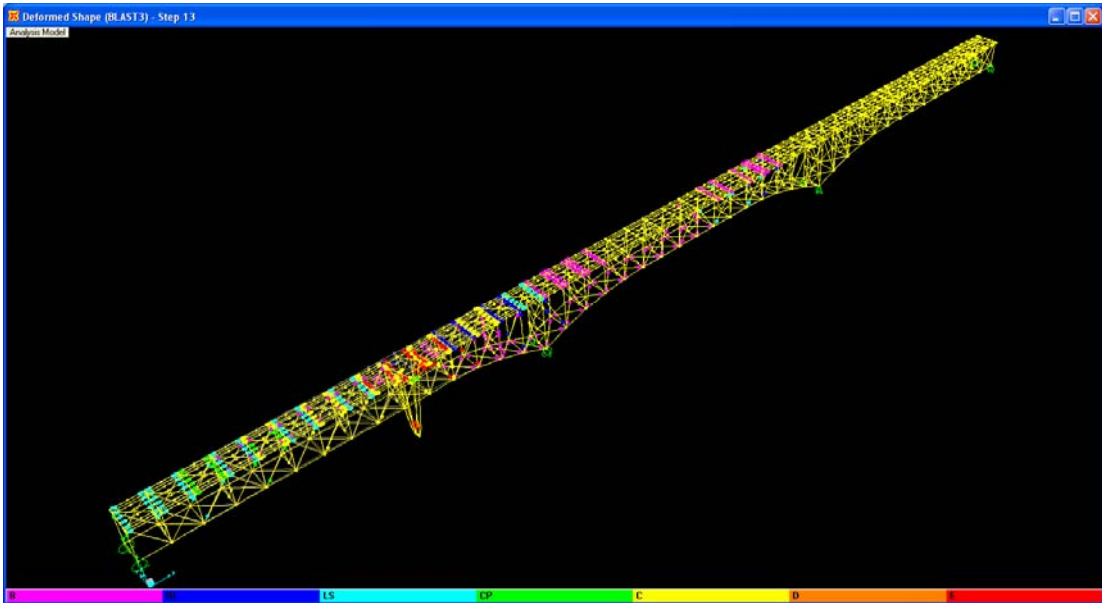


Figure 7-10: Attack Scenario 3 Response (Step 13)

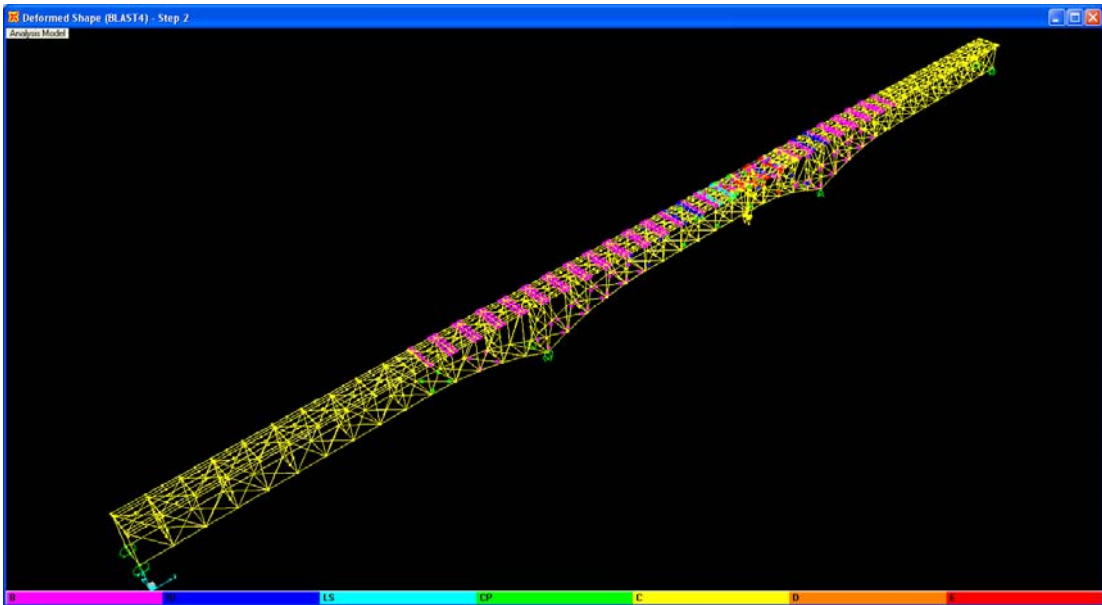


Figure 7-11: Attack Scenario 4 Response (Step 2)

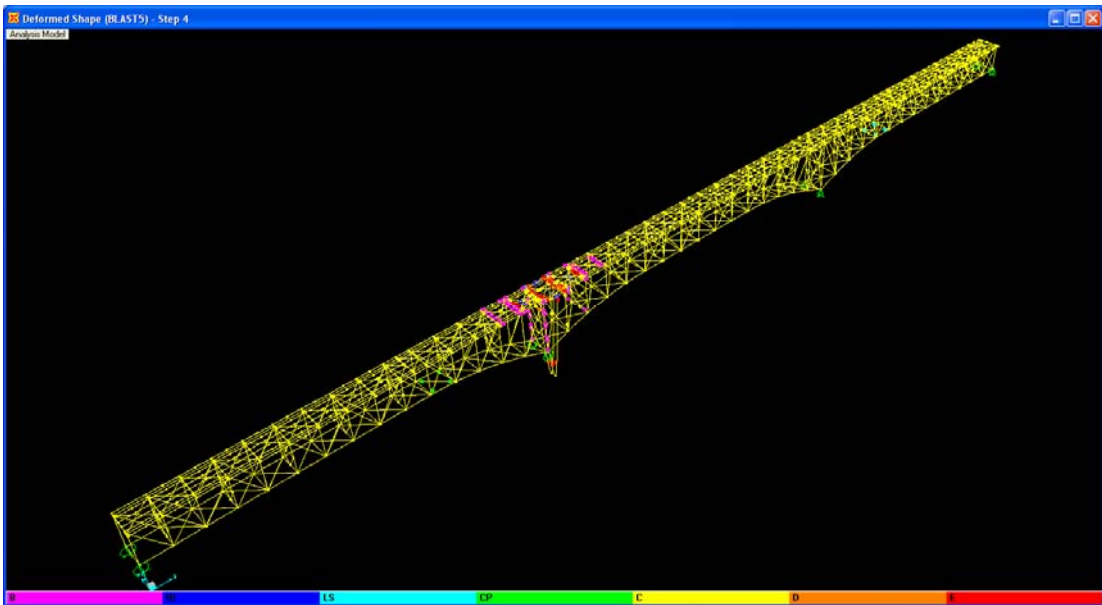


Figure 7-12: Attack Scenario 5 Response (Step 4)

7.6 Consequence Assessment

For the deck cantilever truss bridge, the consequences are estimated using the method described in Section 4.5.

7.6.1 Structural Damage

Figures 7-8 through 7-12 reveal that DT bridge experiences damage in all three performance levels. Table 7-4 summarizes the structural damage and associated costs, calculated using Equations 4.2 and 4.3.

Table 7-4: DT Bridge Structural Damage Costs

Attack Scenario (i)	Damaged Area by Performance Level (ft ²)			Structural Damage Cost (\$) (C _{i,s}) ^{DT}	
	≥ IO	≥ LS	≥ CP	Lower Bound	Upper Bound
1	4,759	-	5,949	\$2,498,580	\$3,640,788
2	1,190	-	4,759	\$1,769,758	\$2,578,790
3	2,380	7,139	8,329	\$4,372,725	\$6,371,685
4	3,569	1,190	4,759	\$2,186,188	\$3,185,588
5	-	-	3,569	\$1,249,290	\$1,820,394

7.6.2 Casualties

Based on the peak hour traffic data, the number of vehicles on the 1350' bridge at any time (V_{peak}) is 90 vehicles. Equations 4.5 and 4.6 yield the estimated cost of casualties, as shown in Table 7-5.

Table 7-5: Cost of Casualties for DT Bridge

Attack Scenario (i)	Failure Ratio (F _i) ^{DT}	(F _i)*V _{peak} (vehicles)	Cost of Casualties (\$) (C _{i,c}) ^{DT}	
			Lower Bound	Upper Bound
1	11%	10	0	36,000,000
2	9%	8	0	28,800,000
3	16%	14	0	50,400,000
4	9%	8	0	28,800,000
5	7%	6	0	21,600,000

7.6.3 Downtime

Using the Failure Ratio and bridge replacement times, Equations 4.7 and 4.8 are used to calculate upper and lower limit of bridge downtime for each attack

scenario, as Table 7-6 displays. Equations 4.9 - 4.12 calculate the cost ranges for toll revenue loss and user delay. The results are shown in Table 7-7.

Table 7-6: DT Bridge Downtime

Attack Scenario (i)	Failure Ratio $(F_i)^{DT}$	Downtime (days) $(D_i)^{DT}$	
		Lower Bound	Upper Bound
1	11%	47	53
2	9%	37	43
3	16%	65	75
4	9%	37	43
5	7%	28	32

Table 7-7: DT Bridge Downtime Costs

Attack Scenario (i)	Lost Toll Revenue (\$) $(C_{i,D1})^{DT}$		User Detour Cost (\$) $(C_{i,D2})^{DT}$	
	Lower Bound	Upper Bound	Lower Bound	Upper Bound
1	2,820,000	3,180,000	52,875,000	59,625,000
2	2,220,000	2,580,000	41,625,000	48,375,000
3	3,900,000	4,500,000	73,125,000	84,375,000
4	2,220,000	2,580,000	41,625,000	48,375,000
5	1,680,000	1,920,000	31,500,000	36,000,000

7.6.4 Total Consequences for Deck Cantilever Truss Bridge

Equations 4.15 and 4.16 calculate the expected cost of the consequences $E[(C_i)^{DT}]$ and standard deviation $(\sigma_i)^{DT}$ for each attack scenario. Finally, the expected consequence cost, $E[C^{DT}]$, and standard deviation (σ^{DT}) for the deck truss bridge type is estimated using Equations 4.17 and 4.18. Table 7-8 summarizes these consequence costs.

Table 7-8: DT Bridge Consequence Costs

i	Consequence	Cost (\$)		Mean (\$) $(C_i)^{DT}$	Std Dev (\$) $(\sigma_i)^{DT}$
		Lower Bound	Upper Bound		
1	Structural Damage	2,498,580	3,640,788	3,069,684	329,727
	Casualties	0	36,000,000	18,000,000	10,392,305
	Downtime	55,695,000	62,805,000	59,250,000	2,052,480
	$E[(C_1)^{DT}]$			80,319,684	10,598,179
2	Structural Damage	1,769,758	2,578,790	2,174,274	233,547
	Casualties	0	28,800,000	14,400,000	8,313,844
	Downtime	43,845,000	50,955,000	47,400,000	2,052,480
	$E[(C_2)^{DT}]$			63,974,274	8,566,634
3	Structural Damage	4,372,725	6,371,685	5,372,205	577,050
	Casualties	0	50,400,000	25,200,000	14,549,227
	Downtime	77,025,000	88,875,000	82,950,000	3,420,800
	$E[(C_3)^{DT}]$			113,522,205	14,957,101
4	Structural Damage	2,186,188	3,185,588	2,685,888	288,502
	Casualties	0	28,800,000	14,400,000	8,313,844
	Downtime	43,845,000	50,955,000	47,400,000	2,052,480
	$E[(C_4)^{DT}]$			64,485,888	8,568,308
5	Structural Damage	1,249,290	1,820,394	1,534,842	164,864
	Casualties	0	21,600,000	10,800,000	6,235,383
	Downtime	33,180,000	37,920,000	35,550,000	1,368,320
	$E[(C_5)^{DT}]$			47,884,842	6,385,881
Expected Consequence Costs, $E[C^{DT}]$				\$74,037,378	\$22,248,466

8.0 CONCLUSIONS

8.1 Study Results

This study analyzes and quantifies the effects of a blast event occurring on a highway bridge deck. The proposed method uses nonlinear structural analysis, probability distributions, and performance level criteria to calculate the expected costs of three consequences: structural damage, casualties, and downtime. Three case studies using different functional bridge types are completed by implementing the proposed method.

Table 8-1 displays the damaged area in square feet by performance level for each bridge type. Table 8-2 summarizes the average results for the applied attack scenarios. Table 8-3 breaks down the expected value of costs by consequence type for each bridge.

Table 8-1: Structural Damage Summary

Bridge Type and Length	Mean Damaged Area by Performance Level (ft ²)		
	≥ IO	≥ LS	≥ CP
60' Prestressed Concrete Beam	0	0	2,380
606' Steel Plate Girder	2,608	1,225	4,105
1350' Deck Cantilever Truss	2,975	4,165	5,473

Table 8-2: Results Summary

Bridge Type and Length	Mean Failure Ratio, F	Expected Value of Consequence Cost, E[C]	Standard Deviation, σ
60' Prestressed Concrete Beam	100%	\$114,397,400	-
606' Steel Plate Girder	18%	\$58,319,625	\$4,334,990
1350' Deck Cantilever Truss	10%	\$74,037,378	\$22,248,466

Table 8-3: Expected Value of Costs by Consequence Type

Bridge Type and Length	Expected Value of Consequence (\$)		
	Structural Damage, C_S	Casualties, C_C	Downtime, C_D
60' Prestressed Concrete Beam	\$547,400	\$7,200,000	\$106,650,000
606' Steel Plate Girder	\$1,637,625	\$12,600,000	\$44,082,000
1350' Deck Cantilever Truss	\$2,967,378	\$16,560,000	\$54,510,000

Table 8-2 shows that the prestressed concrete beam bridge has the highest expected value of consequences. However, this is not because of the structural damage. Table 8-3 sheds light on this result by breaking down the costs by consequence type. It is clear that the PC beam bridge's downtime cost (\$106,650,000) controls. The steel girder and deck truss bridges have higher structural damage and casualty costs; however, since they only require local replacement, the required downtime is less than the prestressed concrete bridge.

8.2 Recommended Areas of Future Research

In closing, the author would like to suggest areas of future research that could build onto this study.

1. The attack scenarios in the case studies are manually applied to each bridge model. Developing user-defined code to automate this process would allow more simulations to be completed in a more time-efficient manner.
2. More research could better define the relationship between structural damage and bridge replacement cost.
3. Official guidelines, perhaps through a national effort by FEMA, for performance-based design criteria for blast loads are needed.

4. Large-scale laboratory testing, although costly, would be valuable in determining the effects of conventional explosives on bridges.
5. In this study, the costs of casualties and downtime are solely dependent on the amount of damaged area in or above the Collapse Prevention performance level. More research could provide a better understanding of these consequences in the other performance levels.
6. The method demonstration only analyzes the effect of conventional explosives over the bridge deck (carried in a vehicle on the bridge). Further research could analyze other weapon and delivery method used by terrorists.
7. The “next generation” seismic performance-based guidelines use analytical models to assess economic consequences. As of now, input data required to apply this concept to blasts limited. More research could assist this effort.
8. Uniform and triangular probability distributions are assigned in this study for demonstration purposes. Characterizing the attack scenarios and consequences with more fitting distributions would decrease uncertainty.

Appendix

Table A-1: PC Beam Attack Scenario 1 Static Equivalent Load Calculations

	Joint No.	Coord. Relative to Origin		X (ft)	Z (ft)	D (ft)	θ_i (°)	Pressure (psi)	Tributary Area (ft ²)	Load on Joint (K)
		x	y							
PC Beam 1	1	0	17.92	38	4	39	84	59.19	27.50	234
	2	10	17.92	30	4	30	82	119.43	55.00	946
	3	20	17.92	23	4	23	80	233.64	55.00	1850
	4	30	17.92	18	4	19	78	312.75	55.00	2477
	5	40	17.92	19	4	19	78	312.75	55.00	2477
	6	50	17.92	24	4	24	81	197.09	55.00	1561
	7	60	17.92	32	4	32	83	100.12	27.50	396
PC Beam 2	1	0	10.75	36	4	36	84	73.51	35.83	379
	2	10	10.75	26	4	27	81	150.43	71.67	1552
	3	20	10.75	18	4	18	77	321.06	71.67	3313
	4	30	10.75	11	4	12	71	784.48	71.67	8096
	5	40	10.75	12	4	13	72	668.49	71.67	6899
	6	50	10.75	19	4	20	78	306.30	71.67	3161
	7	60	10.75	28	4	28	82	137.49	35.83	709
PC Beam 3	1	0	3.58	34	4	34	83	86.82	35.83	448
	2	10	3.58	24	4	25	81	173.95	71.67	1795
	3	20	3.58	14	4	15	75	472.39	71.67	4875
	4	30	3.58	5	4	7	53	7869.88	71.67	81217
	5	40	3.58	7	4	8	60	3487.37	71.67	35990
	6	50	3.58	16	4	17	76	365.83	71.67	3775
	7	60	3.58	26	4	27	81	150.43	35.83	776
PC Beam 4	1	0	-3.58	34	4	34	83	86.82	35.83	448
	2	10	-3.58	24	4	25	81	173.95	71.67	1795
	3	20	-3.58	14	4	15	75	472.39	71.67	4875
	4	30	-3.58	5	4	7	53	7869.88	71.67	81217
	5	40	-3.58	7	4	8	60	3487.37	71.67	35990
	6	50	-3.58	16	4	17	76	365.83	71.67	3775
	7	60	-3.53	26	4	27	81	150.43	35.83	776
PC Beam 5	1	0	-10.75	36	4	36	84	73.51	35.83	379
	2	10	-10.75	26	4	27	81	150.43	71.67	1552
	3	20	-10.75	18	4	18	77	321.06	71.67	3313
	4	30	-10.75	11	4	12	71	784.48	71.67	8096
	5	40	-10.75	12	4	13	72	668.49	71.67	6899
	6	50	-10.75	19	4	20	78	306.30	71.67	3161
	7	60	-10.75	28	4	28	82	137.49	35.83	709
PC Beam 6	1	0	-17.92	38	4	39	84	59.19	27.50	234
	2	10	-17.92	30	4	30	82	119.43	55.00	946
	3	20	-17.92	23	4	23	80	233.64	55.00	1850
	4	30	-17.92	18	4	19	78	312.75	55.00	2477
	5	40	-17.92	19	4	19	78	312.75	55.00	2477
	6	50	-17.92	24	4	24	81	197.09	55.00	1561
	7	60	-17.92	32	4	32	83	100.12	27.50	396

Table A-2: PC Beam Attack Scenario 2 Static Equivalent Load Calculations

	Joint No.	Coord. Relative to Origin		X (ft)	Z (ft)	D (ft)	θ_i (°)	Pressure (psi)	Tributary Area (ft ²)	Load on Joint (K)
		x	y							
PC Beam 1	1	0	17.92	48	4	48	85	48.71	27.50	193
	2	10	17.92	38	4	39	84	84.33	55.00	668
	3	20	17.92	30	4	30	82	156.51	55.00	1240
	4	30	17.92	23	4	23	80	290.26	55.00	2299
	5	40	17.92	18	4	19	78	364.94	55.00	2890
	6	50	17.92	19	4	19	78	364.94	55.00	2890
	7	60	17.92	24	4	24	81	272.50	27.50	1079
PC Beam 2	1	0	10.75	45	4	45	85	57.04	35.83	294
	2	10	10.75	36	4	36	84	101.57	71.67	1048
	3	20	10.75	26	4	27	81	207.45	71.67	2141
	4	30	10.75	18	4	18	77	413.48	71.67	4267
	5	40	10.75	11	4	12	71	971.44	71.67	10025
	6	50	10.75	12	4	13	72	834.12	71.67	8608
	7	60	10.75	19	4	20	78	330.79	35.83	1707
PC Beam 3	1	0	3.58	44	4	44	85	60.49	35.83	312
	2	10	3.58	34	4	34	83	118.77	71.67	1226
	3	20	3.58	24	4	25	81	261.06	71.67	2694
	4	30	3.58	14	4	15	75	598.24	71.67	6174
	5	40	3.58	5	4	7	53	9648.34	71.67	99571
	6	50	3.58	7	4	8	60	4251.71	71.67	43878
	7	60	3.58	16	4	17	76	469.70	35.83	2424
PC Beam 4	1	0	-3.58	44	4	44	85	60.49	35.83	312
	2	10	-3.58	34	4	34	83	118.77	71.67	1226
	3	20	-3.58	24	4	25	81	261.06	71.67	2694
	4	30	-3.58	14	4	15	75	598.24	71.67	6174
	5	40	-3.58	5	4	7	53	9648.34	71.67	99571
	6	50	-3.58	7	4	8	60	4251.71	71.67	43878
	7	60	-3.53	16	4	17	76	469.70	35.83	2424
PC Beam 5	1	0	-10.75	45	4	45	85	57.04	35.83	294
	2	10	-10.75	36	4	36	84	101.57	71.67	1048
	3	20	-10.75	26	4	27	81	207.45	71.67	2141
	4	30	-10.75	18	4	18	77	413.48	71.67	4267
	5	40	-10.75	11	4	12	71	971.44	71.67	10025
	6	50	-10.75	12	4	13	72	834.12	71.67	8608
	7	60	-10.75	19	4	20	78	330.79	35.83	1707
PC Beam 6	1	0	-17.92	48	4	48	85	48.71	27.50	193
	2	10	-17.92	38	4	39	84	84.33	55.00	668
	3	20	-17.92	30	4	30	82	156.51	55.00	1240
	4	30	-17.92	23	4	23	80	290.26	55.00	2299
	5	40	-17.92	18	4	19	78	364.94	55.00	2890
	6	50	-17.92	19	4	19	78	364.94	55.00	2890
	7	60	-17.92	24	4	24	81	272.50	27.50	1079

Table A-3: PC Beam Attack Scenario 3 Static Equivalent Load Calculations

	Joint No.	Coord. Relative to Origin		X (ft)	Z (ft)	D (ft)	θ_i (°)	Pressure (psi)	Tributary Area (ft ²)	Load on Joint (K)
		x	y							
PC Beam 1	1	0	17.92	22	4	22	80	175.26	27.50	694
	2	10	17.92	18	4	19	78	284.21	55.00	2251
	3	20	17.92	19	4	20	78	242.83	55.00	1923
	4	30	17.92	25	4	25	81	132.02	55.00	1046
	5	40	17.92	32	4	33	83	63.90	55.00	506
	6	50	17.92	41	4	41	84	37.34	55.00	296
	7	60	17.92	50	4	50	85	24.52	27.50	97
PC Beam 2	1	0	10.75	17	4	17	77	315.40	35.83	1627
	2	10	10.75	11	4	12	70	630.70	71.67	6509
	3	20	10.75	13	4	13	73	504.91	71.67	5211
	4	30	10.75	20	4	21	79	206.72	71.67	2133
	5	40	10.75	29	4	29	82	91.91	71.67	949
	6	50	10.75	39	4	39	84	41.85	71.67	432
	7	60	10.75	48	4	48	85	26.56	35.83	137
PC Beam 3	1	0	3.58	13	4	14	73	440.48	35.83	2273
	2	10	3.58	5	4	6	49	10023.32	71.67	103441
	3	20	3.58	8	4	9	63	1710.17	71.67	17649
	4	30	3.58	17	4	18	77	304.12	71.67	3139
	5	40	3.58	27	4	28	82	99.90	71.67	1031
	6	50	3.58	37	4	37	84	47.22	71.67	487
	7	60	3.58	47	4	47	85	27.68	35.83	143
PC Beam 4	1	0	-3.58	13	4	14	73	440.48	35.83	2273
	2	10	-3.58	5	4	6	49	10023.32	71.67	103441
	3	20	-3.58	8	4	9	63	1710.17	71.67	17649
	4	30	-3.58	17	4	18	77	304.12	71.67	3139
	5	40	-3.58	27	4	28	82	99.90	71.67	1031
	6	50	-3.58	37	4	37	84	47.22	71.67	487
	7	60	-3.53	47	4	47	85	27.68	35.83	143
PC Beam 5	1	0	-10.75	17	4	17	77	315.40	35.83	1627
	2	10	-10.75	11	4	12	70	630.70	71.67	6509
	3	20	-10.75	13	4	13	73	504.91	71.67	5211
	4	30	-10.75	20	4	21	79	206.72	71.67	2133
	5	40	-10.75	29	4	29	82	91.91	71.67	949
	6	50	-10.75	39	4	39	84	41.85	71.67	432
	7	60	-10.75	48	4	48	85	26.56	35.83	137
PC Beam 6	1	0	-17.92	22	4	22	80	175.26	27.50	694
	2	10	-17.92	18	4	19	78	284.21	55.00	2251
	3	20	-17.92	19	4	20	78	242.83	55.00	1923
	4	30	-17.92	25	4	25	81	132.02	55.00	1046
	5	40	-17.92	32	4	33	83	63.90	55.00	506
	6	50	-17.92	41	4	41	84	37.34	55.00	296
	7	60	-17.92	50	4	50	85	24.52	27.50	97

Table A-4: PC Beam Attack Scenario 4 Static Equivalent Load Calculations

	Joint No.	Coord. Relative to Origin		X (ft)	Z (ft)	D (ft)	θ_i (°)	Pressure (psi)	Tributary Area (ft ²)	Load on Joint (K)
		x	y							
PC Beam 1	1	0	17.92	40	4	40	84	176.11	27.50	697
	2	10	17.92	32	4	32	83	278.72	55.00	2207
	3	20	17.92	24	4	24	81	435.43	55.00	3449
	4	30	17.92	19	4	19	78	677.50	55.00	5366
	5	40	17.92	18	4	19	78	677.50	55.00	5366
	6	50	17.92	23	4	23	80	468.68	55.00	3712
	7	60	17.92	30	4	30	82	296.44	27.50	1174
PC Beam 2	1	0	10.75	38	4	38	84	201.65	35.83	1041
	2	10	10.75	28	4	28	82	326.92	71.67	3374
	3	20	10.75	19	4	20	78	623.02	71.67	6430
	4	30	10.75	12	4	13	72	1413.21	71.67	14584
	5	40	10.75	11	4	12	71	1622.29	71.67	16742
	6	50	10.75	18	4	18	77	756.27	71.67	7805
	7	60	10.75	26	4	27	81	350.41	35.83	1808
PC Beam 3	1	0	3.58	36	4	36	84	232.61	35.83	1200
	2	10	3.58	26	4	27	81	350.41	71.67	3616
	3	20	3.58	16	4	17	76	846.12	71.67	8732
	4	30	3.58	7	4	8	60	6989.00	71.67	72126
	5	40	3.58	5	4	7	53	15886.79	71.67	163952
	6	50	3.58	14	4	15	75	1044.84	71.67	10783
	7	60	3.58	24	4	25	81	404.37	35.83	2087
PC Beam 4	1	0	-3.58	36	4	36	84	232.61	35.83	1200
	2	10	-3.58	26	4	27	81	350.41	71.67	3616
	3	20	-3.58	16	4	17	76	846.12	71.67	8732
	4	30	-3.58	7	4	8	60	6989.00	71.67	72126
	5	40	-3.58	5	4	7	53	15886.79	71.67	163952
	6	50	-3.58	14	4	15	75	1044.84	71.67	10783
	7	60	-3.53	24	4	25	81	404.37	35.83	2087
PC Beam 5	1	0	-10.75	38	4	38	84	201.65	35.83	1041
	2	10	-10.75	28	4	28	82	326.92	71.67	3374
	3	20	-10.75	19	4	20	78	623.02	71.67	6430
	4	30	-10.75	12	4	13	72	1413.21	71.67	14584
	5	40	-10.75	11	4	12	71	1622.29	71.67	16742
	6	50	-10.75	18	4	18	77	756.27	71.67	7805
	7	60	-10.75	26	4	27	81	350.41	35.83	1808
PC Beam 6	1	0	-17.92	40	4	40	84	176.11	27.50	697
	2	10	-17.92	32	4	32	83	278.72	55.00	2207
	3	20	-17.92	24	4	24	81	435.43	55.00	3449
	4	30	-17.92	19	4	19	78	677.50	55.00	5366
	5	40	-17.92	18	4	19	78	677.50	55.00	5366
	6	50	-17.92	23	4	23	80	468.68	55.00	3712
	7	60	-17.92	30	4	30	82	296.44	27.50	1174

Table A-5: PC Beam Attack Scenario 5 Static Equivalent Load Calculations

	Joint No.	Coord. Relative to Origin		X (ft)	Z (ft)	D (ft)	θ_i (°)	Pressure (psi)	Tributary Area (ft ²)	Load on Joint (K)
		x	y							
PC Beam 1	1	0	17.92	28	4	28	82	277.62	27.50	1099
	2	10	17.92	21	4	21	79	426.20	55.00	3376
	3	20	17.92	18	4	18	77	585.76	55.00	4639
	4	30	17.92	20	4	20	79	465.20	55.00	3684
	5	40	17.92	26	4	26	81	296.42	55.00	2348
	6	50	17.92	34	4	34	83	181.69	55.00	1439
	7	60	17.92	43	4	43	85	103.44	27.50	410
PC Beam 2	1	0	10.75	24	4	24	80	325.52	35.83	1680
	2	10	10.75	15	4	16	75	744.45	71.67	7683
	3	20	10.75	11	4	12	70	1336.41	71.67	13792
	4	30	10.75	14	4	15	74	846.62	71.67	8737
	5	40	10.75	22	4	22	80	383.67	71.67	3959
	6	50	10.75	31	4	31	83	235.12	71.67	2426
	7	60	10.75	40	4	41	84	118.25	35.83	610
PC Beam 3	1	0	3.58	21	4	22	79	391.35	35.83	2019
	2	10	3.58	12	4	12	71	1302.15	71.67	13438
	3	20	3.58	4	4	5	43	23749.68	71.67	245097
	4	30	3.58	10	4	10	68	1924.59	71.67	19862
	5	40	3.58	19	4	20	78	476.61	71.67	4919
	6	50	3.58	29	4	29	82	268.05	71.67	2766
	7	60	3.58	39	4	39	84	131.86	35.83	680
PC Beam 4	1	0	-3.58	21	4	22	79	391.35	35.83	2019
	2	10	-3.58	12	4	12	71	1302.15	71.67	13438
	3	20	-3.58	4	4	5	43	23749.68	71.67	245097
	4	30	-3.58	10	4	10	68	1924.59	71.67	19862
	5	40	-3.58	19	4	20	78	476.61	71.67	4919
	6	50	-3.58	29	4	29	82	268.05	71.67	2766
	7	60	-3.53	39	4	39	84	131.86	35.83	680
PC Beam 5	1	0	-10.75	24	4	24	80	325.52	35.83	1680
	2	10	-10.75	15	4	16	75	744.45	71.67	7683
	3	20	-10.75	11	4	12	70	1336.41	71.67	13792
	4	30	-10.75	14	4	15	74	846.62	71.67	8737
	5	40	-10.75	22	4	22	80	383.67	71.67	3959
	6	50	-10.75	31	4	31	83	235.12	71.67	2426
	7	60	-10.75	40	4	41	84	118.25	35.83	610
PC Beam 6	1	0	-17.92	28	4	28	82	277.62	27.50	1099
	2	10	-17.92	21	4	21	79	426.20	55.00	3376
	3	20	-17.92	18	4	18	77	585.76	55.00	4639
	4	30	-17.92	20	4	20	79	465.20	55.00	3684
	5	40	-17.92	26	4	26	81	296.42	55.00	2348
	6	50	-17.92	34	4	34	83	181.69	55.00	1439
	7	60	-17.92	43	4	43	85	103.44	27.50	410

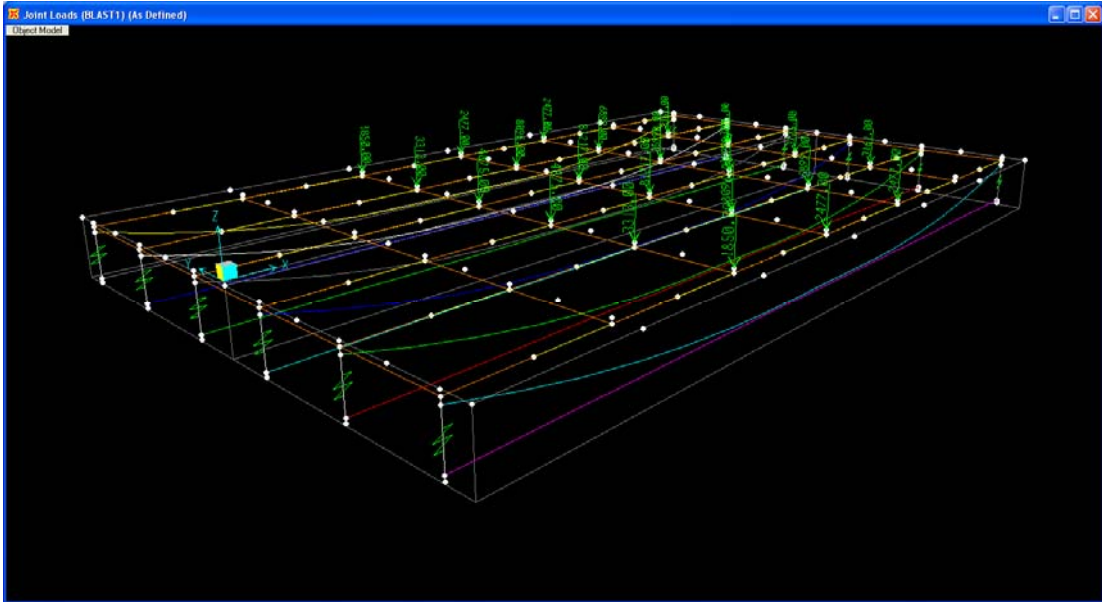


Figure A-1: PC Beam Attack Scenario 1 Static Equivalent Joint Loads

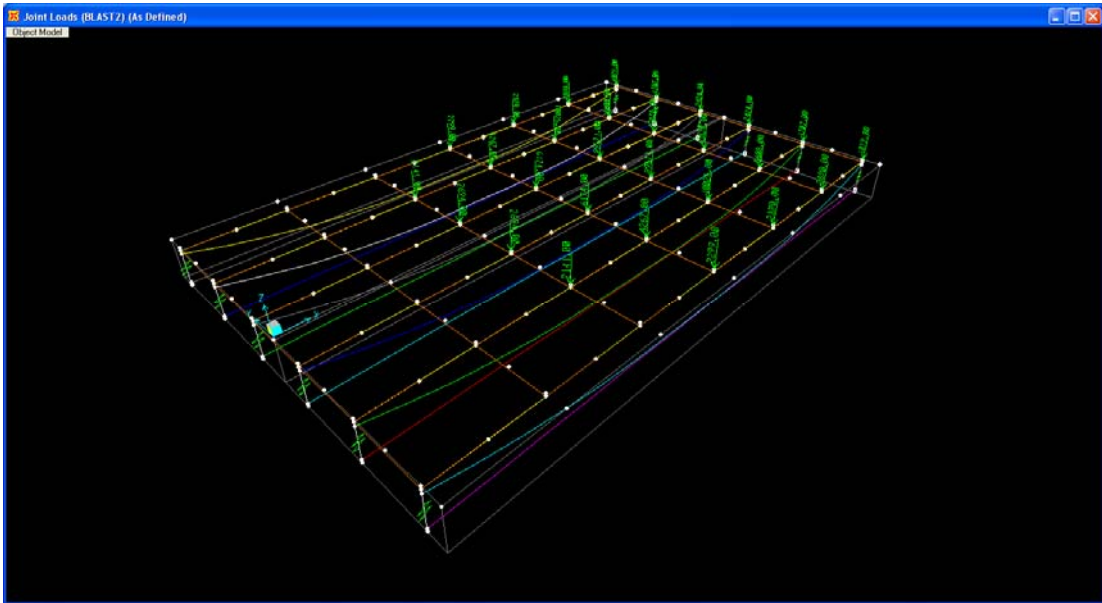


Figure A-2: PC Beam Attack Scenario 2 Static Equivalent Joint Loads

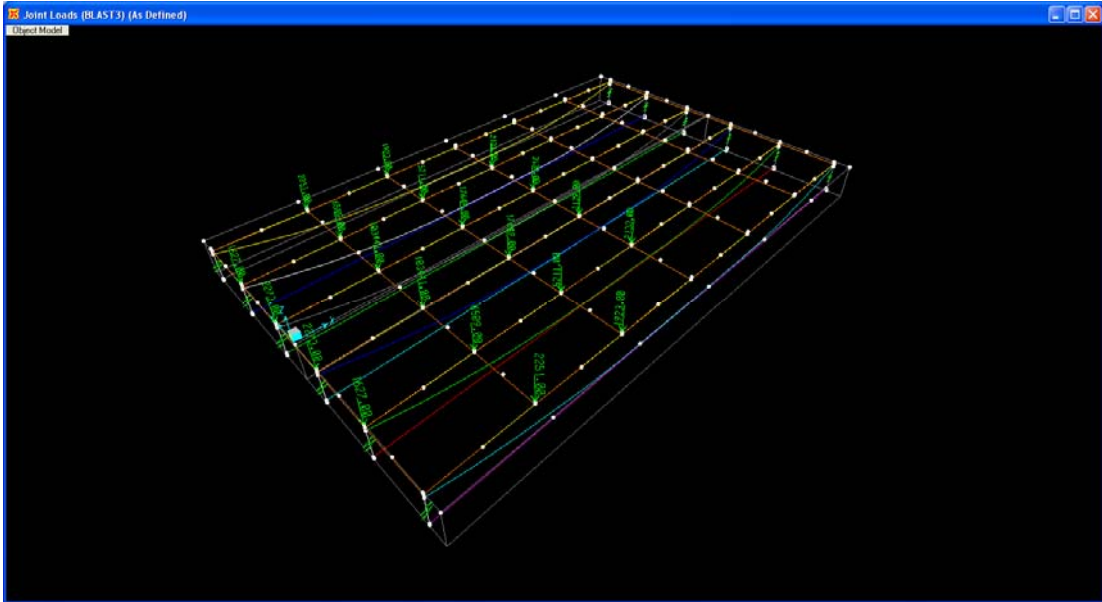


Figure A-3: PC Beam Attack Scenario 3 Static Equivalent Joint Loads

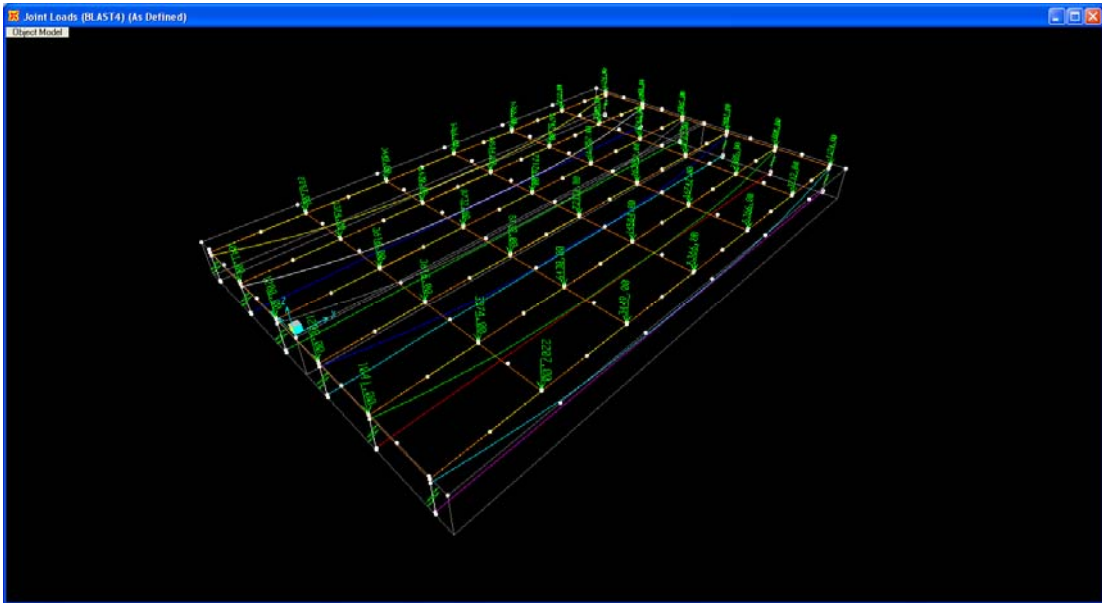


Figure A-4: PC Beam Attack Scenario 4 Static Equivalent Joint Loads

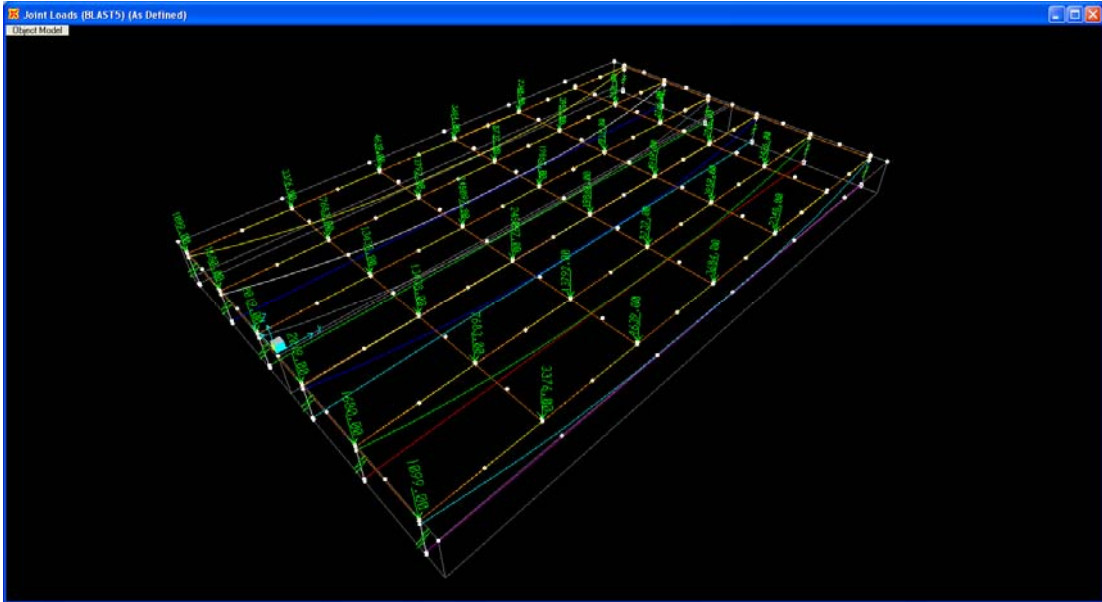


Figure A-5: PC Beam Attack Scenario 5 Static Equivalent Joint Loads

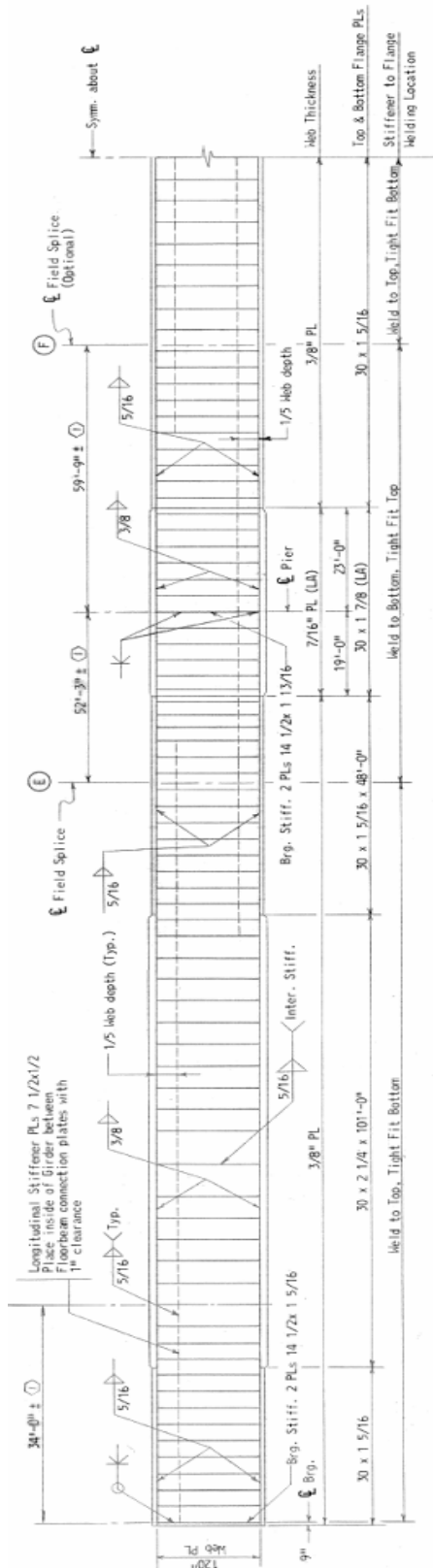


Figure A-6: Plate Girder Elevation

Table A-6: SG Bridge Attack Scenario 1 Static Equivalent Load Calculations

	Joint No.	Coord. Relative to Origin		X (ft)	Z (ft)	D (ft)	θ_i (°)	Pressure (psi)	Tributary Area (ft ²)	Load on Joint (K)
		x	y							
Stringer 1	35	312.75	18.58	39	4	39	84	59.19	27.98	239
	36	322.5	18.58	31	4	31	83	107.86	27.98	435
	37	332.25	18.58	24	4	24	80	205.34	27.98	827
	38	342	18.58	19	4	20	78	306.30	27.98	1234
	39	351.75	18.58	19	4	20	78	306.30	27.98	1234
	40	361.5	18.58	24	4	24	80	205.34	27.98	827
	41	371.25	18.58	31	4	31	83	107.86	27.98	435
	42	381	18.58	39	4	39	84	59.19	25.00	213
Plate Girder 1	35	312.75	14	37	4	37	84	68.22	56.45	555
	36	322.5	14	28	4	29	82	128.05	56.45	1041
	37	332.25	14	20	4	21	79	290.81	56.45	2364
	38	342	14	15	4	15	75	472.39	56.45	3840
	39	351.75	14	15	4	15	75	472.39	56.45	3840
	40	361.5	14	20	4	21	79	290.81	56.45	2364
	41	371.25	14	28	4	28	82	137.49	56.45	1118
	42	381	14	37	4	37	84	68.22	50.43	495
Stringer 2	35	312.75	7	35	4	35	83	81.09	68.25	797
	36	322.5	7	25	4	26	81	161.43	68.25	1587
	37	332.25	7	16	4	17	76	365.83	68.25	3595
	38	342	7	9	4	9	65	1833.63	68.25	18021
	39	351.75	7	8	4	9	65	1833.63	68.25	18021
	40	361.5	7	16	4	17	76	365.83	68.25	3595
	41	371.25	7	25	4	26	81	161.43	68.25	1587
	42	381	7	35	4	35	83	81.09	60.97	712
Stringer 3	35	312.75	0	34	4	34	83	86.82	68.25	853
	36	322.5	0	25	4	25	81	173.85	68.25	1709
	37	332.25	0	15	4	15	75	472.39	68.25	4643
	38	342	0	5	4	6	51	11320.26	68.25	111256
	39	351.75	0	5	4	6	50	12000.89	68.25	117945
	40	361.5	0	15	4	15	75	472.39	68.25	4643
	41	371.25	0	24	4	25	81	173.95	68.25	1710
	42	381	0	34	4	34	83	86.82	60.97	762

Table A-7: SG Bridge Attack Scenario 2 Static Equivalent Load Calculations

	Joint No.	Coord. Relative to Origin		X (ft)	Z (ft)	D (ft)	θ_i (°)	Pressure (psi)	Tributary Area (ft ²)	Load on Joint (K)
		x	y							
Stringer 1	46	413.5	18.58	36	4	36	84	101.57	27.27	399
	47	423	18.58	28	4	28	82	182.96	27.41	722
	48	432.6	18.58	22	4	22	80	296.90	27.55	1178
	49	442.2	18.58	19	4	19	78	364.94	27.55	1448
	50	451.8	18.58	20	4	21	79	306.90	27.55	1218
	51	461.4	18.58	25	4	26	81	232.97	27.55	924
	52	471	18.58	33	4	33	83	126.52	26.95	491
	53	480.18	18.58	41	4	41	84	74.41	26.35	282
Plate Girder 1	45	404	14	42	4	43	85	64.25	49.71	460
	46	413.5	14	34	4	34	83	118.77	55.01	941
	47	423	14	25	4	26	81	232.97	55.29	1855
	48	432.6	14	18	4	18	78	403.81	55.58	3232
	49	442.2	14	14	4	15	74	614.27	55.58	4917
	50	451.8	14	16	4	17	76	469.70	55.58	3760
	51	461.4	14	22	4	23	80	290.26	55.58	2323
	52	471	14	30	4	31	83	144.14	54.37	1128
53	480.18	14	39	4	39	84	84.33	53.15	645	
Stringer 2	45	404	7	41	4	41	84	74.41	60.095	644
	46	413.5	7	31	4	32	83	134.96	66.5	1292
	47	423	7	22	4	22	80	296.90	66.85	2858
	48	432.6	7	13	4	14	73	719.57	67.2	6963
	49	442.2	7	7	4	8	61	3811.33	67.2	36881
	50	451.8	7	10	4	11	69	1181.61	67.2	11434
	51	461.4	7	19	4	19	78	364.94	67.2	3531
	52	471	7	28	4	28	82	182.96	65.73	1732
53	480.18	7	37	4	37	84	95.32	64.26	882	
Stringer 3	45	404	0	40	4	40	84	79.50	60.095	688
	46	413.5	0	31	4	31	83	144.14	66.5	1380
	48	432.6	0	11	4	12	71	971.44	67.2	9400
	49	442.2	0	2	4	4	24	32291.50	67.2	312478
	50	451.8	0	8	4	9	63	2572.80	67.2	24896
	51	461.4	0	17	4	18	77	413.48	67.2	4001
	52	471	0	27	4	27	82	203.52	65.73	1926
	53	480.18	0	36	4	36	84	101.57	64.26	940
	54	489.36	0	45	4	46	85	53.88	64.295	499

Table A-8: SG Bridge Attack Scenario 3 Static Equivalent Load Calculations

	Joint No.	Coord. Relative to Origin		X (ft)	Z (ft)	D (ft)	θ_i (°)	Pressure (psi)	Tributary Area (ft ²)	Load on Joint (K)
		x	y							
Stringer 1	12	98.27	18.58	37	4	37	84	147.65	26.35	560
	13	107.45	18.58	29	4	29	82	268.05	26.36	1018
	14	116.64	18.58	23	4	23	80	353.05	26.36	1340
	15	125.82	18.58	19	4	19	78	521.48	26.35	1978
	16	135	18.58	19	4	20	78	476.61	26.95	1850
	17	144.6	18.58	24	4	24	80	325.02	27.55	1290
	18	154.2	18.58	31	4	31	83	235.12	27.55	933
	19	163.8	18.58	39	4	39	84	131.86	27.55	523
	Plate Girder 1	12	98.27	14	35	4	35	83	167.94	53.15
13		107.45	14	27	4	27	81	290.53	53.18	2225
14		116.64	14	19	4	20	78	476.61	53.18	3650
15		125.82	14	15	4	15	75	824.53	53.15	6311
16		135	14	15	4	15	75	824.53	54.37	6455
17		144.6	14	20	4	21	79	426.20	55.58	3411
18		154.2	14	28	4	28	82	277.62	55.58	2222
19		163.8	14	37	4	37	84	147.65	55.58	1182
Stringer 2		11	89.09	7	42	4	42	84	112.10	64.26
	12	98.27	7	32	4	33	83	197.45	64.26	1827
	13	107.45	7	24	4	24	80	325.52	64.295	3014
	14	116.64	7	15	4	16	75	744.45	64.295	6892
	15	125.82	7	8	4	9	64	3138.30	64.26	29040
	16	135	7	9	4	9	65	2908.67	65.73	27531
	17	144.6	7	16	4	17	76	659.49	67.2	6382
	18	154.2	7	25	4	26	81	296.42	67.2	2868
	19	163.8	7	35	4	35	83	167.94	67.2	1625
Stringer 3	11	89.09	0	41	4	41	84	118.25	64.26	1094
	12	98.27	0	32	4	32	83	215.15	64.26	1991
	13	107.45	0	23	4	23	80	353.05	64.295	3269
	14	116.64	0	13	4	14	73	982.45	64.295	9096
	15	125.82	0	4	4	6	46	21050.34	64.26	194788
	16	135	0	5	4	6	51	18331.72	65.73	173512
	17	144.6	0	15	4	15	75	824.53	67.2	7979
	18	154.2	0	24	4	25	81	300.72	67.2	2910
	19	163.8	0	34	4	34	83	181.69	67.2	1758
	20	173.4	0	43	4	44	85	98.15	67.2	950

Table A-9: SG Bridge Attack Scenario 4 Static Equivalent Load Calculations

	Joint No.	Coord. Relative to Origin		X (ft)	Z (ft)	D (ft)	θ_i (°)	Pressure (psi)	Tributary Area (ft ²)	Load on Joint (K)
		x	y							
Stringer 1	35	312.75	18.58	52	4	52	86	94.04	27.98	379
	36	322.5	18.58	43	4	43	85	147.15	27.98	593
	37	332.25	18.58	34	4	34	83	260.77	27.98	1051
	38	342	18.58	27	4	27	81	350.41	27.98	1412
	39	351.75	18.58	21	4	21	79	560.49	27.98	2258
	40	361.5	18.58	19	4	19	78	677.50	27.98	2730
	41	371.25	18.58	21	4	22	79	517.68	27.98	2086
	42	381	18.58	27	4	28	82	326.92	25.00	1177
	43	388.67	18.58	33	4	34	83	260.77	22.00	826
	44	396.33	18.58	40	4	40	84	176.11	22.00	558
	45	404	18.58	47	4	47	85	120.56	24.64	428
Plate Girder 1	35	312.75	14	50	4	50	85	104.76	56.45	852
	36	322.5	14	41	4	41	84	165.39	56.45	1344
	37	332.25	14	32	4	32	83	278.72	56.45	2266
	38	342	14	24	4	24	80	435.43	56.45	3540
	39	351.75	14	17	4	17	77	826.80	56.45	6721
	40	361.5	14	14	4	15	74	998.19	56.45	8114
	41	371.25	14	17	4	18	77	756.27	56.45	6148
	42	381	14	24	4	25	81	404.37	50.43	2937
	43	388.67	14	31	4	31	83	287.15	44.38	1835
	44	396.33	14	38	4	38	84	201.65	44.38	1289
	45	404	14	45	4	45	85	132.95	49.71	952
Stringer 2	35	312.75	7	49	4	49	85	109.69	68.25	1078
	36	322.5	7	39	4	39	84	188.28	68.25	1850
	37	332.25	7	30	4	30	82	296.44	68.25	2913
	38	342	7	20	4	21	79	560.49	68.25	5508
	39	351.75	7	12	4	12	71	1622.39	68.25	15945
	40	361.5	7	7	4	8	60	6989.00	68.25	68688
	41	371.25	7	12	4	13	72	1413.21	68.25	13889
	42	381	7	21	4	22	79	517.68	60.97	4545
	43	388.67	7	29	4	29	82	305.43	53.655	2360
	44	396.33	7	36	4	36	84	232.61	53.655	1797
	45	404	7	44	4	44	85	139.81	60.095	1210
Stringer 3	34	303	0	58	4	58	86	72.84	68.25	716
	35	312.75	0	48	4	48	85	114.95	68.25	1130
	36	322.5	0	39	4	39	84	188.28	68.25	1850
	37	332.25	0	29	4	29	82	305.43	68.25	3002
	38	342	0	19	4	19	78	677.50	68.25	6658
	39	351.75	0	9	4	10	67	2621.96	68.25	25769
	40	361.5	0	1	4	4	7	59366.49	68.25	583454
	41	371.25	0	10	4	11	69	1947.05	68.25	19136
	42	381	0	20	4	20	79	608.11	60.97	5339
	43	388.67	0	28	4	28	82	326.92	53.655	2526
	44	396.33	0	35	4	36	84	232.61	53.655	1797
45	404	0	43	4	43	85	147.15	60.095	1273	
46	413.5	0	53	4	53	86	90.02	66.5	862	

Table A-10: SG Bridge Attack Scenario 5 Static Equivalent Load Calculations

	Joint No.	Coord. Relative to Origin		X (ft)	Z (ft)	D (ft)	θ_i (°)	Pressure (psi)	Tributary Area (ft ²)	Load on Joint (K)
		x	y							
Stringer 1	20	173.4	18.58	40	4	40	84	124.81	27.55	495
	21	183	18.58	32	4	32	83	215.15	27.41	849
	22	192.5	18.58	25	4	25	81	300.72	27.27	1181
	23	202	18.58	20	4	20	79	465.20	24.64	1651
	24	209.67	18.58	19	4	19	78	521.48	22.00	1652
	25	217.33	18.58	20	4	21	79	426.20	22.00	1350
	26	225	18.58	25	4	25	81	300.72	25.00	1082
	27	234.75	18.58	32	4	32	83	215.15	27.98	867
28	244.5	18.58	40	4	40	84	124.81	27.98	503	
Plate Girder 1	20	173.4	14	38	4	38	84	139.46	55.58	1116
	22	192.5	14	22	4	22	80	383.67	55.01	3039
	23	202	14	16	4	16	76	727.83	49.71	5210
	24	209.67	14	14	4	15	74	846.62	44.38	5411
	25	217.33	14	16	4	17	76	649.49	44.38	4151
	26	225	14	21	4	22	79	391.35	50.43	2842
	27	234.75	14	29	4	30	82	258.06	56.45	2098
	28	244.5	14	38	4	38	84	139.46	56.45	1134
Stringer 2	20	173.4	7	36	4	37	84	147.65	67.2	1429
	21	183	7	27	4	27	82	286.47	66.85	2758
	22	192.5	7	18	4	18	77	585.76	66.5	5609
	23	202	7	10	4	11	68	1686.58	60.095	14595
	24	209.67	7	7	4	8	60	5649.73	53.655	43652
	25	217.33	7	11	4	12	70	1336.41	53.655	10326
	26	225	7	17	4	18	77	585.76	60.97	5143
	27	234.75	7	27	4	27	81	290.53	68.25	2855
28	244.5	7	36	4	36	84	156.49	68.25	1538	
Stringer 3	20	173.4	0	36	4	36	84	156.49	67.2	1514
	21	183	0	26	4	26	81	296.42	66.85	2853
	22	192.5	0	17	4	17	76	659.49	66.5	6315
	23	202	0	7	4	8	60	5649.73	60.095	48891
	24	209.67	0	1	4	4	10	47361.20	53.655	365928
	25	217.33	0	8	4	9	64	3138.30	53.655	24248
	26	225	0	16	4	16	76	727.83	60.97	6390
	27	234.75	0	26	4	26	81	296.42	68.25	2913
28	244.5	0	36	4	36	84	156.49	68.25	1538	

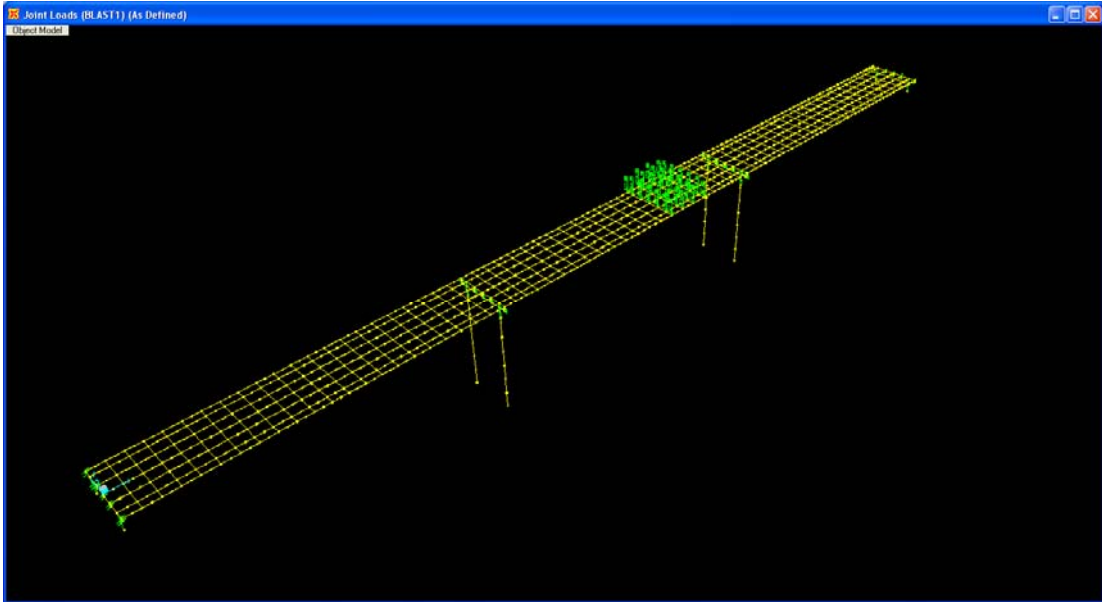


Figure A-7: SG Bridge Attack Scenario 1 Static Equivalent Joint Loads

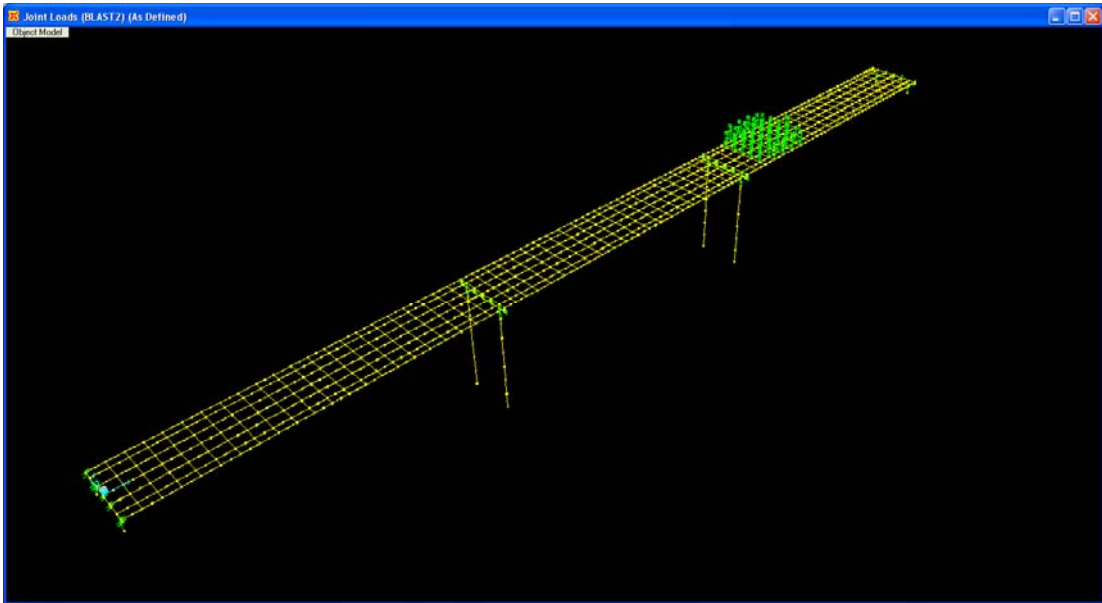


Figure A-8: SG Bridge Attack Scenario 2 Static Equivalent Joint Loads

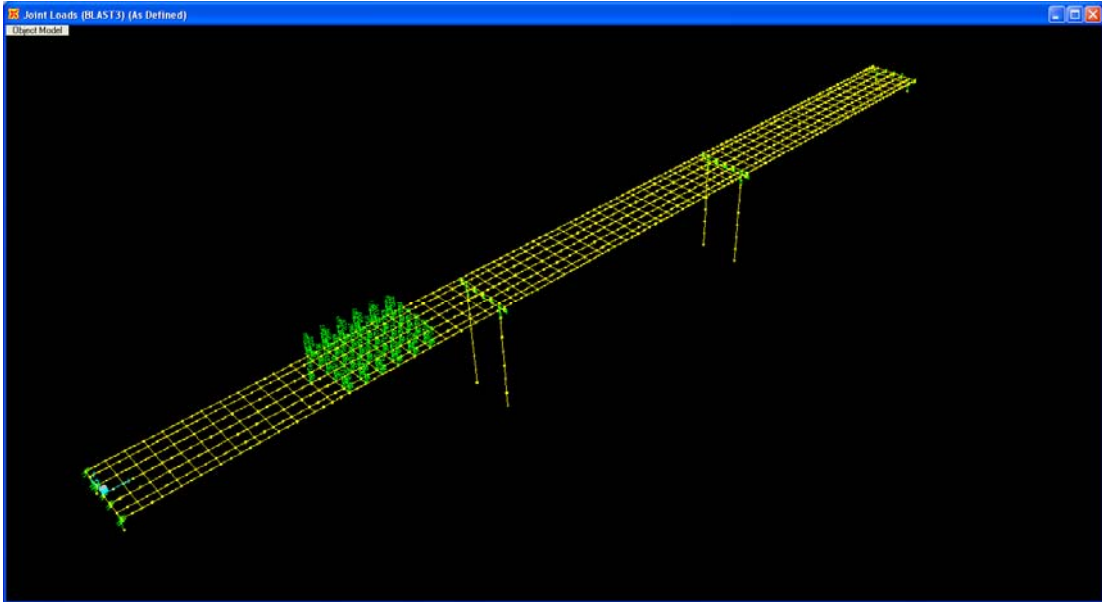


Figure A-9: SG Bridge Attack Scenario 3 Static Equivalent Joint Loads

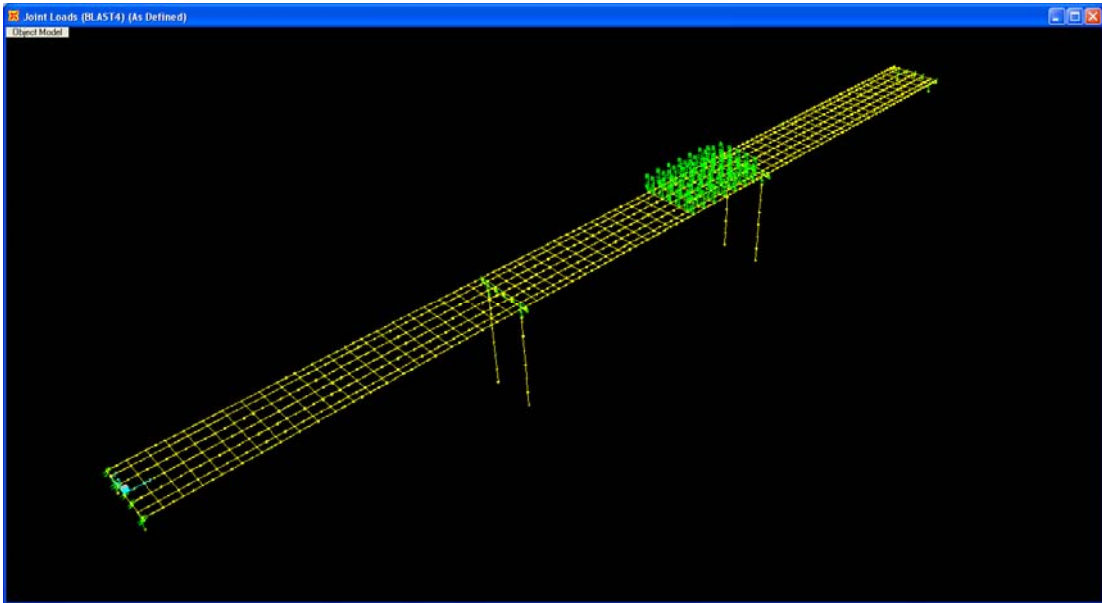


Figure A-10: SG Bridge Attack Scenario 4 Static Equivalent Joint Loads

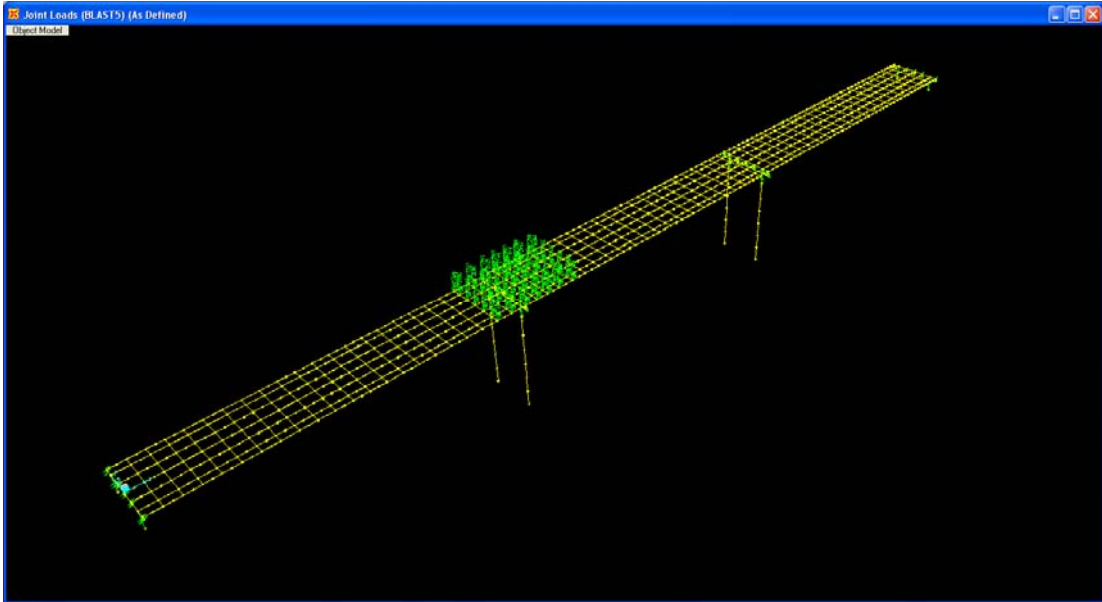


Figure A-11: SG Bridge Attack Scenario 5 Static Equivalent Joint Loads

Table A-11: DT Bridge Attack Scenario 1 Static Equivalent Load Calculations

	Joint No.	Coord. Relative to Origin		X (ft)	Z (ft)	D (ft)	θ_i (°)	Pressure (psi)	Tributary Area (ft ²)	Load on Joint (K)
		x	y							
Stringer 1	1	750	17.5	29	4	29	82	128.05	87.45	1613
	2	765	17.5	19	4	20	78	312.75	87.45	3938
	3	780	17.5	19	4	19	78	306.30	87.45	3857
	4	795	17.5	28	4	28	82	137.49	87.45	1731
Stringer 2	1	750	10.5	25	4	26	81	161.43	105.00	2441
	2	765	10.5	13	4	14	73	572.36	105.00	8654
	3	780	10.5	13	4	13	72	668.49	105.00	10108
	4	795	10.5	24	4	25	81	173.95	105.00	2630
Stringer 3	1	750	3.5	23	4	24	80	205.34	105.00	3105
	2	765	3.5	9	4	10	65	1567.80	105.00	23705
	3	780	3.5	8	4	9	63	2123.15	105.00	32102
	4	795	3.5	22	4	23	80	233.64	105.00	3533

Table A-12: DT Bridge Attack Scenario 2 Static Equivalent Load Calculations

	Joint No.	Coord. Relative to Origin		X (ft)	Z (ft)	D (ft)	θ_i (°)	Pressure (psi)	Tributary Area (ft ²)	Load on Joint (K)
		x	y							
Stringer 1	1	960	17.5	35	4	35	83	111.23	87.45	1401
	2	975	17.5	23	4	23	80	290.26	87.45	3655
	3	990	17.5	18	4	18	77	413.48	87.45	5207
	4	1005	17.5	23	4	23	80	290.26	87.45	3655
	5	1020	17.5	35	4	35	83	111.23	87.45	1401
Stringer 2	1	960	10.5	32	4	32	83	134.96	105.00	2041
	2	975	10.5	18	4	19	78	364.94	105.00	5518
	3	990	10.5	11	4	11	69	1181.61	105.00	17866
	4	1005	10.5	18	4	19	78	364.94	105.00	5518
	5	1020	10.5	32	4	32	83	134.96	105.00	2041
Stringer 3	1	960	3.5	30	4	30	82	156.51	105.00	2366
	2	975	3.5	15	4	16	75	535.11	105.00	8091
	3	990	3.5	4	4	5	41	18319.39	105.00	276989
	4	1005	3.5	15	4	16	75	535.11	105.00	8091
	5	1020	3.5	30	4	30	82	156.51	105.00	2366

Table A-13: DT Bridge Attack Scenario 3 Static Equivalent Load Calculations

	Joint No.	Coord. Relative to Origin		X (ft)	Z (ft)	D (ft)	θ_i (°)	Pressure (psi)	Tributary Area (ft ²)	Load on Joint (K)
		x	y							
Stringer 1	1	270	17.5	27	4	27	81	111.54	87.45	1405
	2	285	17.5	18	4	19	78	284.21	87.45	3579
	3	300	17.5	20	4	21	79	206.72	87.45	2603
	4	315	17.5	31	4	31	83	76.09	87.45	958
Stringer 2	1	270	10.5	23	4	23	80	160.65	105.00	2429
	2	285	10.5	12	4	12	71	614.53	105.00	9292
	3	300	10.5	15	4	15	75	360.58	105.00	5452
	4	315	10.5	27	4	27	82	108.91	105.00	1647
Stringer 3	1	270	3.5	20	4	21	79	206.72	105.00	3126
	2	285	3.5	6	4	7	57	4443.51	105.00	67186
	3	300	3.5	11	4	11	69	760.19	105.00	11494
	4	315	3.5	25	4	26	81	122.10	105.00	1846

Table A-14: DT Bridge Attack Scenario 4 Static Equivalent Load Calculations

	Joint No.	Coord. Relative to Origin		X (ft)	Z (ft)	D (ft)	θ_i (°)	Pressure (psi)	Tributary Area (ft ²)	Load on Joint (K)
		x	y							
Stringer 1	1	765	17.5	42	4	42	85	155.01	87.45	1952
	2	780	17.5	29	4	29	82	305.43	87.45	3846
	3	795	17.5	19	4	20	78	623.02	87.45	7846
	4	810	17.5	19	4	19	78	677.50	87.45	8532
	5	825	17.5	28	4	28	82	326.92	87.45	4117
	6	840	17.5	41	4	41	84	165.39	87.45	2083
Stringer 2	1	765	10.5	39	4	40	84	176.11	105.00	2663
	2	780	10.5	25	4	26	81	376.13	105.00	5687
	3	795	10.5	13	4	14	73	1237.55	105.00	18712
	4	810	10.5	13	4	13	72	1413.21	105.00	21368
	5	825	10.5	24	4	25	81	404.37	105.00	6114
	6	840	10.5	38	4	39	84	188.28	105.00	2847
Stringer 3	1	765	3.5	38	4	38	84	201.65	105.00	3049
	2	780	3.5	23	4	24	80	435.43	105.00	6584
	3	795	3.5	9	4	10	65	3113.57	105.00	47077
	4	810	3.5	8	4	9	63	4142.24	105.00	62631
	5	825	3.5	22	4	23	80	469.68	105.00	7102
	6	840	3.5	37	4	37	84	216.36	105.00	3271

Table A-15: DT Bridge Attack Scenario 5 Static Equivalent Load Calculations

	Joint No.	Coord. Relative to Origin		X (ft)	Z (ft)	D (ft)	θ_i (°)	Pressure (psi)	Tributary Area (ft ²)	Load on Joint (K)
		x	y							
Stringer 1	1	435	17.5	35	4	35	83	167.94	87.45	2115
	2	450	17.5	23	4	23	80	353.05	87.45	4446
	3	465	17.5	18	4	18	77	585.76	87.45	7376
	4	480	17.5	23	4	23	80	353.05	87.45	4446
	5	495	17.5	35	4	35	83	167.94	87.45	2115
Stringer 2	1	435	10.5	32	4	32	83	181.69	105.00	2747
	2	450	10.5	18	4	19	78	521.48	105.00	7885
	3	465	10.5	11	4	11	69	1570.27	105.00	23742
	4	480	10.5	18	4	19	78	521.48	105.00	7885
	5	495	10.5	32	4	32	83	181.69	105.00	2747
Stringer 3	1	435	3.5	30	4	30	82	258.06	105.00	3902
	2	450	3.5	15	4	16	75	744.45	105.00	11256
	3	465	3.5	4	4	5	41	24226.71	105.00	366308
	4	480	3.5	15	4	16	75	744.45	105.00	11256
	5	495	3.5	30	4	30	82	258.06	105.00	3902

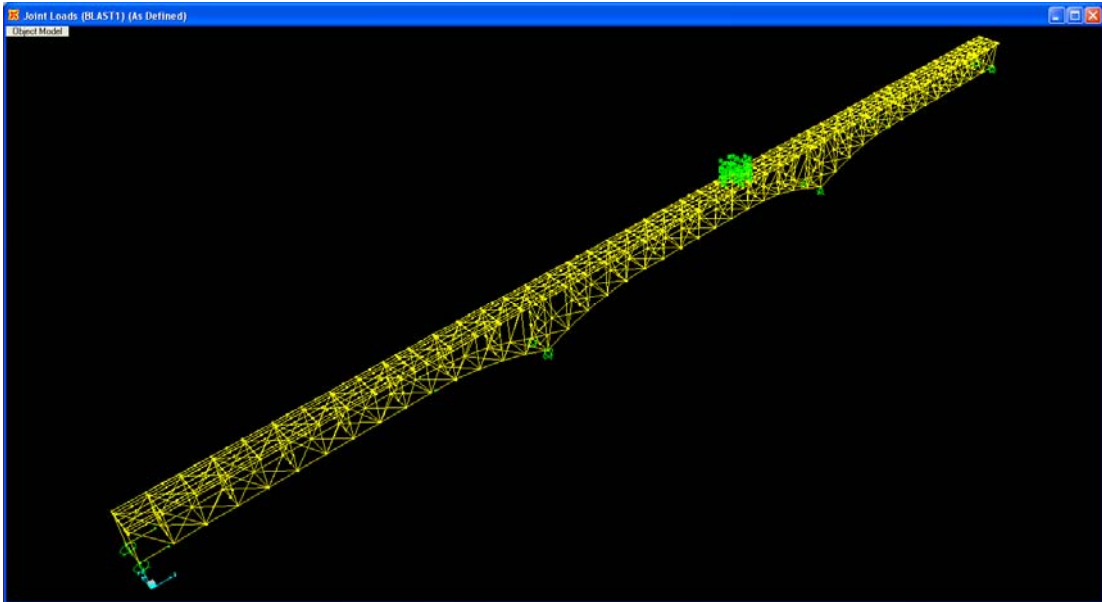


Figure A-12: DT Bridge Attack Scenario 1 Static Equivalent Joint Loads

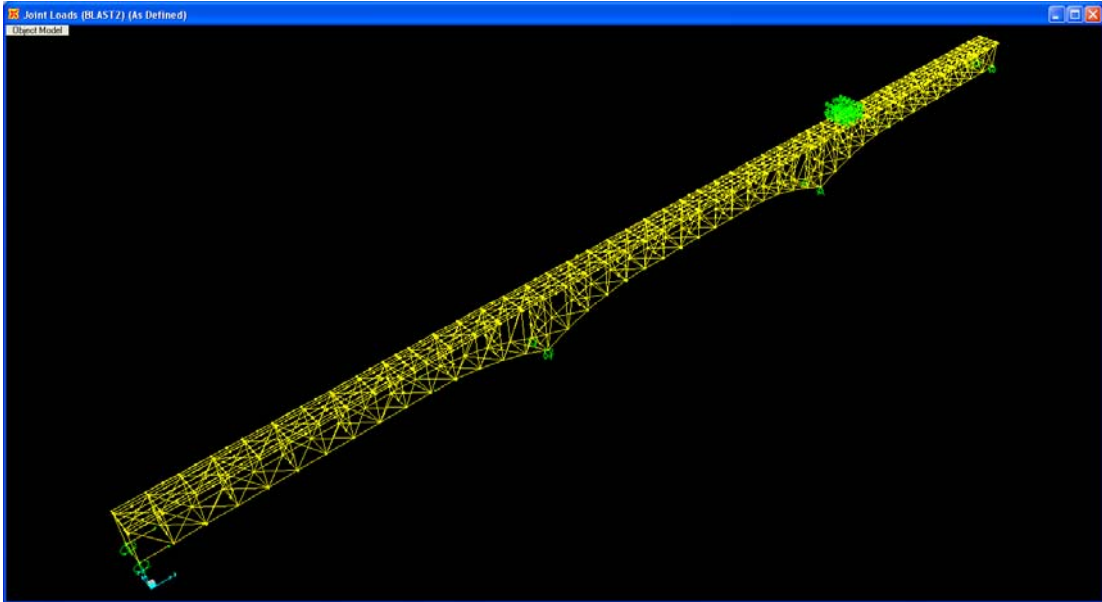


Figure A-13: DT Bridge Attack Scenario 2 Static Equivalent Joint Loads

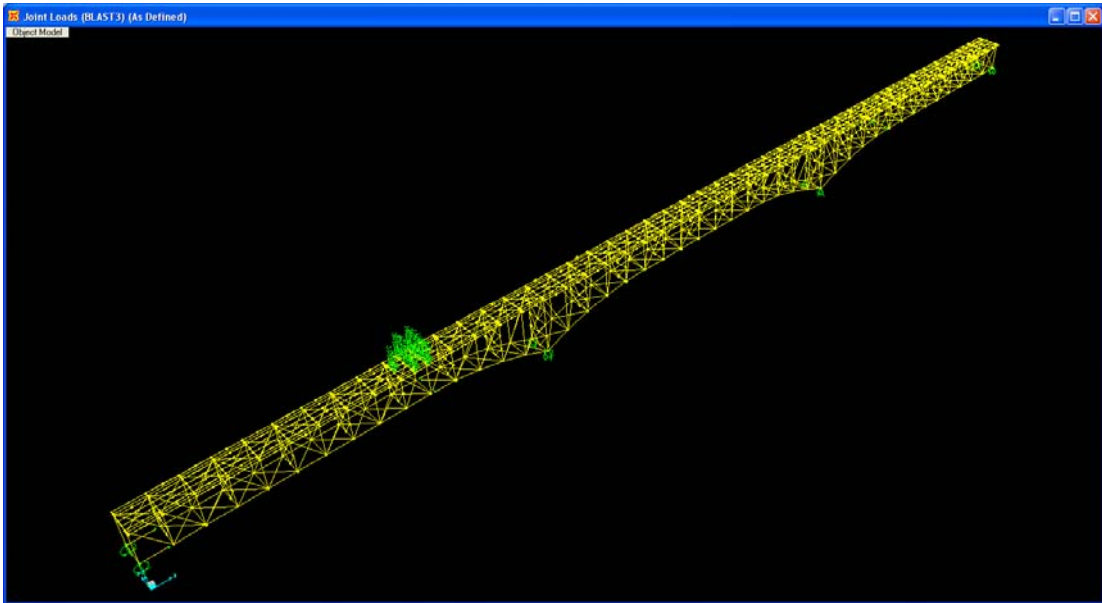


Figure A-14: DT Bridge Attack Scenario 3 Static Equivalent Joint Loads

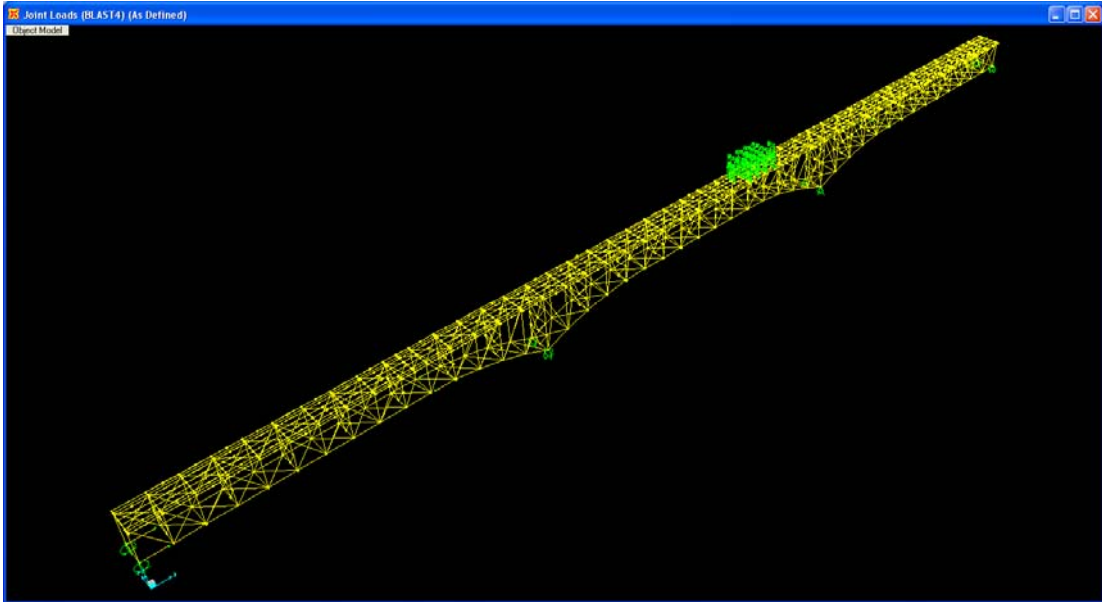


Figure A-15: DT Bridge Attack Scenario 4 Static Equivalent Joint Loads

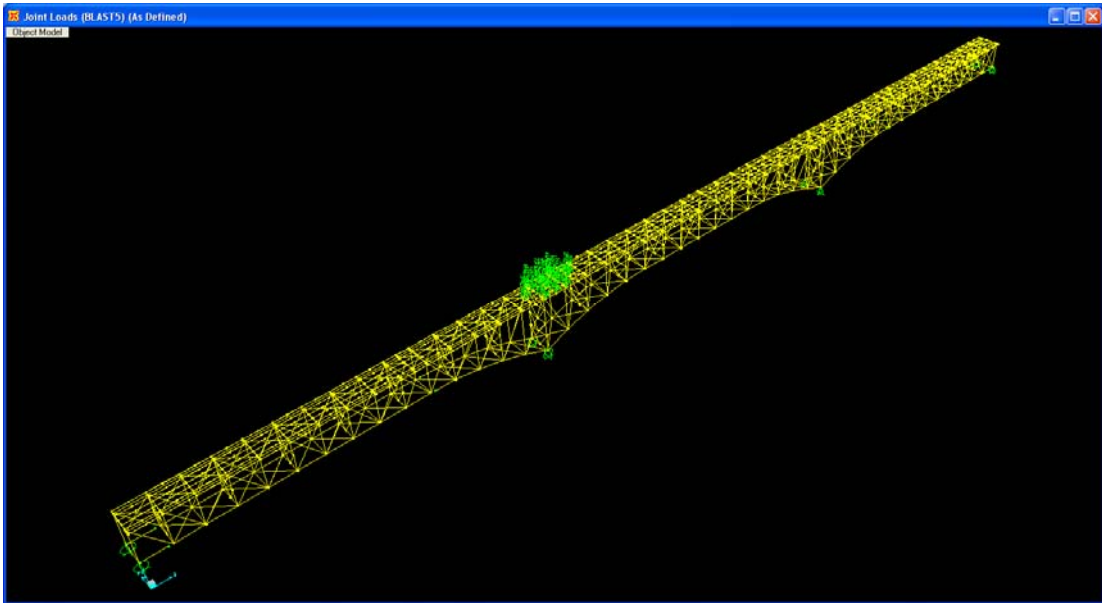


Figure A-16: DT Bridge Attack Scenario 5 Static Equivalent Joint Loads

References

1. AASHTO. (2002). *A Guide to Highway Vulnerability Assessment for Critical Asset Identification and Protection*. <http://security.transportation.org/sites/security/docs/guide-VA_FinalReport.pdf>.
2. AASHTO/FHWA. (2003). Blue Ribbon Panel on Bridge and Tunnel Security. *Recommendations for Bridge and Tunnel Security*. <<http://security.transportation.org/sites/security/brpt/brp.pdf>>.
3. AASHTO. (2002). *National Needs Assessment for Ensuring Transportation Infrastructure Security*. <<http://security.transportation.org/sites/security/docs/NatlNeedsAssess.pdf>>.
4. Al-Wazeer, Adel. (2007). *Risk-Based Bridge Maintenance Strategies*. Ph.D. Dissertation, Department of Civil and Environmental Engineering, University of Maryland, College Park.
5. Applied Research Associates, Inc. (2004). *AT-Blast Version 2.2*.
6. Applied Technology Council (ATC). (2006). *Next-Generation Performance-Based Seismic Design Guidelines: Program Plan for New and Existing Buildings*. <<http://www.atcouncil.org/atc-58.shtml>>.
7. Bensi, Michelle. (2006). *Generalized Assessment of Bridge Vulnerability to Terrorist Threats: A Probabilistic Structural Analysis Based Approach*. Master's Thesis, Department of Civil Engineering, University of Delaware.
8. CALTRANS. (2007). "Comparative Bridge Costs." California Department of Transportation, Division of Structure Earthquake Engineering & Design Support.
9. CALTRANS. (2006). "Sec 11 – Estimating" in *Bridge Design Aids*. California Department of Transportation, Division of Engineering Services. <http://www.dot.ca.gov/hq/esc/techpubs/manual/bridgemanuals/bridge-design-aids/bda.html>.
10. Computers and Structures, Inc. (2005). *SAP2000 Advanced 11.0.2*. Berkeley, California.
11. Ayyub, B. M., McGill, W. L., and Kaminskiy, M. (2007). "Critical Asset and Portfolio Risk Analysis for Homeland Security: An All-Hazards Framework." *Risk Analysis Journal*, Accepted for publication.

12. Ayyub, Bilal M. (2003). *Risk Analysis in Engineering and Economics*. Washington, DC: Chapman and Hall/CRC.
13. Federal Emergency Management Agency (FEMA). (1997). *NEHRP Guidelines for the Seismic Rehabilitation of Buildings*, FEMA Publication 273. Washington, D.C.
14. Federal Emergency Management Agency (FEMA). (2003). *Prestandard and Commentary for the Seismic Rehabilitation of Buildings*, FEMA Publication 356. Washington, D.C.
15. FHWA. (2002). "Accelerated Bridge Repairs: Meeting the Challenge in Oklahoma." <<http://www.tfhr.gov/focus/aug02/01.htm>>.
16. Floren, A., and Mohammadi, J. (2001). "Performance-Based Design Approach in Seismic Analysis of Bridges." *Journal of Bridge Engineering*, 6(1), 37-45.
17. Inel, Mehmet and Ozmen, Hayri B. (2006). "Effects of Plastic Hinge Properties in Nonlinear Analysis of Reinforced Concrete Buildings." *Engineering Structures*, 28(11), 1494-1502.
18. Islam, A.K.M. (2005). *Performance of AASHTO Girder Bridges Under Blast Loading*. Master's Thesis, Department of Civil Engineering, Florida State University.
19. Kunnath, Sashi K. (2007). Application of the PEER PBEE Methodology to the I-880 Viaduct, PEER 2006/10. Pacific Earthquake Engineering Research Center, University of California, Berkeley.
20. Mackie, K., Wong, J-M., and Stojadinovic, B. (2006). "Method for post-earthquake highway bridge repair cost estimation." In Proceedings of the *5th National Seismic Conference on Bridges and Highways*, September 18-20, 2006. San Francisco, CA.
21. McGill, W. L., Ayyub, B. M., and Kaminskiy, M. (2007). "Risk Analysis for Critical Asset Protection." *Risk Analysis*, Accepted for publication.
22. Pacific Earthquake Engineering Research Center. University of California, Berkeley. <<http://peer.berkeley.edu>>.
23. Saiidi, M.S. (1997). "Working Group on Bridge Design Issues." *Conclusions and Recommendations of the Workshop on Seismic Design Methodologies for the Next Generation of Codes*, Bled, Slovenia.

24. Suthar, Kunal. (2007). *The Effect of Dead, Live and Blast Loads on a Suspension Bridge*. Master's Thesis, Department of Civil and Environmental Engineering, University of Maryland, College Park.
25. Thompson, B.P., and Bank, L.C. (2007). "Risk Perception in Performance-Based Building Design and Applications to Terrorism-Resistant Design." *Journal of Performance of Constructed Facilities*, 21(1), 61-69.
26. United States Department of Transportation. (2002). Memorandum (Subject: *Revised Departmental Guidance: Treatment of Value of Life and Injuries in Preparing Economic Evaluations*). <http://ostpxweb.dot.gov/VSL_2002_Guidance.pdf>.
27. Whittaker, A., Hamburger, R., Comartin, C., Mahoney, M., Bachman, R., and Rojahn, C. (2003). "Performance-Based Engineering of Buildings for Extreme Events." *AISC-SINY Symp. On Resisting Blast and Progressive Collapse*, New York.
28. Winget, D.G., K.A. Marchand, and E.B. Williamson. (2005). "Analysis and Design of Critical Bridges Subjected to Blast Loads." *ASCE Journal of Structural Engineering*, 131(8), 1243-1255.